KUNGL TEKNISKA HÖGSKOLAN

TRITA-MEK
Technical Report 2002:11
ISSN 0348-467X
ISRN KTH/MEK/TR--02/11--SE

Simulating Dynamical Behaviour of Wind Power Structures

Anders Ahlström

Licentiate Thesis
Stockholm, 2002

Royal Institute of Technology
Department of Mechanics

Simulating Dynamical Behaviour of Wind Power Structures

by

Anders Ahlström

August 2002
Technical Reports from
Royal Institute of Technology
Department of Mechanics
SE-100 44 Stockholm, Sweden

©Anders Ahlström 2002

Abstract

The work in this thesis deals with the development of an aeroelastic simulation tool for horizontal axis wind turbine applications.

Horizontal axis wind turbines can experience significant time varying aerodynamic loads, potentially causing adverse effects on structures, mechanical components, and power production. The need of computational and experimental procedures for investigating aeroelastic stability and dynamic response have increased as wind turbines become lighter and more flexible.

A finite element model for simulation of the dynamic response of horizontal axis wind turbines has been developed. The simulations are performed using the commercial finite element software SOLVIA, which is a program developed for general analyses, linear as well as non-linear, static as well as dynamic. The aerodynamic model, used to transform the wind flow field to loads on the blades, is a Blade-Element/Momentum model. The aerodynamic code is developed by FFA (The Aeronautical Research Institute of Sweden) and is a state-of-the-art code incorporating a number of extensions to the Blade-Element/Momentum formulation. SOSIS-W, developed by Teknikgruppen AB was used to develop wind time series for modelling different wind conditions.

The model is rather general, and different configurations of the structural model and various type of wind conditions could easily be simulated. The model is primarily intended for use as a research tool when influences of specific dynamic effects are investigated.

Simulation results for the three-bladed wind turbine Danwin 180 kW are presented as a verification example.

Keywords: aeroelastic modelling, rotor aerodynamics, structural dynamics, wind turbine, AERFORCE, SOSIS-W, SOLVIA

Preface

The research work presented in this thesis was carried out at the Department of Structural Engineering and the Department of Mechanics at the Royal Institute of Technology under the supervision of Professor Anders Eriksson.

My thanks go out to my supervisor Professor Anders Eriksson for his guidance, encouragement and valuable comments throughout the process of this work.

I would also like to thank Docent Costin Pacoste for help and supervision at the startup of the project.

I thank Gunnar Larsson at SOLVIA Engineering AB for many fruitful discussions and for his assistance and positive attitude.

I thank Anders Björk at Nordic Wind Power for valuable help with various questions regarding wind turbines and aerodynamics.

Many grateful thanks to Ingemar Carlén and Hans Ganander at Teknikgruppen AB for the data on the Alsvik wind turbine and for their time and assistance.

I am also grateful to Christer Ahlström, Dr. Jean-Marc Battini and Dr. Gunnar Tibert for proof-reading this manuscript.

A warm thank you to colleagues and former colleagues of the Department of Structural Engineering and Department of Mechanics for their contribution to this work and for creating a stimulating working environment.

The project has been primarily financed by a grant from STEM, The Swedish Energy Administration, which is gratefully acknowledged.

Stockholm, June 2002

Anders Ahlström

Contents

List of symbols

a	axial induction factor, 35
a'	tangential induction factor, 37
A_0	area of the actuator disc, 35
A_∞	streamtube area upstream of the actuator disc, 35
α	angle of attack, 36
A_w	streamtube area downstream of the actuator disc, 35
c	blade cord length, 36
C_D	drag coefficient, 36
C_L	lift coefficient, 36
C_N	projected drag coefficient, 37
C_P	power coefficient, 36
$c(r)$	chord at position r, 37
C_T	projected lift coefficient, 37
D	drag force, 36
$\dot{m}$	mass flow, 35
F_N	force normal to rotor-plane, 36
F_T	force tangential to rotor-plane, 36
L	lift force, 36
$\dot{L}$	rate of change of momentum, 35
N	number of blades, 37
ω	rotation speed, 37
P	generated power, 36
p_0^+	pressure upstream of the actuator disc, 35
p_0^-	pressure downstream of the actuator disc, 35
ϕ	angle between disc plane and relative velocity, 36
p_∞	free stream pressure, 35
r	radius of the blade, 37
ρ_0	air density at the actuator disc, 35
ρ_∞	density of the undisturbed air, 35
ρ_w	air density of the wake, 35
σ	solidify factor, 37
T	thrust on the rotor, 35
θ	local pitch of the blade, 36
U_0	air speed at the actuator disc, 35
U_∞	undisturbed air speed, 35
U_w	wake air speed, 35
v	free stream velocity, 35

V_{rel} relative air speed, 36

List of Figures

List of Tables

Chapter 1

Introduction

1.1 Background

For a successful large-scale application of wind energy, the price of wind turbine energy must decrease in order to be competitive with the present alternatives. The behaviour of a wind turbine is made up of a complex interaction of components and sub-systems. The main elements are the rotor, tower, hub, nacelle, foundation, power train and control system. Understanding the interactive behaviour between the components provides the key to reliable design calculations, optimised machine configurations and lower costs for wind-generated electricity. Consequently, there is a trend towards lighter and more flexible wind turbines, which makes design and dimensioning even more important.

Wind turbines operate in a hostile environment where strong flow fluctuations, due to the nature of the wind, can excite intense loads. The varying loads, together with an elastic structure, creates a perfect breeding ground for induced vibration and resonance problems. The need of computational and experimental procedures for investigating aeroelastic stability and dynamic response have increased with the rated power and size of the turbines. The increased size of the rotor requires that the dimension of the other components must be scaled up, e.g., the tower height. With increasing size, the structures behave more flexibly and thus the loads change. As wind turbines become lighter and more flexible, comprehensive systems dynamics codes are needed to predict and understand complex interactions.

1.2 Scope and aims

The goal of this project is to produce a model with such accuracy and flexibility that different kind of dynamic phenomena can be investigated. The majority of the present aeroelastic models are based on a modal formulation and a frequency domain solution. The modal formulation models are computationally time efficient because of the effective way of reducing degrees of freedom (DOF). However, the modal

models are primarily suited for design purposes and will, because of the reduced DOF, often not be suitable for research areas where phenomena such as instabilities may be investigated. In this project, the finite element method (FEM) has been chosen as a means to accurately predict the wind turbine loading and response.

1.3 Outline of thesis

- In Chapter 2, the wind turbine is presented from a historical point of view and a short description of the layout and the general function is given.
- In Chapter 3, the different design concepts are discussed and presented. The purpose of this chapter is to give the unfamiliar reader, a relatively detailed description about the different design concepts, solutions and manufacturing techniques that are used. For instance, different types of generators and power control methods are discussed.
- In Chapter 4, the wind turbine manufacturers are compared regarding design concepts to see if there are any specific trends, e.g. variable or fixed rotor speed, stall or pitch power regulation on today's market.
- In Chapter 5, the current state-of-the-art wind turbine design codes are reviewed. Aspects regarding wind turbine design calculations, e.g. wind field representation, rotor aerodynamics, loads and structural stresses are discussed and explained.
- In Chapter 6, the aspects of modelling a wind turbine within the FEM are described. For example, the modelling of the bedplate, blades and tower. The time-integration method and the different tolerance methods are also discussed.
- In Chapter 7, the three main parts of the simulation program are treated:

  SOSIS-W for generation of the turbulent wind field [8].
  AERFORCE package for the calculation of aerodynamic loads [2].
  SOLVIA commercial finite element program for modelling of the structural dynamics [38].

  Chapter 7 also explains how the three programs are linked together.
- In Chapter 8, the FEM model of the Alsvik turbine is described. Further, results like power curve, flap and edge moment are presented based on numerical simulations.
- Chapter 9 concludes the study and gives some suggestions for further research.
- In Appendix A, the properties of the Alsvik turbine are tabulated.
- In Appendix B, some input files used in the simulations are given.

Chapter 2

A general description of a wind power plant

2.1 Wind power from a historical point of view

Wind energy has been used for a long time. The first field of application was to propel boats along the river Nile around 5000 BC [57]. By comparison, wind turbine is a fairly recent invention. The first simple windmills were used in Persia as early as the 7th century for irrigation purposes and for milling grain [16]. In Europe it has been claimed that the Crusaders introduced the windmills around the 11th century. Their constructions were based on wood. In order to bring the sails into the wind, they were manually rotated around a central post. In 1745, the fantail was invented and soon became one of of the most important improvements in the history of the windmill. The fantail automatically orientated the windmill towards the wind. Wind power technology advanced and in 1772, the spring sail was developed. Wood shutters could be opened either manually or automatically to maintain a constant sail speed in winds of varying speed. The miller was able to adjust the tension of the spring to regulate the needed power and to protect the mechanical parts of the mill [33].

The modern concept of windmills began around the industrial revolution. Millions of windmills were built in the United States during the 19th century. The reason for this massive increase in use of wind energy stems from the development of the American West. The new houses and farms needed ways to pump water. The proceeding of the industrial revolution later led to a gradual decline in the use of windmills.

However, meanwhile the industrial revolution proceeded, the industrialization sparked the development of larger windmills to generate electricity. The first electricity generating wind turbine was developed by Poul la Cour [12]. In the late 1930s Americans started planning a megawatt-scale wind turbine generator using the latest technology. The result of this work was the 1.25 MW Smith-Putnam wind turbine, Figure 2.1. Back in 1941 it was the largest wind turbine ever built and it kept its leading

Figure 2.1: The 1.250 MW Smith-Putnam wind turbine. Reproduced from [35].

position for 40 years [52].

The popularity of using the energy in the wind has always fluctuated with the price of fossils fuels. Research and development in nuclear power and good access to oil during the 1960s led to a decline of the development of new large-scale wind turbines. But when the price of oil raised abruptly in the 1970s, the interest for wind turbines started again [21].

Today, wind energy is the the fastest growing energy technology in the world. The world wind energy capacity installations have surged from under 2000 MW in 1990 to the present level of approximately 24500 MW (January 2002) [66]. By comparison,

the eleven nuclear power plants in Sweden have a gross capacity of 9800 MW [53].

2.2 General description and layout of a wind turbine

Almost all wind turbines that produce electricity for the national grid consists of rotor blades that rotate around a horizontal hub. The hub is connected to a gearbox and a generator (direct-drive generators are present as well and makes the gearbox unnecessary), which are located inside the nacelle, Figure 2.2. The nacelle houses some of the electrical components and is mounted on top of the tower. The electric current is then distributed by a transformer to the grid. Many different design concepts are in use. At present, the most used are two or three bladed, stall or pitch regulated, horizontal-axis machines working at a near fixed rotational speed.

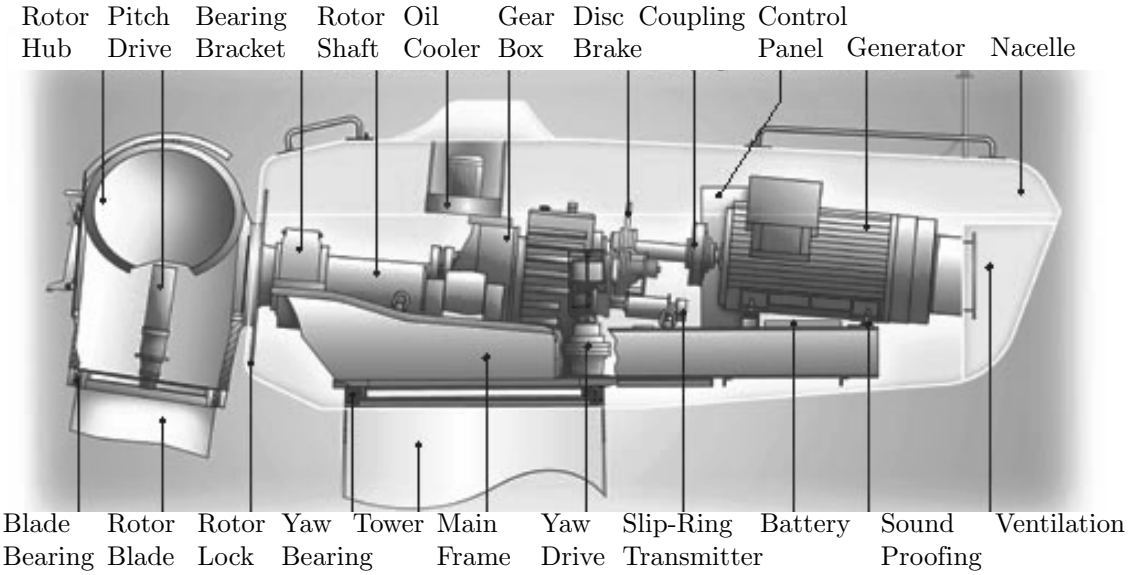

Figure 2.2: Wind turbine layout. Reproduced from [45].

Chapter 3

Wind turbine technology and design concepts

3.1 Blade

All forms of wind turbines are designed to extract power from a moving air stream. The blades have an aerofoil cross-section and extract wind by a lift force caused by pressure difference between blade sides. For maximum efficiency, the blades often incorporate twist and taper. The information in this section is based on [1, 20, 22].

3.1.1 Manufacturing technique and material

Wood has a natural composite structure of low density, good strength and fatigue resistance. The drawbacks are the sensitivity to moisture and the processing costs. There are, however techniques that overcome these problems. Wood veneers are laminated with epoxy resin in a vacuum bag which presses them to the shape of the blade mould. The blade is formed by bonding the top and bottom blade halves. A spar is glued in position between the two halves as a strengthener.

Most larger wind turbine blades are made out of Glass fibre Reinforced Plastics (GRP), e.g. glass fibre reinforced polyester or epoxy. Wet lay-up is a process where fibre, in the form of fabric, mat or roving is placed in a mould and impregnated by hand. This process is labour intensive but offers considerable flexibility in placement of material. A problem with the wet lay-up technique is that the used amount of resin is difficult to control. The result is therefore very much depending on the skills of the worker. Prepreg lay-up is a process where fibers, by a supplier, are pre-impregnated with resin. The process is also manual but assures close control of the resin content. This method also greatly improves the working environment. Another way to impregnate the fibers is to use vacuum infusion moulding (RIM). The difference between wet lay-up and RIM is that vacuum is used to suck the resin in between mould and vacuum bag. This provides better, more uniform product quality and greatly improves the working environment.

Carbon Fibre Reinforced Plastic (CFRP) blades are used in some applications. It has been assumed that this material system was strictly for aerospace applications and too expensive for wind turbines. However, by using effective production techniques, some manufacturers produce cost effective wind turbine blades. The advantage with carbon fibre is the high specific strength.

Figure 3.1 shows the principal blade material used and numbers of each sold until 1999 [22].

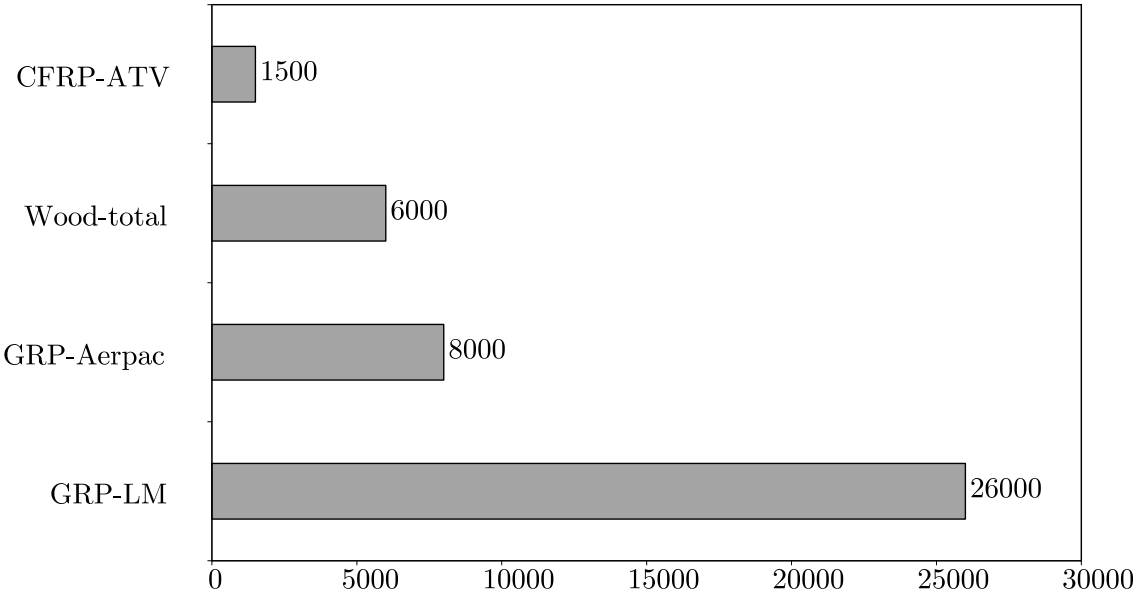

Figure 3.1: Principal blade materials and number sold.

3.1.2 Number of blades

Since the beginning of the modern wind power era, the preferred designs for wind turbines have been with either two or three blades. Many early prototypes have two blades, e.g. Näsudden (Sweden), but the three bladed concept has been the most frequently used during the past years.

Basic aerodynamic principles determine that there is an optimal installed blade area for a given rotational speed. It is more efficient to use many slender blades rather than using few wide ones to make up the required area. A turbine for wind farm applications generally has a tip speed of 60–70 m/s. With these tip speeds a three-bladed rotor is 2–3% more efficient than a two-bladed rotor. It is even possible to use a single bladed rotor if a counterbalance is mounted. The efficiency loss is about 6% compared with the two-bladed rotor construction. Although fewer blades gives lower blade costs, there are penalties. The single-bladed rotor requires a counterbalance and is therefore not lighter than a two-bladed design. The two-bladed rotor must accept very high cycle loading if a rigid hub system is employed. However, by using a teetered hub the loading can be reduced. The teeter system allows the rotor blades to rock as a pair to make it possible for the rotor to tilt backwards and forwards

a few degrees away from the main plane during rotation. The three-bladed rotor is dynamically simpler and a little more aerodynamically efficient. Three-bladed designs have also been preferred since they are considered to look more aesthetic in the landscape and because they make it easier to work within strict ambient sound limits. Against that the two-bladed rotors offer potential reductions in both fabrication and maintenance costs [11].

3.1.3 Aerofoil design

In the beginning, most wind turbine blades where adaptations of aerofoils developed for aircraft and were not optimized for wind turbine uses. In recent years developments of improved aerofoil sections for wind turbines have been ongoing. The prevailing tendency among blade manufacturers is to use NACA 63 sections, [63], that may have modifications in order to improve performance for special applications and wind conditions. Blades tend to have slightly higher lift aerofoils closer to the root and lower lift aerofoils near the tip. To gain efficiency, the blade is both tapered and twisted. The taper, twist and aerofoil characteristic should all be combined in order to give the best possible energy capture for the rotor speed and site conditions.

A number of technologies known from aircraft industry are being adapted for use in wind turbine applications. A problem with wind turbine blades is that even at relatively low wind speed, the innermost part of some blades begin to stall. When parts of the blades stall, it has a braking effect on the rotor. Normally stall-controlled wind turbine blades are supposed to control power at 14–15 m/s when the outer part of the blade begins to stall. If the innermost part of the blade will stall, say around 8–9 m/s, the efficiency will decline. In practice, however, it is not possible to design a thick profile that does not suffer from premature stall, but with ways such as vortex generators there are methods to improve the dynamic behaviour. Vortex generators are a number of small fins which stick out above the boundary layer close to the surface of the blade, Figure 3.2. The fins are alternately skewed a few degrees to the right or left to make the generated eddies turn alternately. When two eddies collide the generated flow will be going in the same direction, which reduces the aerodynamic drag on the rotor blades. On the lee side of the rotor blade it is possible to use the effect from the eddies to pull fresh air in close to the surface of the blade and thereby avoid the premature stall. The company LM Glasfiber claims that improvements of up to 4–6% of the annual production can be obtained using vortex generators [41].

Figure 3.2: Vortex generators in aeroplane use. Reproduced from [61].

3.1.4 Lightning protection

Lightning damage to wind turbines has been a serious problem for power companies since towers have become higher each year. The off-shore installations that currently are being raised will be even more exposed to lightning threats. Experiences with lighting damage to wind turbines in Denmark in the years 1985–1997 shows that the average damage occurrence was 4.1% per wind turbine year. About 50% of the reported damages are related to the control system, 20% to the power system and 18% are connected to the mechanical components [51].

Lightning protection of wind turbines can be accomplished in many ways, but the common idea is to lead the lightning from the tip of the blade, down to the blade hub from where it is led through the nacelle and the tower down into the ground. The *Vestas Total Lightning Protection* uses this kind of lightning route through the turbine.

Blade: each blade is protected by a 50 mm^2 copper conductor, which stretches between the blade tip and the hub. Should lightning strike, it is led through the conductor along the spar of the blade down to the aluminium section at the root of the blade.

Nacelle: the lightning is then led from the hub into the nacelle and there via the machine bed into the tower. A conductor is also fitted at the rear of the nacelle. If the wind turbine is struck directly to the nacelle this conductor ensures that wind vane and anemometer will be protected.

Tower: the lightning is here led either by copper conductors or by the tower itself down to the earthing system.

Earthing system: in Vestas lightning system, a thick copper ring conductor is placed a metre below the surface at a distance of one metre from the concrete foundation of the turbine. The ring conductor is attached to two diametrically opposite points on the tower. The ring is also attached to two copper coated earthing rods placed on either side of the foundation. This arrangement will minimise the danger to both humans and animals in the vicinity of the tower.

Electrical system: control systems are protected by using fibre optic cables for communication and a shielding system. To protect the entire electrical installation overvoltage protections are included.

A lightning protected turbine blade is illustrated in Figure 3.3. An interesting detail is that the blades are equipped with a magnetic card that registers the number of lightning strikes.

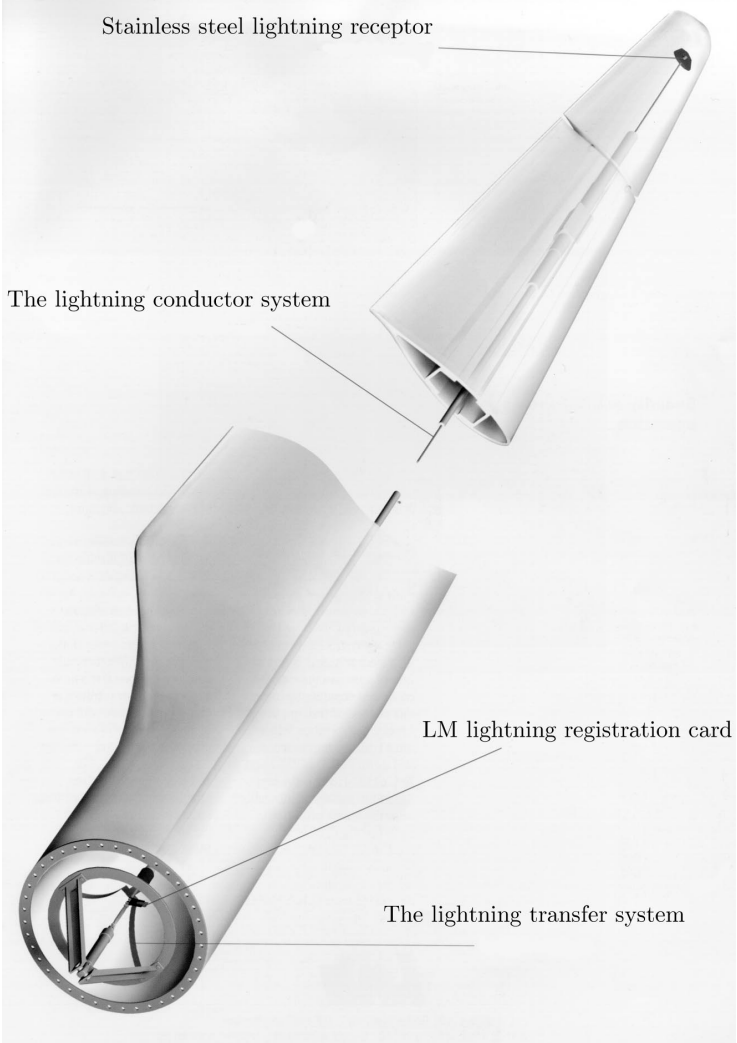

Figure 3.3: Lightning protected turbine blade by LM Glasfiber A/S. Reproduced from [40].

3.2 Tower

The most common types of towers are the lattice and tubular types constructed from steel or concrete. For small wind turbines, the tower may be supported by guy wires.

The tower can be designed in two ways, soft or stiff. A stiff tower has a natural frequency which lies above the blade passing frequency. Soft towers are lighter and cheaper but have to withstand more movement and will suffer higher stress levels.

3.2.1 Tubular steel towers

Most modern wind turbines have conical towers made of steel. The tubular shape allows access from inside the tower to the nacelle, which is preferred in bad weather conditions. The towers are manufactured in sections of 20–30 metres with flanges at both ends. Sections are then transported to the foundation for the final assembly.

3.2.2 Lattice towers

Lattice towers are assembled by welded steel profiles. Lattice towers are cheap but the main disadvantages are the poor visual appeal and the fact that access to the nacelle is exposed. In most of the world, lattice towers are quite rare, but e.g. in the uninhabited desert of California lattice towers may still be found. [26, 63].

3.3 Hub

The hub connects the turbine blades to the main shaft. Blades are bolted to the hub flanges by threaded bushes that are glued into the blade root. The flange bolt holes can be elongated, in order to enable the blade tip angle to be adjusted. As mentioned in Section 3.1.2, the hub type can be either rigid or teetered.
Because of the often complicated hub shape, which is difficult to make in any other way, it is convenient to use cast iron. The hub must also be highly resistant to metal fatigue, which is difficult to achieve in a welded construction. Normal cast iron has the disadvantage of being rather fragile and may fracture under impact type loads. Special types of strong iron alloy are used for overcoming the disadvantages, e.g. Spherical Graphite (SG) cast iron.

3.4 Nacelle

The nacelle contains the key components of the wind turbine, including the gearbox and the electrical generator. The nacelle is generally made of GRP or steel. In

modern wind turbines, service personnel may enter the nacelle from the tower of the turbine.

3.5 Braking system

The power in the wind is proportional to the cube of the wind speed. Considerable forces must therefore be controlled during high winds in order to attain safe operation. There are usually at least two independent systems, each capable of bringing the wind turbine to a safe condition in the case of high winds, loss of connection to the network or other emergencies [63].

3.5.1 Aerodynamic brakes

Aerodynamic brakes operate by turning the blades or turning the blade tip (depending on the power control system) in order to prevent the aerodynamic forces from assisting rotation of the blades. The aerodynamic brake is the preferred brake for stopping because less stress is being placed on the working components than if mechanical brakes are used. The systems are usually spring or hydraulic operated and constructed to work in the case of electrical power failure. In the case of tip brakes, the tip blade is fixed on e.g. a carbon fibre shaft, mounted on a bearing inside the main body of the blade. For instance, the company Bonus, is using such a system [55]. A device is fixed on the end of the shaft inside the blade. The mechanism will rotate the blade tip if subjected to an outward movement. The movement is accomplished by a wire connected between the device and a hydraulic cylinder located in the hub. When it becomes necessary to stop the rotor, the restraining power is cut off by release of oil from the hydraulic cylinder and thereby permitting the centrifugal force to pull the blade tip forwards. When the tip shaft is released the mechanism will rotate the blade tip 90° into a braking position. By letting the hydraulic oil flow through a rather small hole, the blade tip will rotate slowly for a couple of seconds before it is fully in position. This thereby avoids excessive shock loads during braking.

3.5.2 Mechanical brakes

To bring the rotor to a complete stop a mechanical brake is fitted to the main transmission shaft. It is desirable to fit the brake between the rotor and the gearbox in case of a gearbox failure. However, the torque on the low speed shaft can be very large, so manufacturers often fit the brake on the high speed shaft between the gearbox and the generator. The mechanical brake is generally a disc brake made of steel. Like the aerodynamic brake this is also a fail-safe system. For instance, to prevent the brakes from locking, hydraulic oil pressure can be used. Should oil pressure be lacking, a powerful spring will cause the wind turbine to stop by

activating the brakes. The brake disc is made of a special metal alloy to endure the generated heat, which can give temperatures of up to 700°C.

3.6 Yaw mechanism

It is necessary to align the rotor axis with the wind in order to extract as much energy from the wind as possible.

Most horizontal axis wind turbines use forced yawing. An electrical or hydraulic system is used to align the machine with the wind. The yaw drive reacts on signals from, e.g. a wind vane on top of the nacelle. Almost all manufacturers, of upwind machines, brake the yaw mechanism whenever it is not used. In slender wind turbines, like the Swedish Nordic 1000, the yaw mechanism is of importance for the dynamic behavior of the system. The yaw mechanism must fulfil the requirements of a soft and damped connection between the nacelle and the tower. A hydraulic system is used to give the right characteristics whether it is yawing or not. This specific system is not furnished with any mechanical brakes.

In some wind situations, the turbine will rotate in the same direction for a long time. The cables that transport current from the generator down the tower will then be twisted. By using a device that counts the number of twists the cable can be twisted back [13, 59, 63].

3.7 Generator

The wind turbine generator converts mechanical energy to electrical energy. The size of the generator is determined by the rated power. The efficiency of an electrical generator usually falls off rapidly below its rated output. Since the power in the wind fluctuates widely, it is important to consider the relation between rated wind speed and rated power. In order to make the wind turbine as efficient as possible manufactures have developed techniques to rise effectiveness even at low revolution velocities. Whether it is worthwhile to use techniques able to efficiently handle low wind speeds depends on the local wind distribution and the extra cost associated with more expensive equipment.

The usual generator in wind turbines is the induction generator, sometimes called the asynchronous generator. One other type of generator is the synchronous one. The synchronous generator dominates in direct driven turbines, but is not very common in other wind power applications. The advantages of the induction generator are mechanical simplicity, robustness and closed cooling. A weakness could be that the stator needs to be magnetized from the grid before it works. It is possible to run an asynchronous generator in a stand alone system if it is provided with additional components. The synchronous generator is more complicated than the induction one. It has more parts and is normally cooled with ambient air internally. Compared

to the induction generator, a synchronous generator can run without connection to the [14, 56].

3.7.1 Constant speed generators

3.7.1.1 Two generators

To increase efficiency in low wind speed, solutions with two generators of different sizes are used. The smaller generator operates near its rated power at low wind speed and the bigger one is taking over at higher winds.

3.7.1.2 Pole changing generators

Pole changing generators are more common than two generator systems these days. A pole changing generator is made, e.g. with twice as many magnets (generally 4 or 6). Depending on the local wind distribution, the generator is designed for different velocities. For example, the 600 kW Bonus Mk IV is equipped with an asynchronous generator. At low wind speeds the small 6-pole generator winding is used for power production, running at two thirds of the nominal speed. At higher wind speeds, the generator is switched to the 4-pole main winding, operating at nominal speed [5]. An example of such generator is the FLENDER 600/150 kW shown in Figure 3.4.

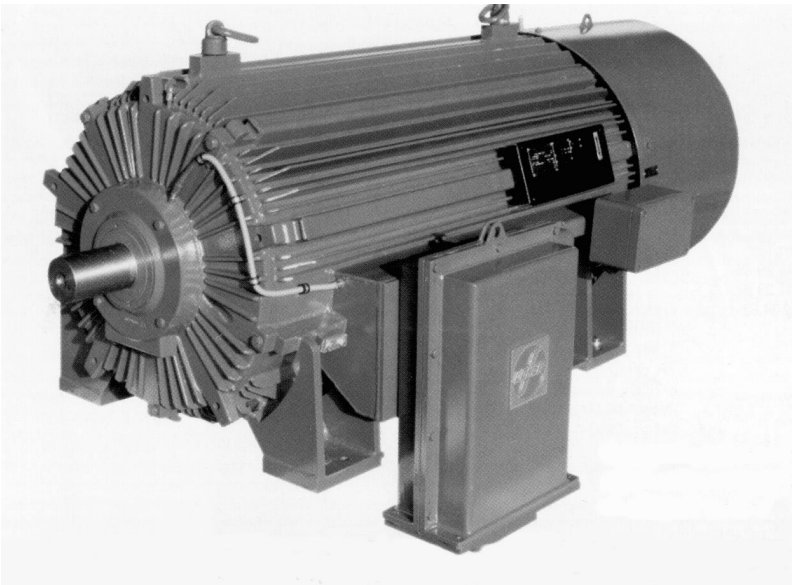

Figure 3.4: Flender two-speed asynchronous generator AGUA-400LX-64A, 600/150 kW, 4/6-poles with forced air-cooling. Reproduced from [23].

3.7.2 Variable speed generators

There are several advantages in operating wind turbines at variable speed:

- The increase in aerodynamic efficiency, which makes it possible to extract more energy than in fixed speed operation.
- The possibility to decrease turbine speed in low wind speeds to reduce noise while avoiding too much torque and cost in the drive train at a relatively high top speed.
- The capability to prevent overloading of the gearbox or generator in pitch controlled turbines.

3.7.2.1 Variable slip generators

Usually the slip in an asynchronous generator will vary about 1% between idle and full speed. By changing the resistance in the rotor windings, it is possible to increase generator slip to e.g. 10% to cope with violent gusts of winds.

The slip is very useful in pitch controlled turbines. The pitch control is a mechanical device controlling the torque in order to prevent overloading of the gearbox and generator by pitching the wings. In fluctuating wind speeds, the reaction time for pitching the wings is critical. Increasing the slip while nearing the rated power of the turbine makes it possible for the wings to pitch. When the wings have pitched, the slip is decreased again. In the opposite situation, when wind suddenly drops, the process is applied in reverse.

3.7.2.2 Optislip®

The Optislip® is a special kind of asynchronous generator with a winded rotor and an integrated system for controlling the current in the rotor. By introducing a system called Rotor Current Controller (RCC), problems with introducing slip rings, brushes and external resistors can be avoided. The RCC unit is mounted on the generator rotor and consists of resistors, sensors and a microprocessor based control unit. An electrical control called Vestas Multi Processor controller (VMP), is placed on the generator itself. The communication between the two devices are made by using optical fibre techniques. By sending a reference current to the RCC unit and comparing it to the actual current in the rotor, the resistance can be changed continuously in order to get the required slip [14, 60]. The system is produced by Vestas but is used by some other manufactures as well.

3.7.2.3 Indirect grid connection

With indirect grid connection it is possible to let the wind turbine rotate within a wide range. On the market there are manufactures offering turbines with a slip of up to $\pm 35\%$.

If the generator is operated by variable speed, the frequency will fluctuate widely. The alternating current needs, therefore, to be transformed to match the frequency

of the public electrical grid. There are three major parts in such systems, generator, direct current (DC)-rectifier and an alternating current (AC)-inverter.

The first step is to convert the fluctuating current into DC. This can be done e.g. by using diode, thyristor or Insulated Gate Bipolar Transistor (IGBT) rectifiers. Today it seems like the IGBT rectifier is the most commonly used. An advantage with the IGBT rectifier compared to the diode rectifier is that both generator voltage and generator current can be controlled.

The DC is then inverted to AC with exactly the same frequency as the public grid. The conversion to AC can be done by using either thyristors or transistors (like the IGBT). The inverter produces different kinds of harmonics that have to be filtered before reaching the public grid [14, 37, 56].

3.7.2.4 Direct drive system

The rotational speed of a standard wind turbine generator is about 1500 revolution per minute (r.p.m.) while a typical turbine speed is 20 to 60 r.p.m. Therefore a gearbox is needed between generator and rotor. By using a low speed generator, the turbine could be directly coupled to the generator. Direct driven generators are commercially in use by e.g. Enercon and Lagerwey, Figure 3.5.

The expected benefits of direct driven systems are:

- Lower cost than a gearbox system.
- Reduced tower-head mass and nacelle length.
- Efficiency savings of several percents.

Both Enercon and Lagerwey use synchronous generators. As mentioned before, the generator speed needs to be around 20–60 r.p.m. to make the gearbox unnecessary. That requires that the number of poles have to be sufficiently large to produce a suitable output frequency. In comparison to an ordinary generator, the direct-driven generator is bigger [22, 28].

3.7.2.5 High voltage direct drive system

Windformer is an integrated system for offshore and coastal wind power generation and transmission of electricity to the high voltage grid developed by ABB. By producing high voltage directly from the generator, the need of transformation is unnecessary. Windformer is fitted with a synchronous generator with a permanent magnet rotor. The generator is directly driven which means that no gearbox is required. The ABB project is currently abandoned due to economical difficulties. However, the high voltage direct drive system technique may still be used in the future [46].

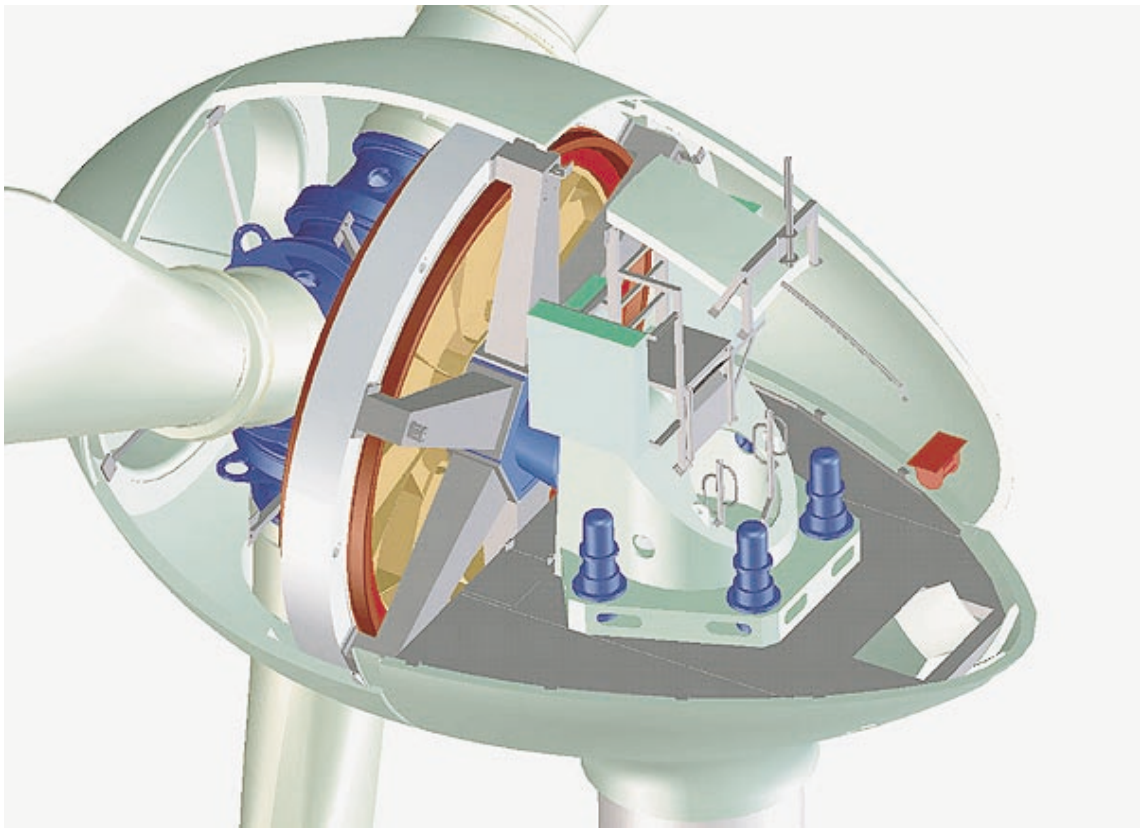

Figure 3.5: Enercon E-40 direct drive system. Reproduced from [19].

3.8 Power control

Wind turbines are designed to produce electricity as cheaply as possible. Since wind speeds rarely exceed 15 m/s, wind turbines are generally designed to yield maximum output (rated power) at a speed around 10-15 m/s (rated wind speed). As the wind speed increases past the turbines rated speed, the control mechanism of the rotor, limits the power drawn from the wind in order to keep the drive train torque constant. To avoid damage the generator and excessive mechanical stresses, the wind turbine is shut off when reaching a predetermined speed, normally about 25 m/s. Figure 3.6 shows the variation of a turbine's power output as a function of the wind speed; the graph is generally known as a power curve.

3.8.1 Pitch controlled wind turbines

On pitch regulated turbines, the blades are mounted on the rotor hub with turntable bearings. They can be turned around their longitudinal axis during operation. In high winds, the pitch setting is continuously adjusted away from stall point to reduce lift force and thereby actively adjust the generated power. As mentioned in Section 3.7.2.1, the reaction time for pitching the wings is critical in order to follow the variations in wind speed to prevent excessive peak loads. Therefore, pitch

regulation in practice requires a generator with full or partial speed, allowing a slight acceleration in rotor speed at wind gusts. The pitch mechanism is usually operated using hydraulics.

3.8.2 Stall controlled wind turbines

Passive control relies on the turbine's inherent machine characteristics, where the aerodynamic properties of the rotor limit the torque produced at high wind speeds. The geometry of the rotor blade has been designed to create turbulence on the side of the rotor blade that faces the wind, if the wind speed becomes too high. A blade is said to stall when the laminar flow over the airfoil breaks down and it loses lift. The blade on a stall-regulated turbine is slightly twisted to ensure that the stall conditions occur progressively from the blade root. The higher the wind speed, the greater the area of the blade is in stall.

The basic advantages of stall regulated wind turbines are the lack of moving parts and an active control system. However, stall regulation presents a highly complex aerodynamic design problem and related design challenges in the structural dynamics of the whole wind turbine, like stall introduced vibrations, etc.

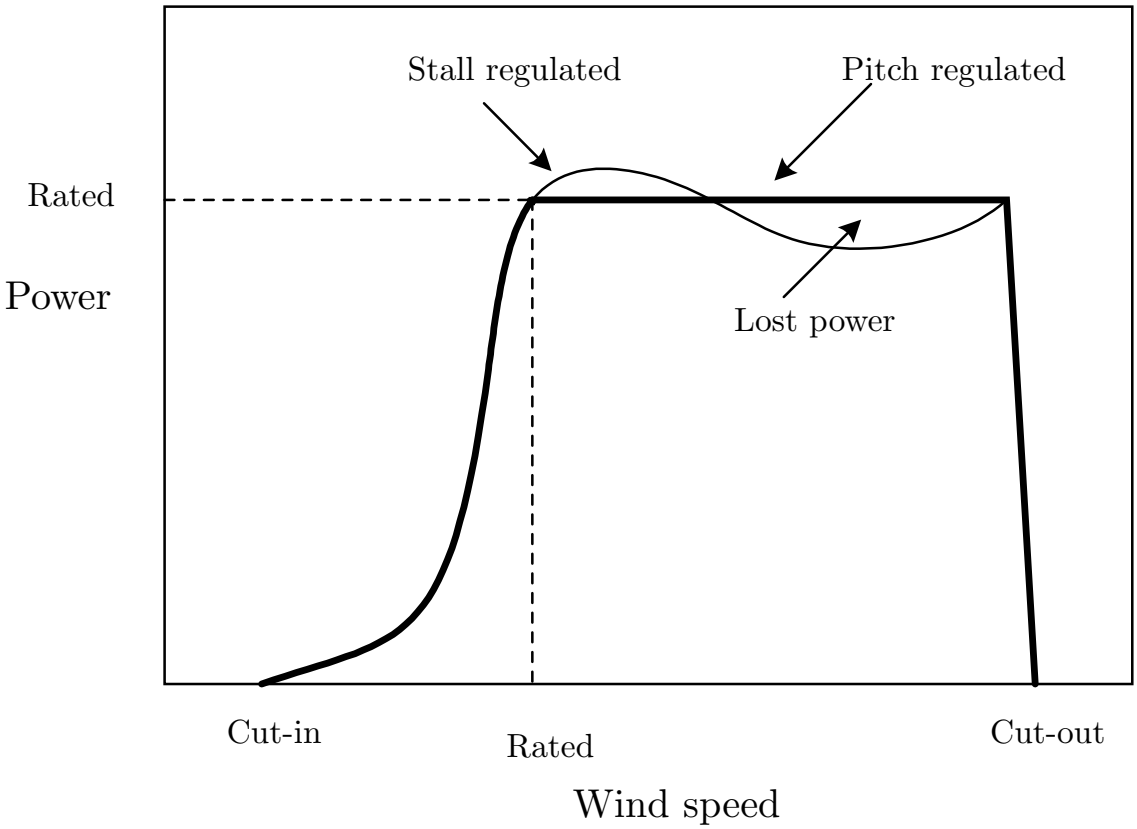

Figure 3.6: Power curves for stall and pitch regulated machines.

3.8.3 Active stall controlled wind turbines

Active stall is a combination of the two above mentioned methods for power limitation. In low and medium wind speeds the pitch method is used to yield maximum power output at any given wind speed. However, the actual power limitation in high wind speeds is obtained by using the stall phenomena. When the rated power is reached, the blades are adjusted to a more negative pitch setting in the opposite direction from the normal pitch regulation method. By adjusting the pitch setting in the negative direction, stall occurs at exactly the power level decided. The benefits is that the power level can be maintained at a constant level with a simple constant speed generator when exceeding rated wind speed.

3.8.4 Other control mechanisms

Some older machines use ailerons to control the power of the rotor. Aileron control is common in aircraft for take-off and landing. However, the use of ailerons in modern wind turbines is not very common.

3.9 Gearbox

The gearbox is required to slow rotational speed of the shaft for several reasons. The speed of the blade is limited by efficiency and also by limitations in the mechanical properties of the turbine and supporting structure. The gearbox ratio depends on the number of poles and the type of generator. As mentioned in Section 3.7.2.4, there are direct driven generators. A direct driven generator would require a generator with 600 poles to generate electricity at 50 Hz. A fixed speed generator generally has a gearbox ratio of 50:1 to give accurate frequency.

Wind turbine gearboxes have been developed for quiet operation. One way to keep the noise down is to produce the steel wheels of the gearbox with a semi-soft, flexible core and with a hard surface to ensure strength and long time wear. It is done by heating the gear wheels after their teeth have been ground, and then let them cool off slowly while they are packed in a special high carbon-content powder. The carbon will be transferred to the gear wheel teeth surfaces. This ensures a high carbon content and high durability in the surface of the metal, while the steel alloy in the interior remains softer and more flexible.

Chapter 4

Trends and statistics

This chapter presents a review of today's suppliers and the design concepts that are used. The idea is to see if there are any specific concept trends and, if possible, trends that are depending on the size of the turbine.

4.1 Suppliers

European wind turbine manufacturers have dominated the market the last years. According to [22], 1292 wind turbine installations were recorded in 1996 and out of them 80% were supplied from European manufacturers. Table 4.1, based on [6], show the top-ten suppliers ranked by sold MW in 1999.

Table 4.1: Top-ten list of suppliers 1999 [6].

Manufacturer	**Sold MW 1999**	**Share 1999**	**Accu. MW 1999**	**Share accu. %**	**Origin**
Neg-Micon	761	19.4%	3034	21.8%	Denmark
Vestas	652	16.6%	2530	18.2%	Denmark
Gamesa	494	12.6%	853	6.1%	Spain
Enercon	488	12.5%	1553	11.1%	Germany
Enron (Zond/Tacke)	360	9.2%	1153	8.3%	USA, Germany
Bonus	338	8.6%	1197	8.6%	Denmark
Nordex	306	7.8%	638	4.6%	Denmark Germany
MADE	218	5.6%	450	3.2%	Spain
Ecotecnia	59	1.5%	136	1.0%	Spain
DeWind	58	1.5%	86	0.6%	Germany
Others	298	4.7%	2839	15.3%	
Sum	4032	100%	14469	100%	

4.2 Trends

In the following section, wind turbines of manufacturers, Table 4.1, are divided into four power classes: 600–999, 1000–1299, 1300–1999 and 2000–2500 kW. See Tables 4.2–4.5 for machines commercially available in the summer of 2000. The point is to clarify if different design solutions are depending on the size of the turbine. Out of the ten manufacturers listed, seven of them will be discussed further, namely *Neg-Micon, Vestas, Enercon, Tacke, Bonus, Nordex* and *DeWind*. The three other *Gamesa, MADE* and *Ectotecnia* are not discussed due to difficulties in finding information. The number of installed turbines are dominated, in terms of world-wide installed capacity, by units rated around 100–600 kW. However, the size range seems to be out of date and therefore the classification starts at 600 kW.

Table 4.2: Product range 600–999 kW.

Operation class 600–999 kW						
Type	**Rated power (kW)**	**Rotor dia. (m)**	**Hub height (m)**	**Nacelle weight (metric tonnes)**	**Control**	**Speed**
Neg-Micon NM60043/48	600	43/48	40/46/56 60/70	-	Stall	Two speed
Neg-Micon NM75044/48	750	44/48	40/45/50 55/60/70	-	Stall	Two speed
Neg-Micon NM90052	900	52.2	44/49/55 60/70	40	Stall	Two speed
Vestas V47	660	47	40/45/50 55	42	Pitch	Variable (10%)
Vestas V47	660/200	47	40/45/50 55/60/65	-	Pitch	Two generators, variable (10%)
Vestas V52	850	52	44/49/55 60/65	32	Pitch	Variable (60%)
Enercon E40	600	44	46/50/55 58/65/78	30.7	Pitch	Variable, multi-poled ring generator
Enron/Tacke 750i	750	46/48/50	55/65	-	Pitch	variable
Bonus MkIV	600	44	40/45/50 60	36.7	Stall	Two speed
Nordex N43	600	43	40/46/50 60	35.5	Stall	Two speed
Nordex N50	800	50	46/50/70	35.4	Stall	Two speed
DeWind D4	600	46/48	40/55/60 70	-	Pitch	variable (±35%)

Table 4.3: Product range 1000–1299 kW.

Operation class 1000–1299 kW						
Type	**Rated power (kW)**	**Rotor dia. (m)**	**Hub height (m)**	**Nacelle weight (metric tonnes)**	**Control**	**Speed**
Neg-Micon NM100060	1000	60	59/70	-	Stall	Two speed
Enercon E58	1000	58	70	92	Pitch	Variable, multi-poled ring generator
Bonus 1 MW	1000	54.2	45/50/60 70	69.1	Active stall	Two speed
Nordex N54	1000	54	60/70	80.1	Stall	Two speed
DeWind D6	1000	60/62/64	69/92	-	Pitch	Variable (±35%)
DeWind D6	1250	60/62/64	56/65/69 92	-	Pitch	variable (±35%)

Table 4.4: Product range 1300–1999 kW.

Operation class 1300–1999 kW						
Type	**Rated power (kW)**	**Rotor dia. (m)**	**Hub height (m)**	**Nacelle weight (metric tonnes)**	**Control**	**Speed**
Neg-Micon NM1500C64	1500	64	60/68/80	75	Stall	Two speed
Vestas V66	1650	66	60/67/78	78	Pitch	Variable (10%)
Vestas V66	1750	66	60/67/78	80	Pitch	Variable (60%)
Enercon E66	1500	66	65/67/85 98	97.4	Pitch	Variable, multi-poled ring generator
Enercon E66	1800	70	65/67/85 98	101.1	Pitch	Variable, multi-poled ring generator
Enron/Tacke TW 1.5	1500	65/71/77	61/65/80 85/100	74	Pitch	Variable (±30%)
Bonus 1.3 MW	1300	62	45/49/68	80.9	Active stall	Two speed
Nordex N60	1300	60	46/50/60 65/69	87.1	Stall	Two speed

Table 4.5: Product range 2000–2500 kW.

Operation class 2000–2500 kW						
Type	**Rated power (kW)**	**Rotor dia. (m)**	**Hub height (m)**	**Nacelle weight (metric tonnes)**	**Control**	**Speed**
Neg-Micon NM200072	2000	72	-	114	Active stall	Two speed
Vestas V66	2000	66	60/67/78	80	Pitch	Variable (60%)
Vestas V80	2000	66	60/67/78 100	94	Pitch	Variable (60%)
Enron/Tacke TW 2.0	2000	70.5	65	-	Pitch	Variable (±30%)
Bonus 2 MW	2000	76	60/68	135	Active stall	Two speed
Nordex N80	2500	80	60/80	138.6	Pitch	Variable

The tables show that the manufacturers offer wide ranges of configurations. In some cases, manufacturers offer tower heights in a 40 m span to suit specific wind and landscape conditions. Figure 4.1 shows the number of power control methods in the rated power classes. For turbines below 1300 kW the frequency for stall, see Section 3.8.2, and pitch control, see Section 3.8.1, are about the same. Between 1300–1999 kW pitch regulation is the dominating one and for turbines with rated power over 2000 kW, stall regulation is not used at all. Active stall power controlled machines, see Section 3.8.3, can be found from 1000 kW and up. For turbines over 2000 kW the active stall control is almost as common as the pitch control. An interesting fact is that *Neg-Micon*, which company supplies turbines in all classes, uses stall regulation in class 1–3 and active stall regulation in class 4. Concern about power quality of stall regulated machines may be the reason for changing their design feature in the megawatt class. Increased interest in variable speed coupled with the uncertainty about how the variable speed stall control mechanism will operate is another explanation for the lack of stall regulated machines at large scale. As explained in Section 3.7, a wind turbine may be designed for either constant or variable speed. Figure 4.2 shows the different speed operation modes for the classes. There are no big differences between the use of two speed or variable speed design. The variable speed operation is generally obtained by using some kind of slip device or with indirect grid connection. *Enercon* is the only one of the mentioned companies that uses a direct drive system, their products reaches from 600–1800 kW.

In Figures 4.3 and 4.4, the weight to swept area ratio is compared between the manufacturers. It is difficult to see any clear differences between ratio in relation to kW size, Figure 4.3. However, it seems like turbines with rated power around 1000–1500 kW have a higher weight to swept area ratio than the others. The explanation is probably that this specific class represents the basis for bigger turbines built on the same concept. Figure 4.4 shows that there are no big differences in weight to swept area ratio between the producers of the wind turbines.

In Figures 4.5 and 4.6 the weight to power ratio is compared. Figure 4.5 shows that

turbines with rated power around 1000–1500 kW have a higher ratio than the other turbines. The explanation is the same as mentioned previously. The other machines show no big differences compared to each other. When comparison is made between manufacturers, the direct driven *Enercon E-66* is the heaviest and *Vestas V52* the lightest per rated kilowatt.

In Figures 4.9 and 4.10, the weights for the nacelle including rotor, m, are plotted as a function of rated power, P. The function is, when all turbines are included from Tables 4.2–4.5, represented as a power function. The data gives, $m = 0.090P^{0.93}$. In other words, the relation between weight and rated power seems to follow an nearly linear path. When different design solutions are compared, the power exponent varies between 0.87 and 1.22. However, there are too few data given in each specific design class to draw any certain conclusions.

The variation of wind speed is often represented by a power law with exponent α, where α is the surface roughness exponent. Empirical results indicate that the 1/7 power law fits many sites around the world [26]. According to [22], the power output of geometrically similar wind turbines will then be scaled with diameter, D, as $D^{(2+3\alpha)}$. The rated power is then depending on the diameter as $D^{2.43}$. Figures 4.7 and 4.8 indicate that such is the case. When all wind turbines listed in Tables 4.2–4.5 are included, the rated power, P depends on the diameter D as, $P = 0.070D^{2.40}$. The figures also include functions for different power control methods and speed operations to see if there are any differences between different design solutions. The only obvious observation is that stall regulation yields higher output for a given rotor diameter.

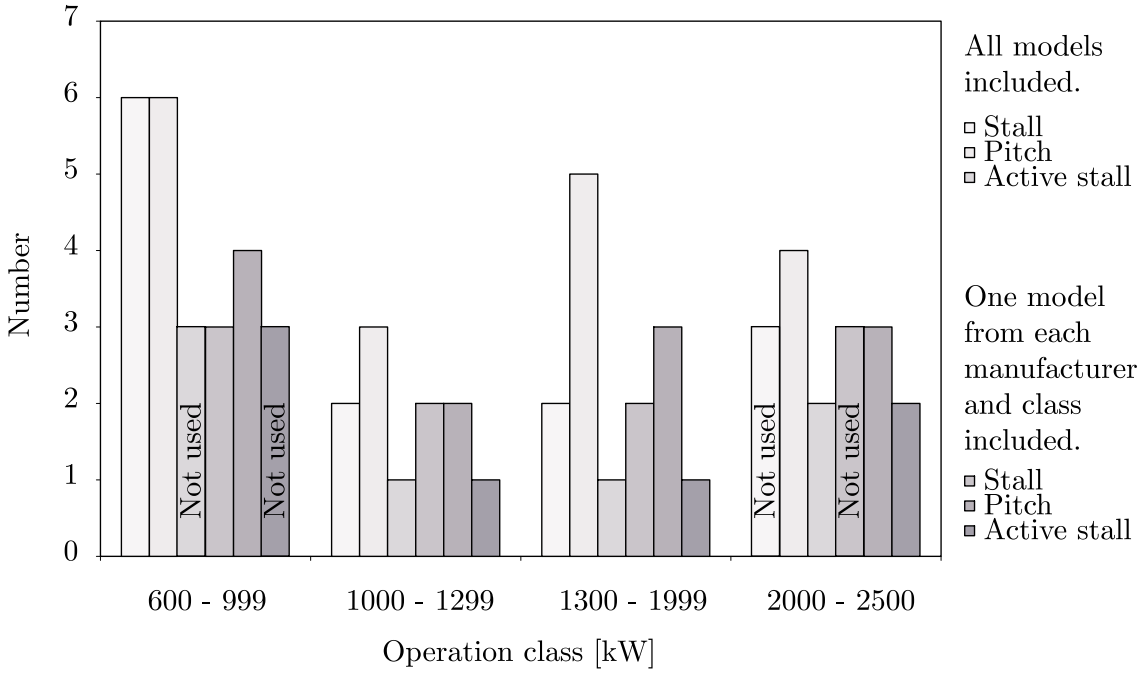

Figure 4.1: Number of power control methods in the 600–999, 1000–1299, 1300–1999 and the 2000–2500 kW classes.

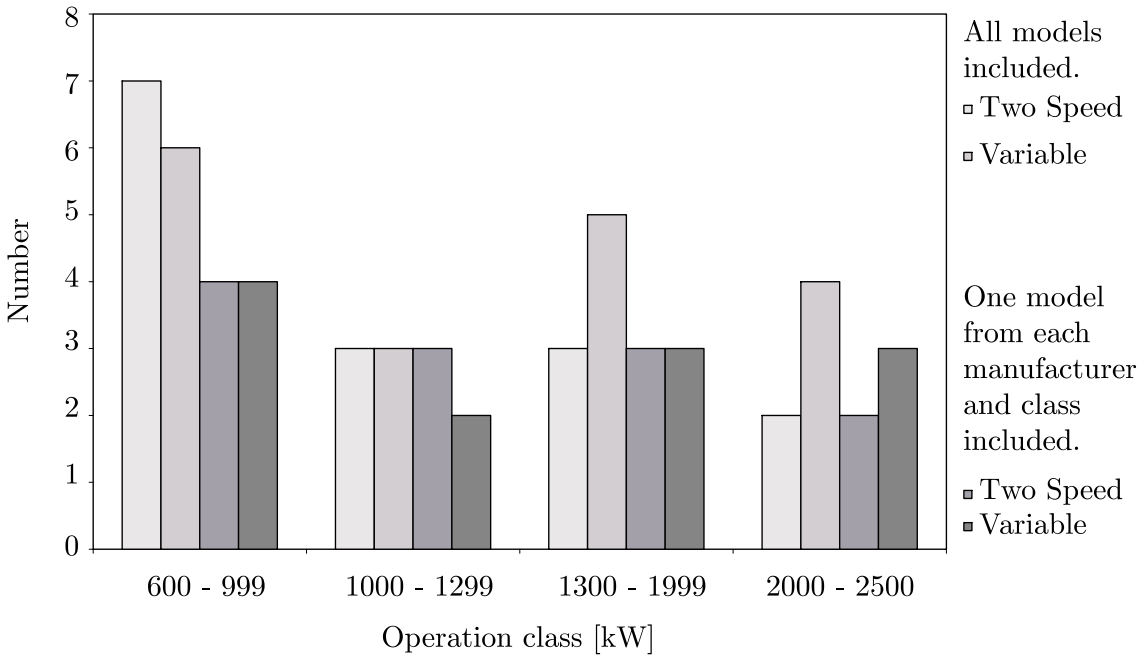

Figure 4.2: Number of speed operation modes in the 600–999, 1000–1299, 1300–1999 and the 2000–2500 kW classes.

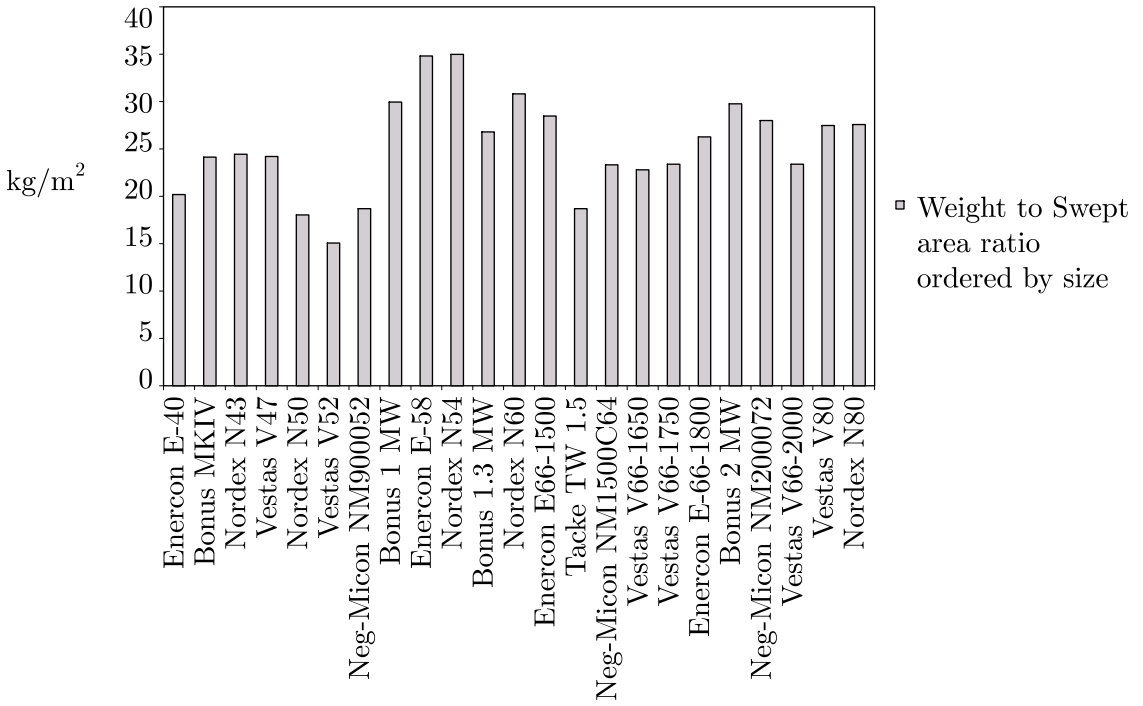

Figure 4.3: Weight to swept area ratio, manufacturers ordered by kW size.

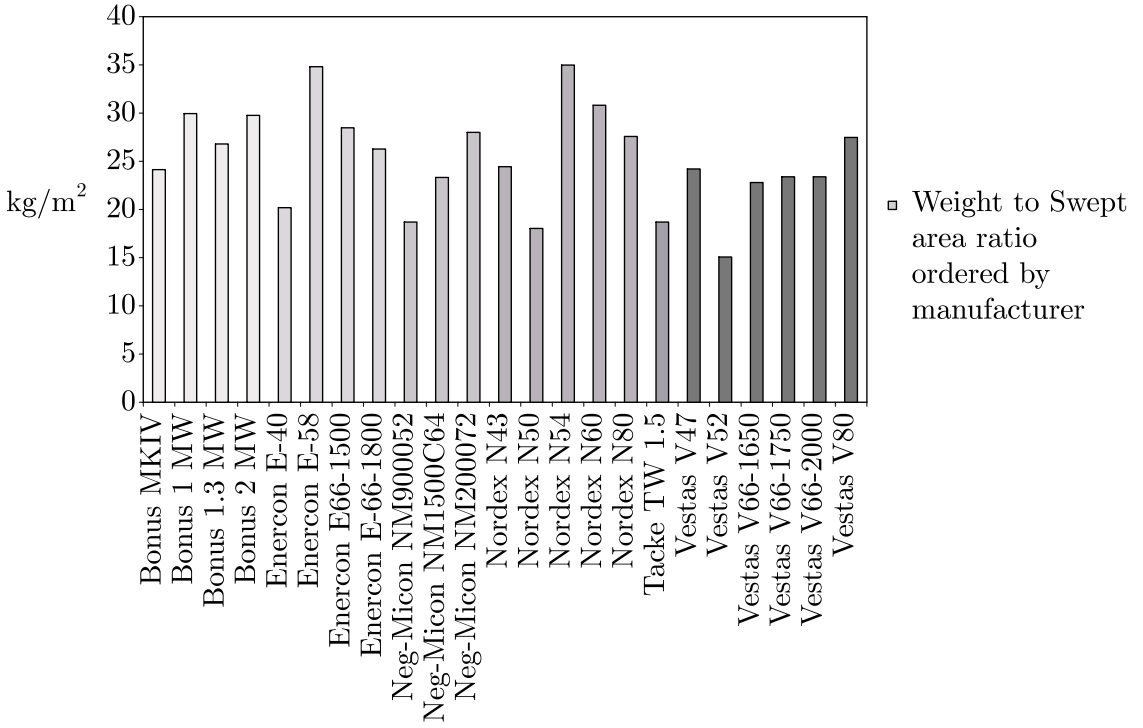

Figure 4.4: Weight to swept area ratio, manufacturers in alphabetical order.

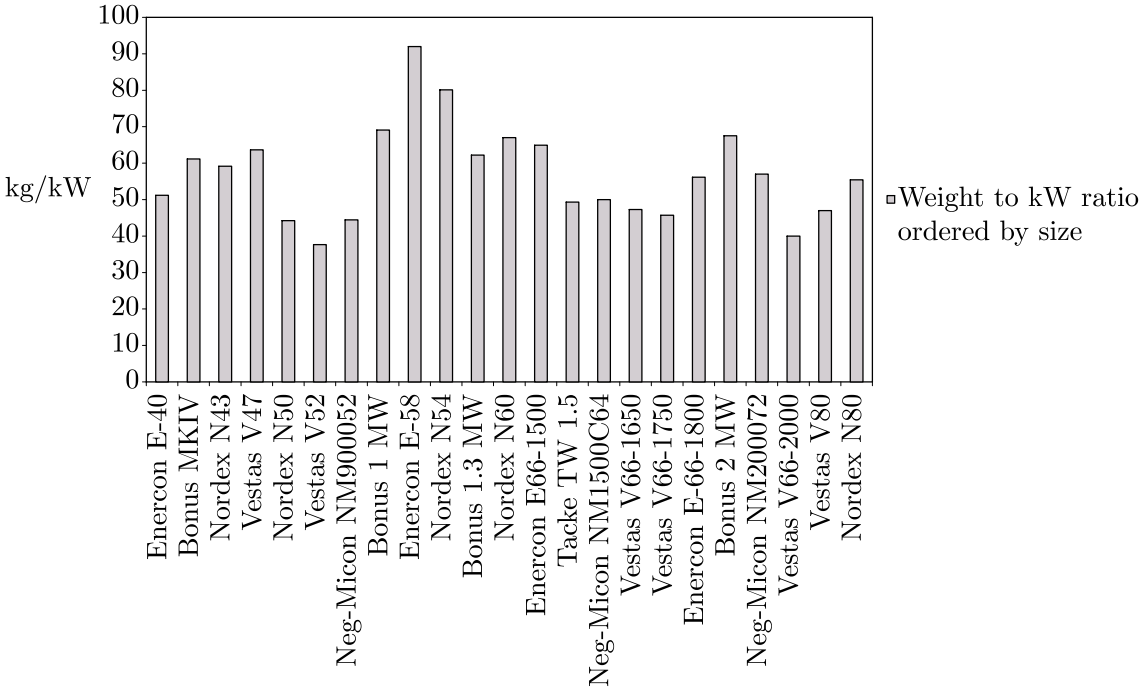

Figure 4.5: Weight to Power ratio, manufacturers ordered by power.

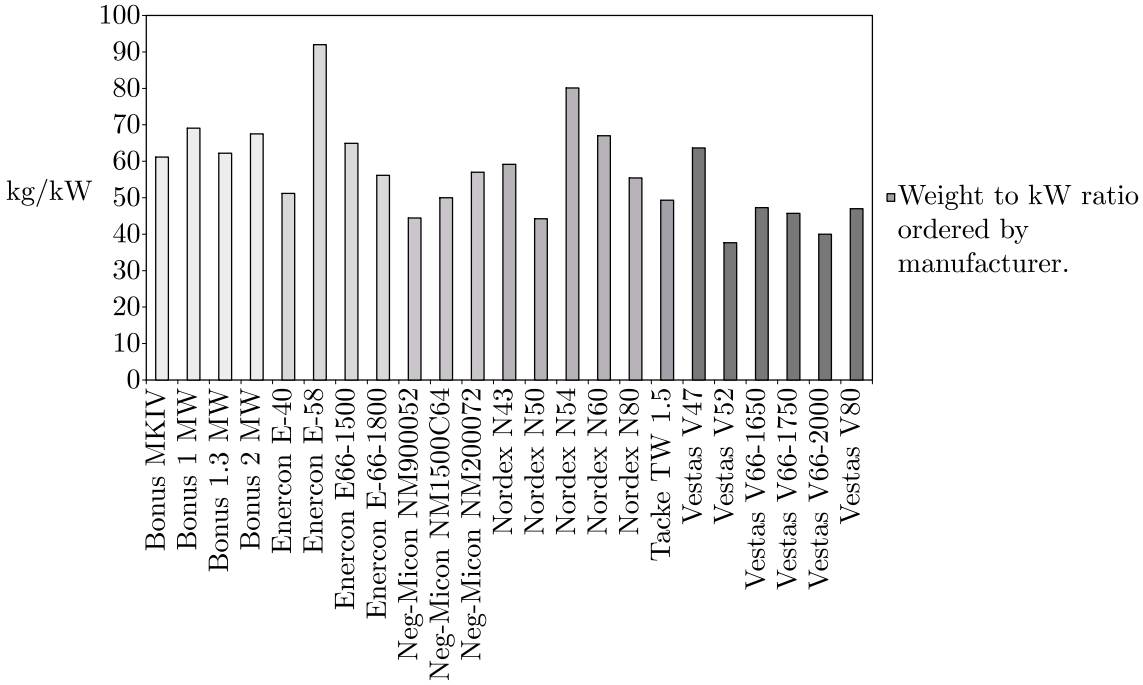

Figure 4.6: Weight to power ratio, manufacturers in alphabetical order.

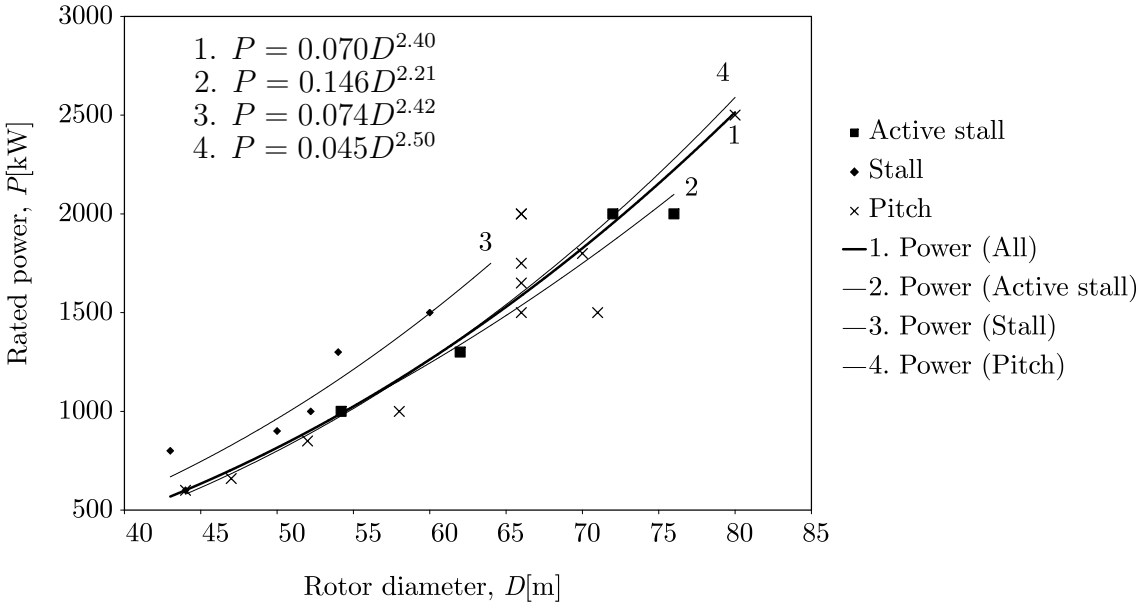

Figure 4.7: Rated power as a function of rotor diameter for different control mechanism types.

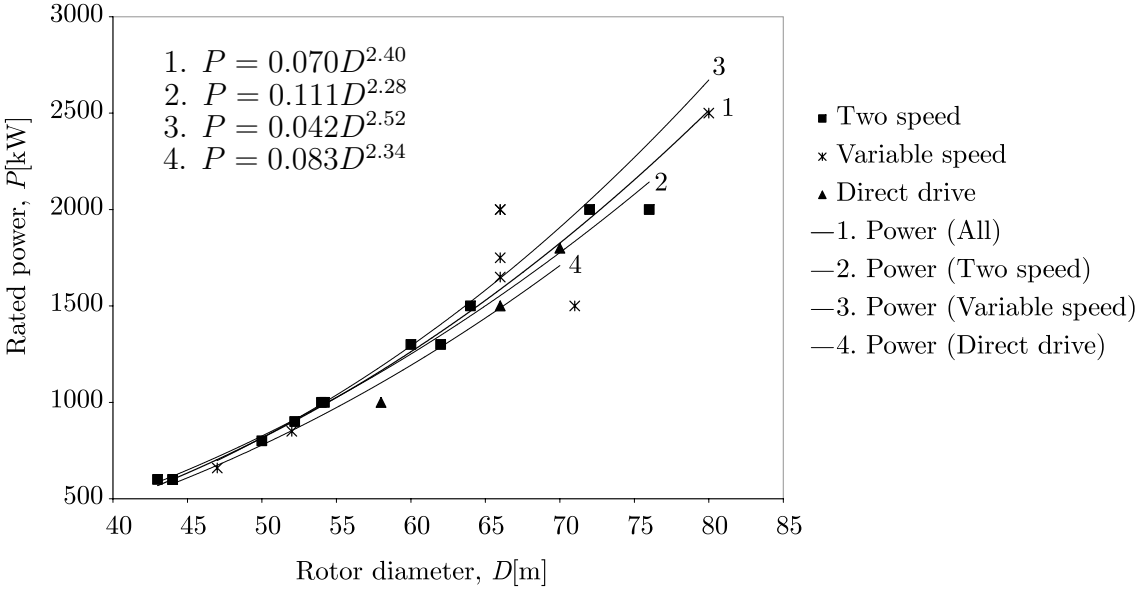

Figure 4.8: Rated power as a function of rotor diameter for different speed operation types.

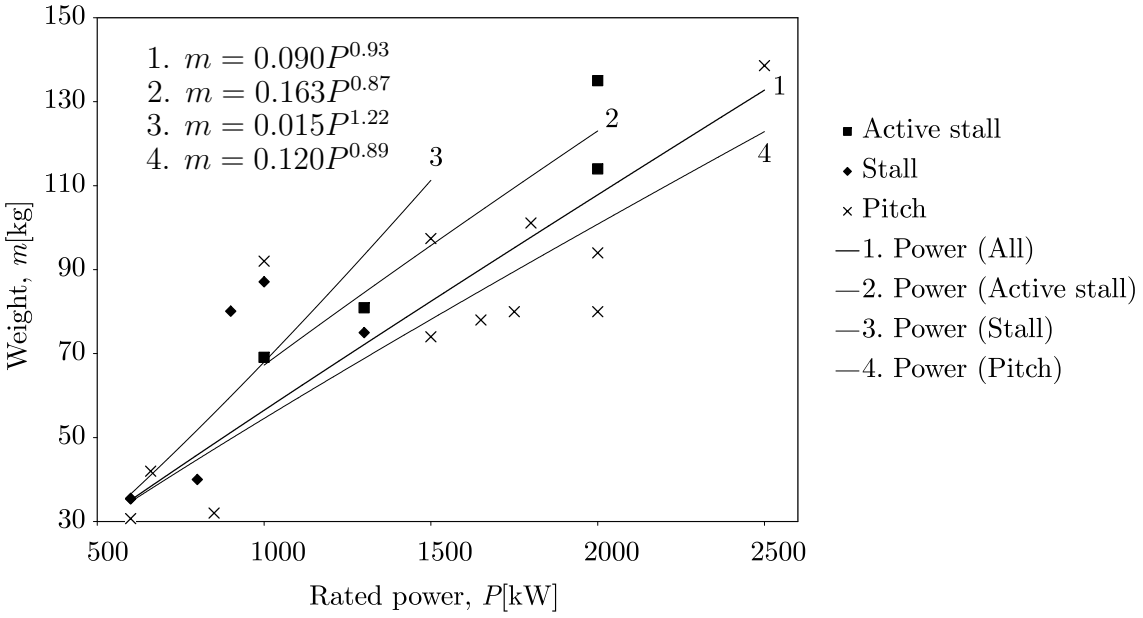

Figure 4.9: Nacelle (rotor included) mass as a function of rated power for different control mechanism types.

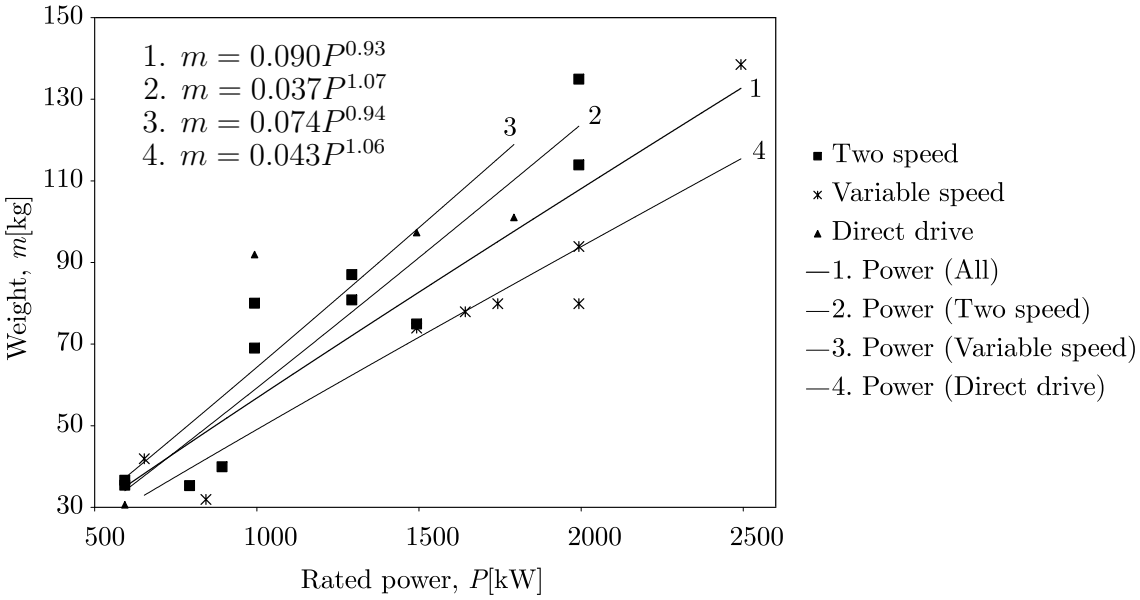

Figure 4.10: Nacelle (incl. rotor) mass as a function of rated power for different speed operation types.

Chapter 5

Wind turbine design calculations

5.1 Introduction

Wind energy technology has developed rapidly over the last 10 years. Larger machines as well as new design trends are introduced, which demands more sophisticated design tools, capable of providing more accurate predictions of loads. The need and interest of placing wind turbines in complex terrain areas has increased. In such sites, high wind speed, high turbulence levels and strong gusts are frequently present. The weather conditions need careful consideration as they are suspected to seriously affect the reliability of the wind turbines. In order to back-up further exploitation of wind energy it is important to provide the industry and the certifying institutions with computational tools capable of performing complete simulations of the behaviour of wind turbines over a wide range of different operational conditions [58].

5.2 Present wind turbine design codes

A number of design codes have been used over the last ten years to model the wind turbine's dynamic behaviour, or to carry out design calculations [44, 49].

In the wind energy community, the following wind turbine design codes are commonly used. A short description and the features of the design codes will be presented.

- ADAMS/WT (Automatic Dynamic Analysis of Mechanical Systems – Wind Turbine). ADAMS/WT is designed as an application-specific add-on to ADAMS/SOLVER and ADAMS/View. The ADAMS package is developed by Mechanical Dynamics, Inc., and the add-on module WT is developed under contract to the National Renewable Energy Laboratory (NREL) [48].
- BLADED for Windows. BLADED for Windows is an integrated simulation package for wind turbine design and analysis. The software is developed by

Garrad Hassan and Partners, Ltd. The Garrad Hassan approach to the calculation of wind turbine performance and loading has been developed over the last fifteen years and has been validated against monitored data from a wide range of turbines of many different sizes and configurations [25].

- DUWECS (Delft University Wind Energy Converter Simulation Program). DUWECS has been developed at the Delft University of Technology with financial support from the European Community. The program has been improved in order to make DUWECS available for simulating offshore wind turbines. Lately the code has been extended to incorporate wave loads, and a more extensive soil model [36].

- FAST (Fatigue, Aerodynamics, Structures, and Turbulence). The FAST code is being developed through a subcontract between National Renewable Energy Laboratory (NREL) and Oregon State University. NREL has modified FAST to use the AeroDyn subroutine package developed at the University of Utah to generate aerodynamic forces along the blade. This version is called FAST-AD [65].

- FLEX4 The code is developed at the Fluid Mechanics Department at the Technical University of Denmark. The program simulates, e.g., turbines with one to three blades, fixed or variable speed generators, pitch or stall power regulation. The turbine is modelled with relatively few degrees of freedom combined with a fully nonlinear calculation of response and loads [47].

- FLEXLAST (Flexible Load Analysing Simulation Tool). The development of the program started at Stork Product Engineering in 1982. Since 1992, FLEXLAST has been used by Dutch industries for wind turbine and rotor design. The program has also been used for certification calculations by a number of foreign companies [62].

- FOCUS (Fatigue Optimization Code Using Simulations). FOCUS is an integrated program for structural optimization of turbine blades. It is the outcome from a cooperation between Stork Product Engineering, the Stevin Laboratory and the Institute for Wind Energy, Netherlands. FOCUS consists of four main modules, SWING (stochastic wind generation), FLEXLAST (calculation load time cycles), FAROB (structural blade modelling) and Graph (output handling).

- GAROS (General Analysis of Rotating Structures). GAROS is a general purpose program for the dynamic analysis of coupled elastic rotating and non-rotating structures with special attention to horizontal-axis wind turbines. The program is developed by Aerodyn Energiesysteme, GmbH [44].

- GAST (General Aerodynamic and Structural Prediction Tool for Wind Turbines). GAST is developed at the fluid section, of the National Technical University of Athens. The program includes a simulator of turbulent wind fields, time-domain aeroelastic analysis of the full wind turbine configuration and post-processing of loads for fatigue analysis [58].

- PHATAS-IV (Program for Horizontal Axis Wind Turbine Analysis Simulation, Version IV). The PHATAS programs are developed at ECN Wind Energy of the Netherlands Energy Research Foundation. The program is developed for the design and analysis of on-shore and offshore horizontal axis wind turbines. The program include, e.g., a model for wave loading [39].

- TWISTER. The program is developed at Stentec B.V. The development of the aeroelastic computer code of Stentec was started in 1983 and was called FKA. For commercial reasons, the name has been changed to TWISTER in 1997. Since 1991 the code supports stochastic windfield simulation and has been used for the development and certification of a number of wind turbines, mainly from Dutch manufacturers, like Lagerwey, DeWind and Wind Strom Frisia [54].

- VIDYN. VIDYN is a simulation program for static and dynamic structural analysis for horizontal axis wind turbines. The development of VIDYN began in 1983 at Teknikgruppen AB, Sollentuna, Sweden, as a part of a evaluation project concerning two large Swedish prototypes: Maglarp and Näsudden [24].

- YawDyn. YawDyn is developed at the Mechanical Engineering Department, University of Utah, US with support of the National Renewable Energy Laboratory (NREL), National Wind Technology Center. YawDyn simulates e.g. the yaw motions or loads of a horizontal axis wind turbine, with a rigid or teetering hub. In 1992, the aerodynamics analysis subroutines from YawDyn were modified for use with the ADAMS program, which is mentioned above [29].

The benefits with the developed simulation tool is described in Chapter 7.

5.3 Wind field representation

It is very important for the wind industry to accurately describe the wind. Turbine designers need the information to optimize the design of their turbines and turbine investors need the information to estimate their income from electricity generation. As is well known, the highest wind velocities are generally found on hill tops, exposed coasts and out at sea. Various parameters need to be known concerning the wind, including the mean wind speed, directional data, variations about the mean in the short term (gusts), daily, seasonal and annual variations, and variations with height. These parameters are highly site specific and can only be determined with sufficient accuracy by measurements at a particular site over a sufficiently long period.

From the point of view of wind energy, the most striking characteristic of the wind resource is its variability. The wind is changing both geographically and temporally. Furthermore, this variability persists over a wide range of time scales, both in space and time, and the importance of this is amplified by the cubic relationship to the available power [42].

There are many computer programs available to numerically simulating the fluctuating wind fields. A review of the underlying theory will not be presented in this thesis. However, a relatively detailed description is given in e.g. [7].

5.4 Rotor aerodynamics

Various methods can be used to calculate the aerodynamic forces acting on the blades of a wind turbine. The most advanced are numerical methods solving the Navier-Stokes equations for the global compressible flow as well as the flow near the blades. The two major approaches to calculating the forces are the *Actuator Disc Model* and the *Blade Element Model*. In the following two sections a brief introduction to the above mentioned methods will be presented. The introduction will focus on the qualitative results and the basic assumptions that is made.

5.4.1 Actuator disc model

The actuator disc model is based on Bernoulli's equation and energy balances [18,34].

Suppose that the rotor is replaced by an actuator disc, through which the static pressure decreases discontinuously. By examining the flow through a control volume, the extractable power from the turbine can be calculated, Figure 5.1.

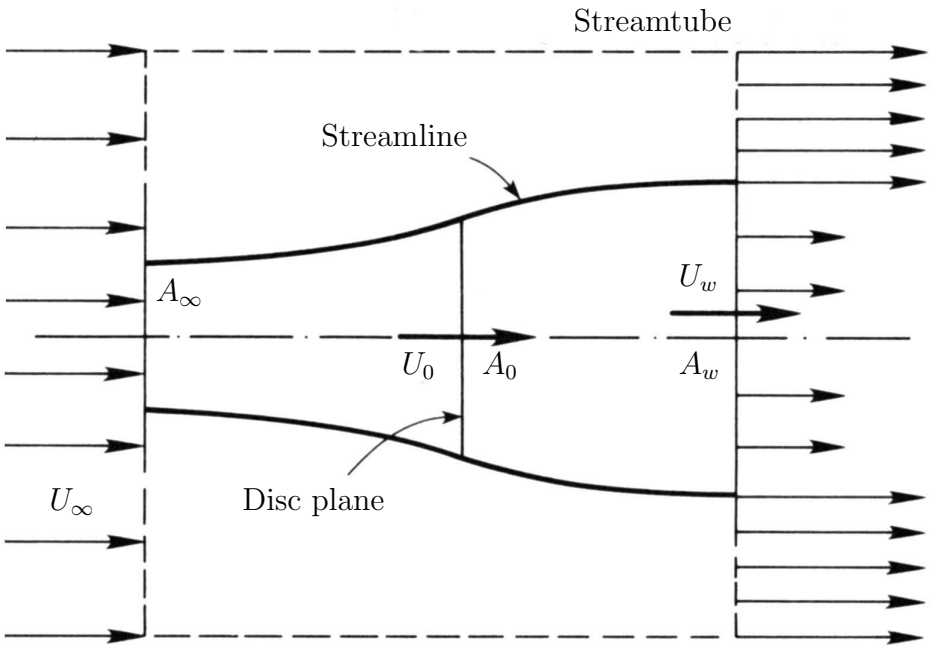

Figure 5.1: Flow pattern inside the streamtube. Reproduced from [17].

The streamtube has a cross-sectional area smaller than the cross-sectional area for the upstream disc and a larger area than the downstream disc. Within the streamtube, continuity is required and the rate of the mass flow must be constant.

$$\dot{m} = |\rho_\infty A_\infty U_\infty| = |\rho_0 A_0 U_0| = |\rho_w A_w U_w| \tag{5.1}$$

By introducing an axial interference factor, a, as the fractional decrease in wind velocity between the free stream and the rotor plane represented by

$$a = \frac{v}{U_\infty} \tag{5.2}$$

it is found that

$$U_0 = U_\infty(1-a) \tag{5.3}$$

The air which passes through the disc undergoes an overall change in velocity. The velocity multiplied by the flow rate gives the rate of change of momentum, more known as a force

$$T = \dot{L} = \dot{m}(U_\infty - U_w) \tag{5.4}$$

Combining the equations above with the fact that the change of momentum comes entirely from the pressure difference across the actuator disc, it is obtained that

$$p_0^+ - p_0^- = (U_\infty - U_w)\rho_0 A_0 (1-a) U_\infty \tag{5.5}$$

To obtain the pressure difference, the Bernoulli´s equation is applied separately to the upstream and downstream section of the streamtube. For the upstream section it becomes

$$\frac{1}{2}\rho U_\infty^2 + p_\infty = \frac{1}{2}\rho U_0^2 + p_0^+ \tag{5.6}$$

Similary, downstream

$$\frac{1}{2}\rho U_w^2 + p_\infty = \frac{1}{2}\rho U_0^2 + p_0^- \tag{5.7}$$

Subtracting (5.6) from (5.7) yields

$$p_0^+ - p_0^- = \frac{1}{2}\rho(U_\infty^2 - U_w^2) \tag{5.8}$$

Equation (5.8) and (5.5) gives

$$U_w = (1-2a)U_\infty \tag{5.9}$$

The force, T, is obtained by substituting (5.9), (5.3) and (5.1) into (5.4), which gives

$$T = 2\rho A_0 U_\infty^2 a(1-a) \tag{5.10}$$

Combining (5.3), (5.9) and the rate of work done by the force, $P = TU_0$, the power extraction from the air is obtained as

$$P = 2\rho A_0 U_\infty^3 a(1-a)^2 \tag{5.11}$$

or, by introducing the dimensionless power-coefficient, $C_P = 4a(1-a)^2$,

$$P = \frac{1}{2}\rho A_0 U_\infty^3 C_P \tag{5.12}$$

The power-coefficient represents the efficiency of the turbine, which depends on variables like the wind speed, the rotor speed and the pitch angle. The coefficient shows how much of the kinetic energy in the air stream that is transformed into mechanical energy. The maximum C_P as a function of a is $C_P = 16/27 \approx 0.59$, at $a = 1/3$.

5.4.2 Blade element theory

For the use of aeroelastic codes in design calculations, the aerodynamic method has to be very time efficient. The Blade Element Momentum (BEM) theory, has been shown to give good accuracy with respect to time cost.

In this method, the turbine blades are divided into a number of independent elements along the length of the blade. At each section, a force balance is applied involving 2D section lift and drag with the thrust and torque produced by the section. At the same time, a balance of axial and angular momentum is applied. This produces a set of non-linear equations which can be solved numerically for each blade section. The description follows [30, 34].

In Section 5.4.1, only the force in the flow direction was regarded. The BEM theory also takes notice of the tangential force due to the torque in the shaft. The lift force L per unit length is perpendicular to the relative speed V_{rel} of the wind and equals

$$L = \frac{\rho c}{2} V_{\text{rel}}^2 C_L \tag{5.13}$$

where c is the blade cord length. The drag force D per unit length, which is parallel to V_{rel} is given by

$$D = \frac{\rho c}{2} V_{\text{rel}}^2 C_D \tag{5.14}$$

Since we are interested only in the forces normal to tangential to the rotor-plane, the lift and drag are projected on these directions, Figure 5.2.

$$F_N = L\cos\phi + D\sin\phi \tag{5.15}$$

and

$$F_T = L\sin\phi - D\cos\phi \tag{5.16}$$

The theory requires information about the lift and drag aerofoil coefficients C_L and C_D. Those coefficients are generally given as functions of the angle of incidence, Figure 5.3.

$$\alpha = \phi - \theta \tag{5.17}$$

Further, it is seen that

$$\tan\phi = \frac{(1-a)U_\infty}{(1+a')\omega r} \tag{5.18}$$

In practice, the coefficients are obtained from a 2D wind-tunnel test. If α exceeds about 15°, the blade will stall. This means that the boundary layer on the upper surface becomes turbulent, which will results in a radical increase of drag and a decrease of lift. The lift and drag coefficients need to be projected onto the NT-direction.

$$C_N = C_L \cos\phi + C_D \sin\phi \tag{5.19}$$

and

$$C_T = C_L \sin\phi - C_D \cos\phi \tag{5.20}$$

Further, a solidify σ is defined as the fraction of the annular area in the control volume, which is covered by the blades

$$\sigma(r) = \frac{c(r)N}{2\pi r} \tag{5.21}$$

where N denotes the number of blades.

The normal force and the torque on the control volume of thickness $\mathrm{d}r$, is since F_N and F_T are forces per length

$$\mathrm{d}T = NF_N\mathrm{d}r = \frac{1}{2}\rho N\frac{U_\infty^2(1-a)^2}{\sin^2\phi}cC_N\mathrm{d}r \tag{5.22}$$

and

$$\mathrm{d}Q = rNF_T\mathrm{d}r = \frac{1}{2}\rho N\frac{U_\infty(1-a)\omega r(1+a')}{\sin\phi\cos\phi}cC_t r\mathrm{d}r \tag{5.23}$$

Finally, the two induction factors are declared by

$$a = \frac{1}{\dfrac{4\sin^2\phi}{\sigma C_N} + 1} \tag{5.24}$$

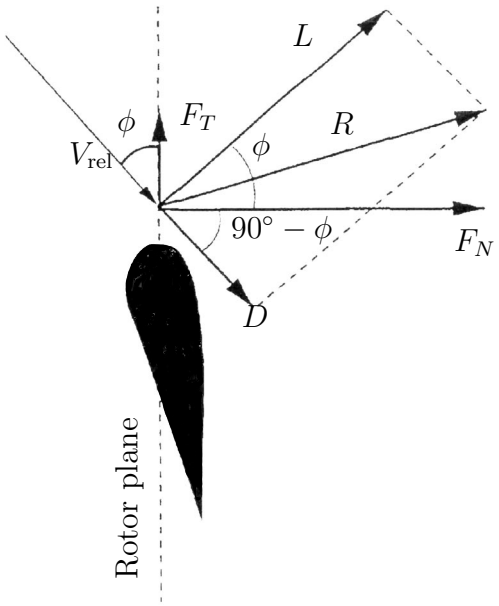

Figure 5.2: The local forces on the blade. Reproduced from [30].

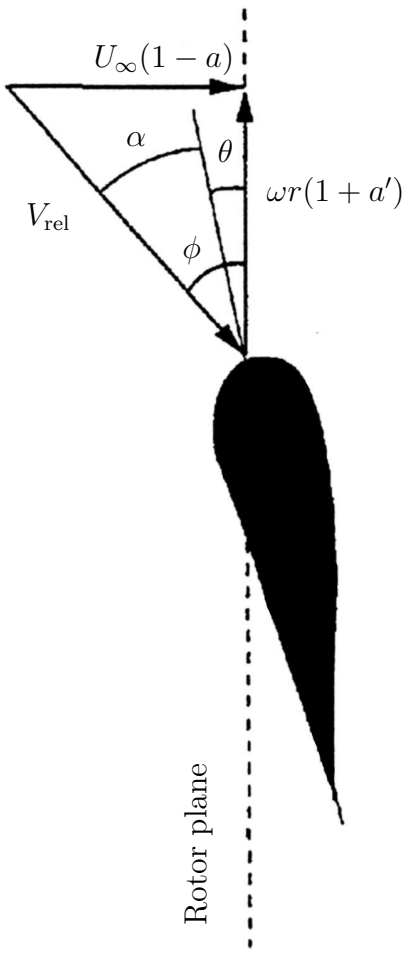

Figure 5.3: Velocities at the rotorplane. Reproduced from [30].

and

$$a' = \frac{1}{\frac{4\sin\phi\cos\phi}{\sigma C_T} - 1} \tag{5.25}$$

All necessary equations have now been derived for the BEM model. Since the different control volumes are assumed to be independent, each strip may be treated separately and therefore the results for one radius can be computed before solving for another radius. For each control volume, the algorithm can be divided into eight steps:

1. Initialize a and a', typically $a = a' = 0$.
2. Compute the flow angle, ϕ, using (5.18).
3. Compute the local angle of attack using (5.17).

4. Read $C_L(\alpha)$ and $C_D(\alpha)$ from the aerofoil data table.
5. Compute C_N and C_T from (5.19) and (5.20).
6. Calculate a and a' from (5.24) and (5.25).
7. If a and a' has changed more than a certain tolerance: goto step 2, else continue.
8. Compute the local forces on each element of the blades.

In a FEM point of application, the loads of each blade element are transformed to respective node in the FEM model. It is of course possible to use more elements in the BEM method, compared to the FEM model, and then integrate the loads to the available FEM node.

This is, in principle, the BEM method, but in order to get better results, the BEM model needs to be extended. For instance, in AERFORCE [2], a package for calculation of the aerodynamic forces, the BEM method has been extended to incorporate:

- Dynamic inflow: unsteady modelling of the inflow for cases with unsteady blade loading or unsteady wind.
- Extensions to BEM theory for inclined flow to the rotor disc (yaw model).
- Unsteady blade aerodynamics: the inclusion of 2D attached flow, unsteady aerodynamics and a semi-empirical model for 2D dynamic stall.

The theory has been found to be very useful for comparative studies in wind turbine developing. In spite of a number of limitations, it is still the best tool available for getting good first order predictions of thrust, torque and efficiency for turbine blades under a large range of operating conditions.

5.5 Loads and structural stresses

As mentioned in the introduction to this chapter, a wind turbine is made up of a number of interconnected mechanical elements. The aerodynamic forces acting on the rotor will not only contribute to the production of electrical power, they will also result in loads on the structure. Since the components are more or less flexible, these loads will create deformations and displacements.

Wind turbines are exposed to very specific loads and stresses. Due to the nature of the wind, the loads are highly changeable. Varying loads mean that the material of the structure is subjected to fatigue which must be accounted for in the dimensioning of the wind turbine. Further, because of the low density of the working medium, air, the blades need a large area in order to capture the wind efficiently. However, with increasing size, the structure will behave more elastically. The combination of

the flexible structure and the varying loads will create a complex interplay, which induces vibrations and resonances and can cause dynamic loading and in stability problems. According to [32] there are three different aspects of the structural design that must be considered:

- The strength of the turbine and its fundamental components must be able to withstand the highest wind speeds that may occur.
- Fatigue life of the components must be ensured for their service life, 20 to 30 years.
- The vibrational behaviour of a wind turbine can be kept under control only when the stiffness parameters of all its components are carefully matched.

There are three categories of forces acting on the wind turbine:

- Inertial forces
- Aerodynamic forces
- Structural forces

The *inertial forces* come as a result of introducing mass, motion and gravity to the static forces. Gyroscopic and gravity forces are examples of inertial forces acting on the wind turbine. The *aerodynamic forces* are the most difficult to visualize and test. The forces are both unsteady and nonlinear, and are further complicated by the influence of rapidly changing wind speed, gusts, etc. The *structural forces* are forces due to the flexible structure. Calculations of the structural and inertial forces would be routine and straightforward if it were not for the complication of the changes in aerodynamic forces when the motions and deflections occur.

5.5.1 Uniform and steady flow

The most simple load case for the primary function of the turbine is assuming uniform and steady flow. That assumption is of course an idealization which does not exists in the free atmosphere. The concept is nevertheless useful for calculating the mean load level, occurring over a longer period of time. The wind loads on the rotor blades, when assuming uniform and steady flow, will depend mainly on the effective wind speed increasing from blade root to blade tip. The bending moments on the rotor blades in the chordwise direction, Figure 5.4 results from the tangential loading and the thrust force distribution, Figure 5.5, is generating the moments in flapwise direction. The thrust and tangential force distributions change distinctly with wind speed or from start-up speed to the shut-down speed. The rotor blade twist is the main reason for this. The blade twist is optimised for nominal wind speed only, so that the aerodynamic forces correspond to an optimum only for the nominal speed.

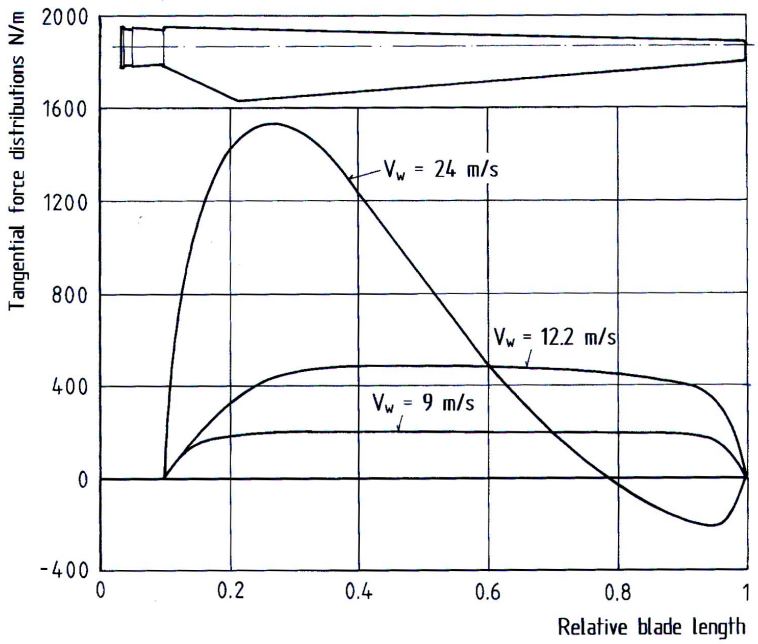

Figure 5.4: Aerodynamic tangential load distribution over the blade length of the experimental WKA-60 wind turbine. Reproduced from [32].

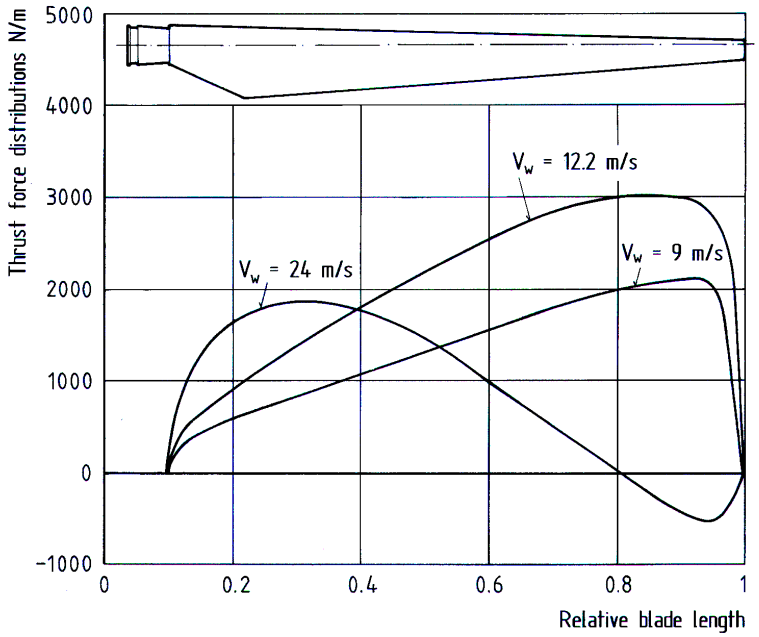

Figure 5.5: Aerodynamic thrust load distribution over the blade length of the experimental WKA-60 wind turbine. Reproduced from [32].

5.5.2 Vertical wind shear and crosswinds

The increase of wind speed with altitude is known as wind shear. The asymmetry of the incoming wind flow will make the rotor blades in the upper rotational sector, due to higher wind speed, more exposed to higher loads than in the sector near the ground. A similar asymmetry is the crosswinds which are caused by fast changes in wind direction. The vertical wind shear and crosswinds on the rotor lead to cyclic increasing and decreasing load distribution over the rotor blades. The variation will cause a blade root bending moment, which causes varying loads for the remaining parts of the turbine.

5.5.3 Tower interference

The air flow is blocked by the presence of the tower, which results in regions of reduced wind speed both upwind and downwind the rotor. In order to keep the nacelle length as short as possible, the clearance of the rotor rotational plane to the tower is small. However, the small distance creates an aerodynamic flow around the tower which will influence the rotor. The reduced flow to the rotor blades, when the tower's wake is being passed, leads to a sudden decrease of the rotor blade lifting forces. The sharp dip in blade loading caused by tower shadow is more prone to excite blade oscillations than the smooth variations in load due to wind shear, shaft tilt and yaw [7].

5.5.4 Wind turbulence and gusts

While long-term variations of the mean wind speed are of interest for the generated power, short-term variations, or turbulence, has a major impact on the design loading. Turbulence is the source of both the extreme gust loading and a large part of the blade fatigue loading. From the simulation viewpoint, turbulence can be seen as random wind speed fluctuations imposed on the mean wind speed. These fluctuations occur in all three directions: longitudinal (in the direction of the wind), lateral (perpendicular to the average wind) and vertical.

5.5.5 Gravitational, centrifugal and gyroscopic forces

It is fairly straightforward to calculate the loads caused by the weight of the components and by centrifugal and gyroscopic forces when the masses are known. As mass can only be calculated as a consequence of the complete load spectrum, several iterations are required in the structural dimensioning before the final properties can be decided. It is noted that several off these effects will only be complicated in an analysis if a detailed discretisation is used.

5.5.5.1 Gravity loads

Naturally, the weight from all the different components must be taken into account for a correct physical model of the wind turbine. The rotor blade weight is of special significance for the blades themselves, but also for the connected components. Due to the rotor revolution, the blade weight will generate sinusoidally varying tensile and compressive forces along the length of the blade, but, above all, a varying moment around the chordwise and flapwise (edgewise) axis of the blades, Figure 5.6. As is the case with any other structure, when scaling up the dimension, the gravity induced loads will be a problem. The effects of the increased gravity loads will be even more evident in the case of a rotating rotor where alternating loads occur.

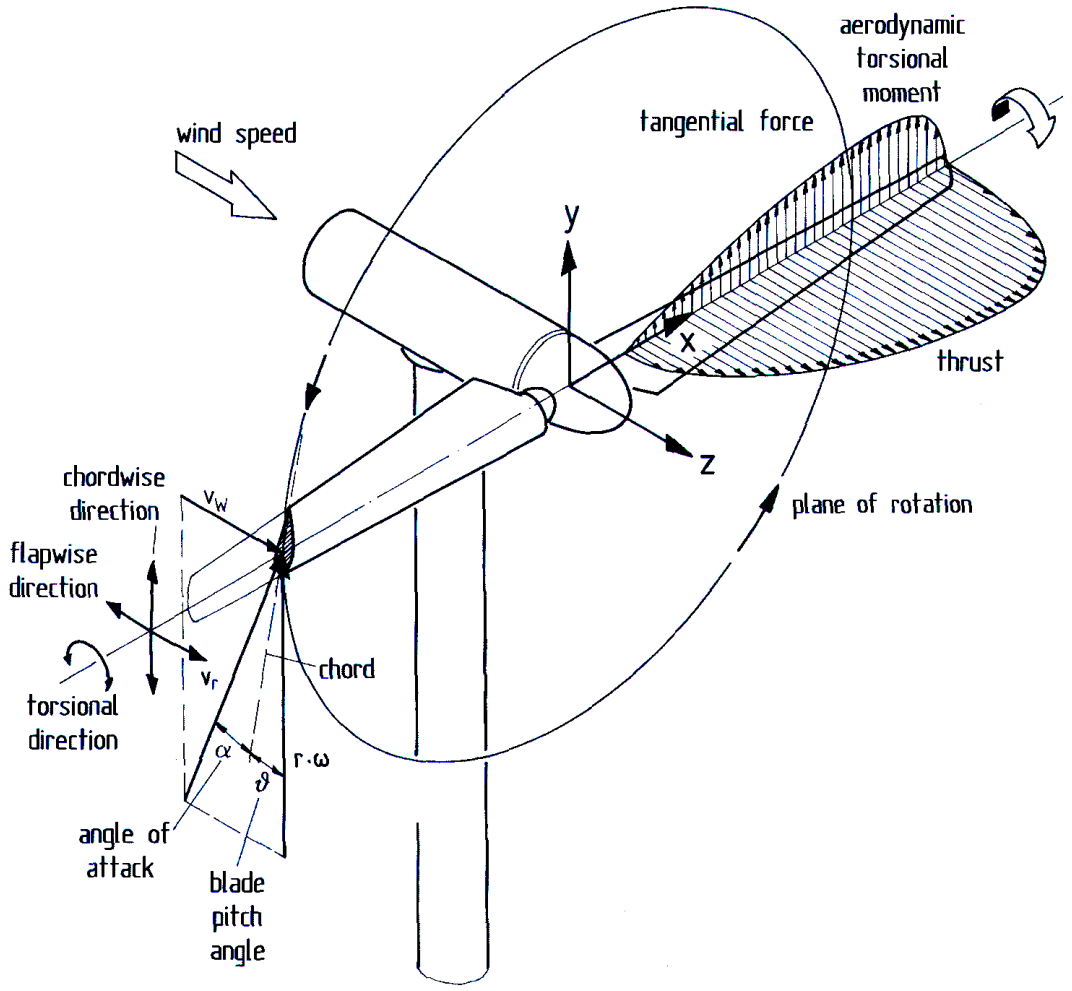

Figure 5.6: Coordinates and technical terms for representing loads and stresses on the rotor. Reproduced from [32].

5.5.5.2 Centrifugal loads

Due to their relatively low speed of revolution, centrifugal forces are not very significant for wind rotors. Thrust loading causes flexible blades to deflect downwind, with the result that centrifugal forces will generate out-of-plane moments in opposition to those due to the thrust. This reduction of the moment due to thrust loading is known as centrifugal relief [32].

5.5.5.3 Gyroscopic loads

When the turbine yaws, the blades experience gyroscopic loads perpendicular to the plane of rotation. A fast yaw motion leads to large gyroscopic moments that act on the rotor axis. In practice, the controller is programmed to yaw the rotor so slow that gyroscopic moments do not play a role.

Chapter 6

Finite element model of a wind turbine

This chapter treats some aspects about modelling wind turbines within the FE method in general and the use of the FEM program SOLVIA in particular.

The choice of FEM program is always a compromise since all FEM programs have their strengths and drawbacks. A fundamental requirement for this specific application was the possibility to write user supplied load subroutines. For instance ABAQUS, ANSYS and SOLVIA have this support, but because of the easy access to SOLVIA at the department, the decision was taken to use SOLVIA in this phase of the project. Further information about SOLVIA is given in Section 7.1.

6.1 Tower

The tower is one of the main components of a wind turbine and its physical properties will highly influence the overall dynamics. By using a commercial FEM program, it is possible to relatively easily model different types of tower concepts, like tubular or lattice towers, different geometries and materials, and of course it is possible to change the number and type of elements. In most cases, it is sufficient to describe the tower with a rather sparse beam element model in order to catch the overall structural behaviour. If the purpose of the model is to study the tower in detail, e.g. optimizing dimension or study buckling phenomena, a shell element formulation might be a better choice, but this would only lead to minor modifications of an existing model. The number and type of element is always a balance between computational cost and accuracy.

The Alsvik wind turbine, described in the numerical example in Section 8.1, has a conical tower and is modelled in SOLVIA with pipe elements. The procedure in SOLVIA to model the tower is to create a number of pipe elements between nodes. The next step is to create section data with thickness and diameter properties. The last step is to associate a specific section to a specific element.

6.2 Blades

The function of the rotor is to convert part of the power contained in the wind stream into mechanical energy. While it is theoretically possible to design a turbine with any number of blades, current technology mainly uses three blade rotors even if two bladed rotors are present.

In the current version of SOLVIA, the blades are limited to be modelled with pipe elements (the next version of SOLVIA will support both iso-beam and general beam elements in large rotation simulations), Figure 6.1. The main advantage with a beam formulation is that the blades could be given different stiffness properties in flap and edge direction.

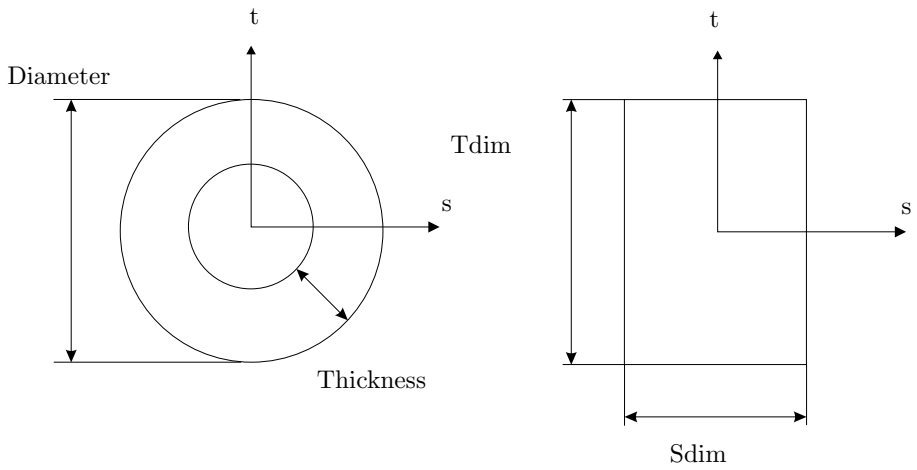

Figure 6.1: Pipe and iso-beam cross-sections.

Diameter	The outer diameter of the pipe cross-section
Thickness	The wall thickness of the pipe cross-section
Tdim	The dimension of the rectangular section in the s-direction
Sdim	The dimension of the rectangular section in the t-direction

The mass of the blade can be calculated automatically from the mass density or be specified as concentrated nodal masses. Further, the mass matrix can be specified to be either consistent or lumped.

6.3 Drive train and bedplate modelling

A variety of different drive train layouts are used by manufacturers. The drive train and support structure have a two-fold function. The first function is to increase the rotational speed of the rotor shaft from about 30 r.p.m. to the value needed by the generator (about 1000–1500 r.p.m.). This is done by the gearbox, which transforms

the incoming power (high torque, low rot. vel.) of the low speed shaft to low torque and high r.p.m. in the high speed shaft. The second function is to transfer loads from the rotating system to the tower.

In most cases it is possible to model the drive train with finite elements. By using constraint equations it is possible to accomplish the speed ratios between the different shafts. Figure 6.2 shows a schematic example of four different drive train configurations:

- A. Long shaft with separate bearings; gearbox supported by the shaft with torque restraints.
- B. Rear bearing integrated in the gearbox; gearbox mounted on the bedplate.
- C. Rotor bearings completely integrated in the gearbox.
- D. Rotor bearings on a stationary hollow axle; power transmission by a torque shaft.

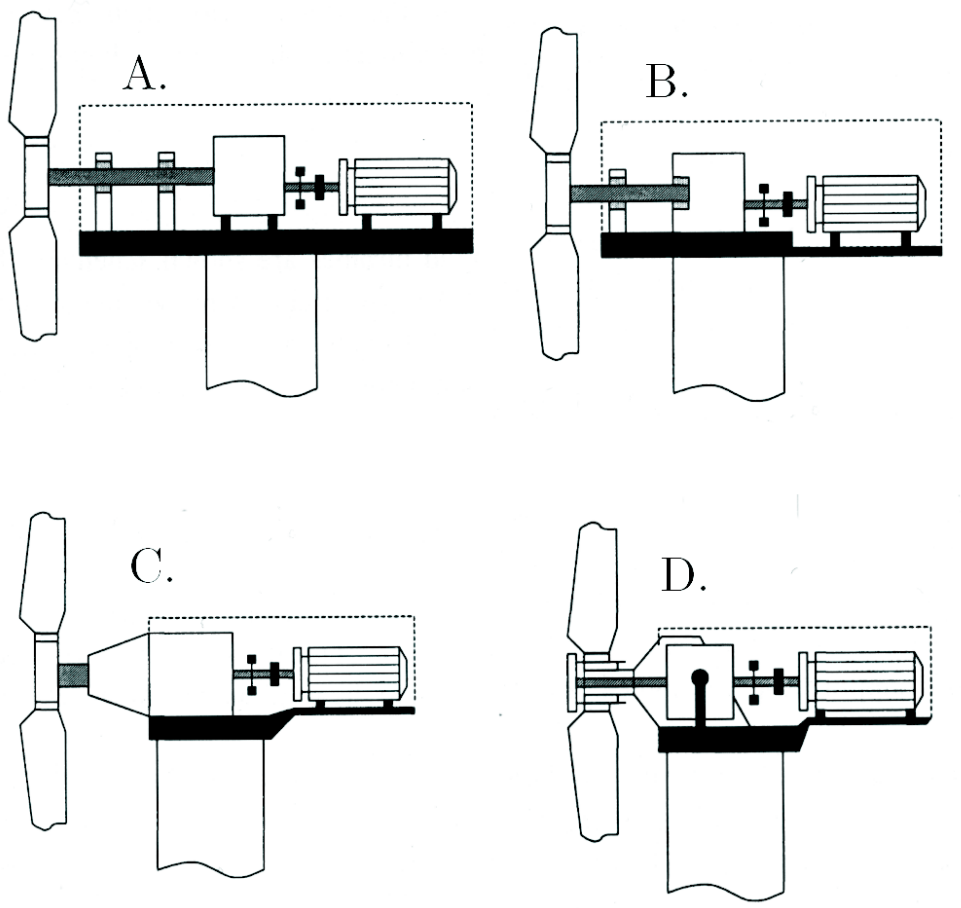

Figure 6.2: Schematic examples of drive train configurations. Reproduced from [31].

Figure 6.3 illustrates the bedplate and the rotor axle as a FEM model. In the figure, the node pairs *A-B*, *C-D*, *E-F* should in fact be located at the same coordinates, but for illustrative reasons the axle is shown above the bedplate. The double nodes are used to specify constraint equations expressing slave (dependent) degrees of freedom as linear combinations of master (independent) degrees of freedom. In the figure, the nodes *A, C, E* are modelled as master nodes and the nodes *B, D, F* as slaves. For each master/slave node combination, constraints are set for translation in *X, Y, Z*, respectively. In this specific example, no constraints are set for the rotational degrees of freedom.

SOLVIA makes it possible to use constraint equations in order to accomplish the speed ratios between the different shafts. The form of the constraint equations is

$$U_s = \sum_m (\beta_m \cdot U_m) \tag{6.1}$$

where U_s is the displacement slave degrees of freedom, U_m the displacement master degrees of freedom and β_m the factors of the linear combination.

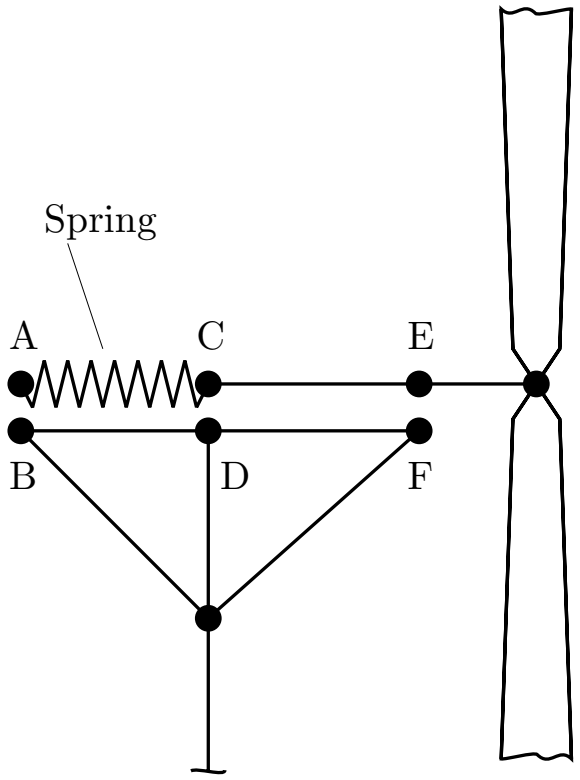

Figure 6.3: Bedplate model.

A constant speed generator may be modelled as described below. In the Alsvik example in Chapter 8, the generator is modelled as a moment derived as a function of the rotational speed.

- A constant rotational displacement acting on node A, with the generator output as a reactive moment to keep this rotation.
- A moment, derived as function of the rotational speed, acting on node A, constraining the rotation value.

In the constant rotational generator/control model the speed is held constant by applying a prescribed displacement to node A in Figure 6.3. The prescribed value of the rotation together with a time function gives the desired rotor speed. Figure 6.4(a) shows the time function and 6.4(b) the corresponding angular velocity. In this particular example, the speed is ramped up linearly during 15 s and then kept constant.

The power is then calculated from the resulting reactive moment in the rotor axle and the rotor speed, as:

$$P = M\omega \tag{6.2}$$

The intension with ramping up the speed is to avoid sudden jumps in acceleration, which otherwise will cause convergence difficulties.

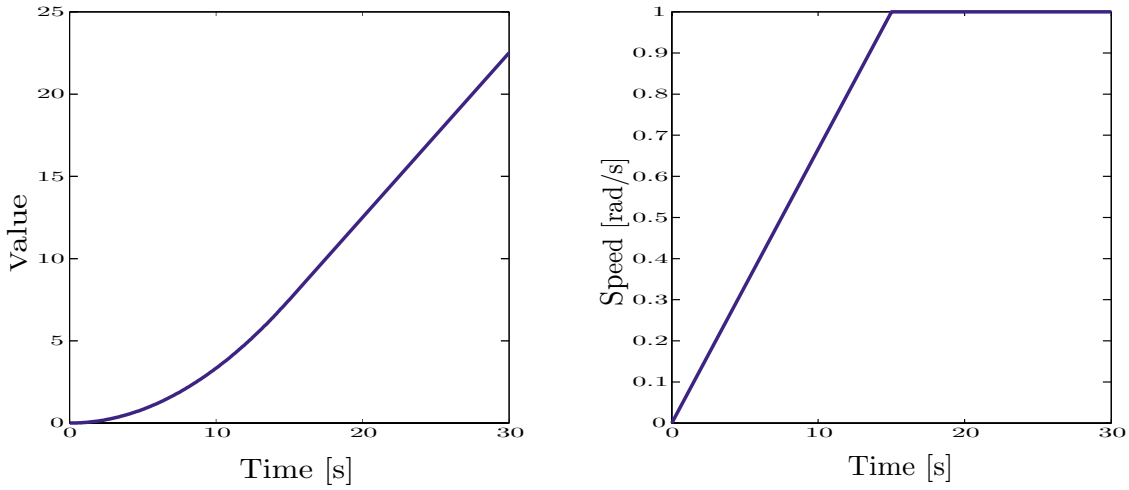

Figure 6.4: SOLVIA time function and the corresponding rotor speed.

In the second model, the generator is modelled as an asynchronous generator. The rotational speed of an asynchronous generator varies with the load. However, in every day language a wind turbine equipped with a asynchronous generator is said to operate at constant speed.

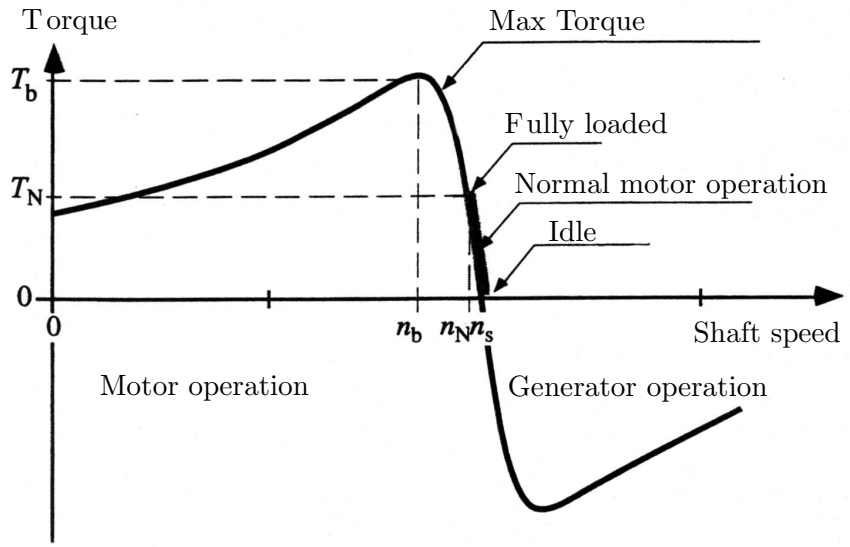

Figure 6.5: Torque as a function of the shaft speed for an asynchronous machine. Reproduced from [64].

When the current is connected, the machine starts turning like a motor at a speed which is just slightly below the synchronous speed of the rotating magnetic field from the stator. However, the wind causes the turbine to run faster than the rotating magnetic field from the stator and a strong current in the stator is induced. The higher the wind velocity, the more power will be transferred as an electromagnetic force to the stator, and the more electricity is transferred into the grid.

The speed of the asynchronous generator will vary with the turning moment applied to it. In practice, the difference between the rotational speed at peak power and at idle is very small, about 2–3%. This difference in per cent of the synchronous speed, is called the generator's slip.

The generator's ability to slightly vary its speed, caused by e.g. gusts, is a very useful mechanical property. The variation means that there will be, due to lower peak torque, less fatigue in the gearbox.

The mathematical formulation and notation are the same as used in VIDYN (aeroelastic code) [24]. The stator is assumed to be rigidly connected to the bedplate.

$$\begin{aligned} M_{\text{gen}} = G_{\text{enm1}} + G_{\text{enk}} \cdot (Omgen - Fip0 - Rollfak \cdot Q_{\text{txp}}) \\ -G_{\text{enk}} \cdot Fip0 \cdot A_{\text{gen}} \cdot \sin(W_{\text{gen}} \cdot Tid) \end{aligned} \tag{6.3}$$

where

M_{gen} generator moment.

G_{enm1} generator moment constant.

G_{enk} generator moment constant.

$Omgen$ angular velocity of the generator.

$Fip0$ angular velocity of the turbine.

$Rollfak$ factor depending on the direction of rotation. $Rollfak = 1$ if the rotation direction of the generator and the rotor coincide.

Q_{txp} bedplate angular velocity around the x-axis.

W_{gen} frequency of the variation in grid frequency.

A_{gen} relative amplitude of the variation in grid frequency.

Tid time elapsed from the beginning of the calculation.

A simplified model is used in the numerical example, where only G_{enm1}, G_{enk}, $Omgen$ and $Fip0$ are used. Equation (6.3), with the Alsvik data, becomes:

$$M_{\text{gen}} = 457600(\omega_{\text{rot}} - \frac{42.35\pi}{30}) \tag{6.4}$$

where ω_{rot} is the generator rotational velocity, measured in each time iteration. The expression introduces a penalty moment, striking towards the correct rotational speed.

The linear function derived in (6.4) above is a simplification of the torque-speed graph in Figure 6.5 around the idle speed.

A modification is made to equation (6.4) in order to prevent overloading at startup. The modified equation is in use the first 20 seconds of simulation and will give a softer startup sequence. A time variable t is introduced as:

$$M_{\text{gen}} = 457600(\omega_{\text{rot}} - \frac{42.35\pi \cdot t}{30 \cdot 20}) \tag{6.5}$$

In performed experiments, this method has been found successful.

6.4 Integration method and tolerances

Numerical simulations in the time domain highly depend on the time integration algorithm concerning accuracy, numerical stability and calculation effort. Many time integration schemes are available, all of which have some advantages and disadvantages in special cases.

Explicit schemes are only conditionally stable and very short steps are mostly necessary. In explicit methods dynamic equilibrium is considered at time t to evaluate the solution at time $t + \Delta t$. If Δt exceeds a certain fraction of the smallest vibration period of the structure, computed displacements and velocities grow without bound. For this reason, these algorithms are commonly used for simulations of very short periods (e.g. impact or crash simulations). In civil engineering structures these schemes are rarely needed as most systems respond in low frequencies [50].

Implicit methods, such as Newmark methods, attempt to satisfy the differential equation at time $t + \Delta t$ after the solution at time $t - i\Delta t \;\; (i = 0, 1, 2, ..., n)$ is found. These methods require the solution of a set of linear equations at each time step. However, larger time steps may be used. Implicit methods are conditionally or unconditionally stable.

While unconditional stability can be guaranteed in linear analysis for most methods, nonlinear simulations are stable only when there is no additional dissipation of energy due to numerical characteristics (especially due to geometrical nonlinearities). An arbitrary increase of energy arises from very high modes oscillating within the current time step. By suppressing these oscillations sufficiently, the calculation can be stabilized.

The Hilber-Hughes method used in SOLVIA introduces damping in the Newmark method without degrading the order of accuracy. With appropriate choice of parameters, this method retains the second order accuracy and provides effective high-frequency dissipation. If the integration parameter is selected so that $\gamma \in [-\frac{1}{3}, 0]$, $\delta = \frac{1}{2} + \gamma$, and $\alpha = \frac{1}{4}(1 + \gamma)^2$, the method is implicit, unconditionally stable, and second-order accurate [10, 27]. When these guidelines are used, with $\gamma = 0$, the method reduces to the trapezoidal rule, which has no dissipation. Decreasing γ increases the amount of numerical damping.

The basic equation that SOLVIA operates on, in implicit time integration, is:

$$\begin{aligned} \mathbf{M}^{t+\Delta t}\ddot{\mathbf{U}}^{(i+1)} + \mathbf{C}^{t+\Delta t}\dot{\mathbf{U}}^{(i+1)} +^{t} \mathbf{K}\Delta\mathbf{U}^{(i+1)} &=^{t+\Delta t} \mathbf{R} -^{t+\Delta t} \mathbf{F}^{(i)} \\ {}^{t+\Delta t}\mathbf{U}^{(i+1)} &=^{t+\Delta t} \mathbf{U}^{(i)} + \Delta\mathbf{U}^{(i+1)} \end{aligned} \tag{6.6}$$

where

M constant mass matrix.

C constant damping matrix.

${}^{t}\mathbf{K}$	tangent stiffness matrix at time t.
${}^{t}\mathbf{R}$, ${}^{t+\Delta t}\mathbf{R}$	external load vector applied at time t and time $t + \Delta t$, respectively.
${}^{t}\mathbf{F}$, ${}^{t+\Delta t}\mathbf{F}^{(i)}$	nodal point internal force vector equivalent at time t, and after iteration (i) at time $t + \Delta t$, respectively.
${}^{t+\Delta t}\mathbf{U}^{(i)}$	vector of nodal point displacements after iteration (i) at time $t + \Delta t$.

A superimposed dot denotes time derivative, e.g., ${}^{t}\dot{\mathbf{U}}$=nodal point velocity vector at time t.

In SOLVIA, Equation (6.6) can be integrated over a time interval using the modified or full Newton-Raphson methods with or without line searches, or the Broyden-Fletcher-Goldfarb-Shanno (BFGS) method.

The tolerances in the analysis must be set when equilibrium iterations are performed. The type of tolerances used in SOLVIA are the *energy tolerance criterion* and the *force/moment tolerance criteria*. It is also possible to combine the two types mentioned above. The choice of criterion is a balance between performance and accuracy. Tests have been made in this project and the conclusion is that the energy criterion, when the tolerance is set relatively tight, alone fulfils the requirements of performance and accuracy.

Chapter 7

Program structure

The developed wind turbine simulating tool consists of three main parts: The SOLVIA finite element program for modelling the structural dynamics, AERFORCE for the calculation of the aerodynamic loads and SOSIS-W for the generation of the turbulent wind field. The idea with using a commercial FEM program is the stability and versatility a well documented program offers. Another advantage is that the software may be used as a tool throughout the complete design process. For instance to dimension specific parts off the structure and include effects from waves etc.

7.1 SOLVIA

SOLVIA is a commercial finite element program for modelling of e.g. structural dynamics [38]. The program is used in its Fortran objective version for the possibility to link user-supplied loads, e.g. wind loads, to the SOLVIA package.

The communication between the aerodynamic code and SOLVIA is done by using the possibility to include user-supplied loads. The user-supplied load is defined as a follower-load type in the SOLVIA program. During the step-by-step response calculation, the user-supplied loads are evaluated in each time step and in each iteration. These loads are added to the global load vector normally established in the response calculation for the time steps.

The user-supplied loads can be calculated based on a number of different nodal parameters. Typical nodal parameters available are e.g. lumped mass components, information about current and incremental solution time, displacements, velocities and accelerations. The load contribution calculated for a node may depend on nodal quantities for other nodes.

7.2 AERFORCE

For the calculation of the aerodynamic forces acting on the blades of the wind turbine, a subroutine package named AERFORCE [2] has been used. The aerodynamic model used in this package is based on the BEM method which has been found to be very time efficient, see Section 5.4.2. In spite of a number of limitations in the method itself, the BEM method is still the best tool available for getting good first order predictions of thrust, torque and efficiency for turbine blades under a large range of operating conditions. The AERFORCE subroutine is called with a number of formal parameters but communication via common blocks is also used.

7.2.1 Coordinate systems

Forces and velocities in AERFORCE are described in three coordinate systems. The coordinate systems are obtained from the structural dynamic program and are utilized by the AERFORCE subroutine:

- The global system: the system in which the free wind is given. The system is designated the g-system.
- The rotor system: a system that is attached to the rotor. The system is rotating with the rotor and has its Y and Z-axis laying in the disc-plane. In this system the normal induction is in the X-axis direction and the tangential induced velocity is an in-plane velocity. The system is designated the r-system, Figure 7.1.
- The blade-element system: a coordinate system that is attached to each blade element. The blade-element system has its Y-axis aligned with the local blade chord axis. The Z-axis is aligned with the blade 25% chord axis. The system is designated the e-system. Figure 7.2 shows the relation between the r- and e-systems.

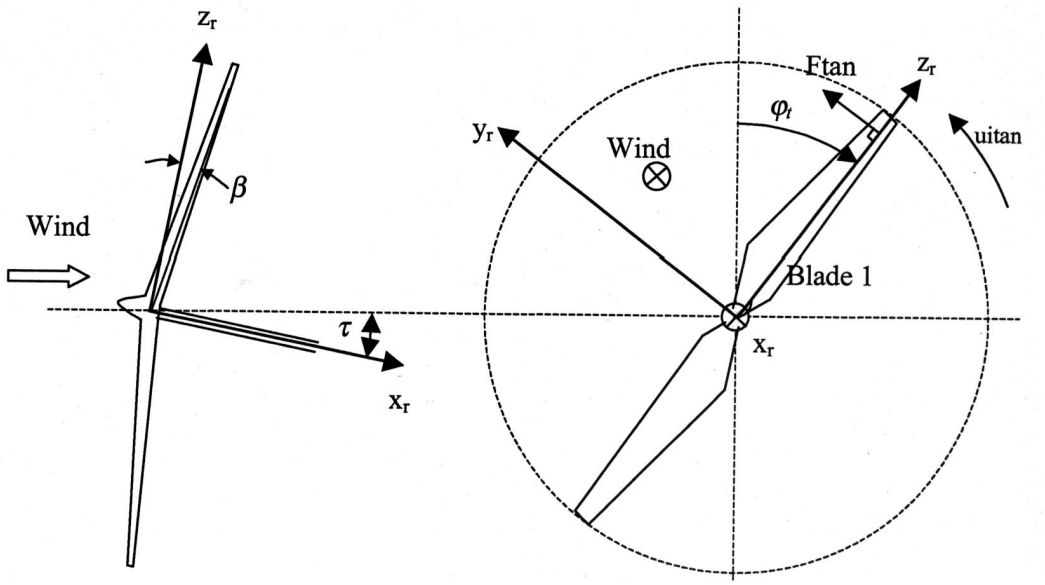

Figure 7.1: View of the rotor in the Y_r-direction and view in the X_r-direction. Reproduced from [2].

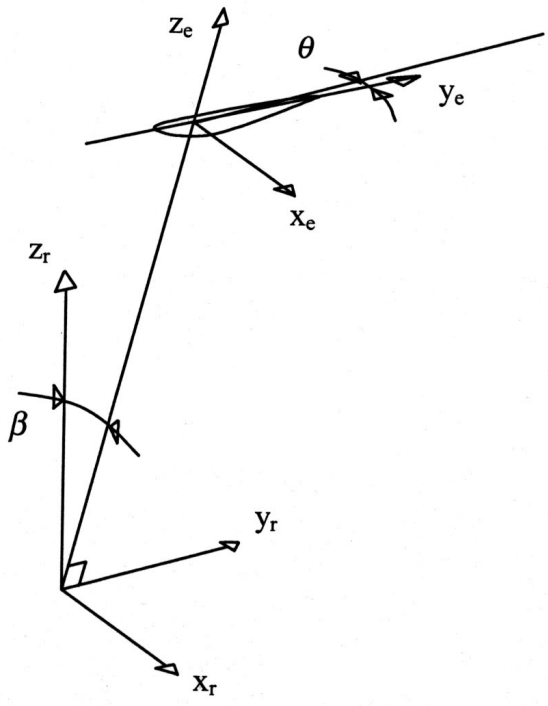

Figure 7.2: Element coordinate system. Reproduced from [2].

In AERFORCE, three transformation matrices are needed. Figure 7.3 illustrates a overview of the the different systems and transformation matrices that are used in

AERFORCE. The transformation matrices are named:

- Transformation from the global system to the rotor system, $\mathbf{S}_{\mathrm{gr}}$.
- Transformation from the global system to the element system, $\mathbf{S}_{\mathrm{ge}}$.
- Transformation from the rotor system to the element system, $\mathbf{S}_{\mathrm{re}}$.

The derivation of the transformation matrices is further explained in Section 7.4.1.

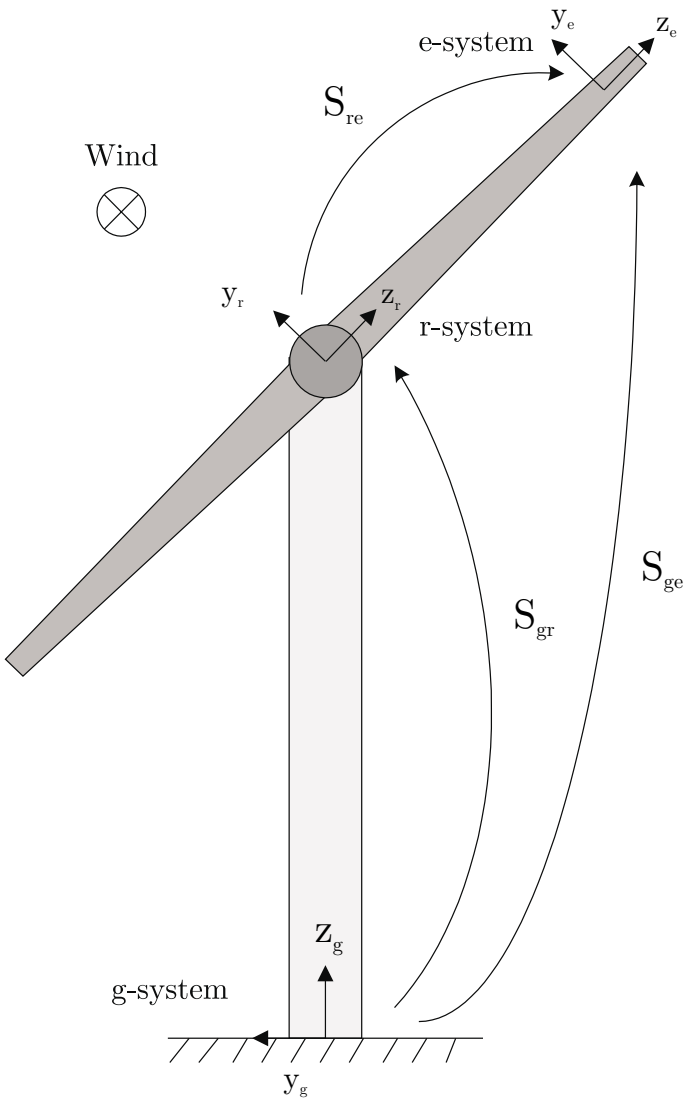

Figure 7.3: Overview of the the different systems and transformation matrices used in AERFORCE.

Each blade is divided into a number of blade elements. The positions of the blades and the blade elements are determined by a number of parameters. Figure 7.4 illustrates some of the parameters needed. Other blade specific parameters are needed, e.g. the chord and area of each blade element. These data are constant for a given structural configuration and are defined as:

r radius to each blade element.

r_{tip} tip radius.

r_{tipmom} radius r_{tip} projected perpendicular to the X_r-axis.

r_{mom} projection of each radius r perpendicular to the X_r-axis.

$\mathrm{d}r_{\text{mom}}$ blade element length $\mathrm{d}r$ projected perpendicular to the X_r-axis.

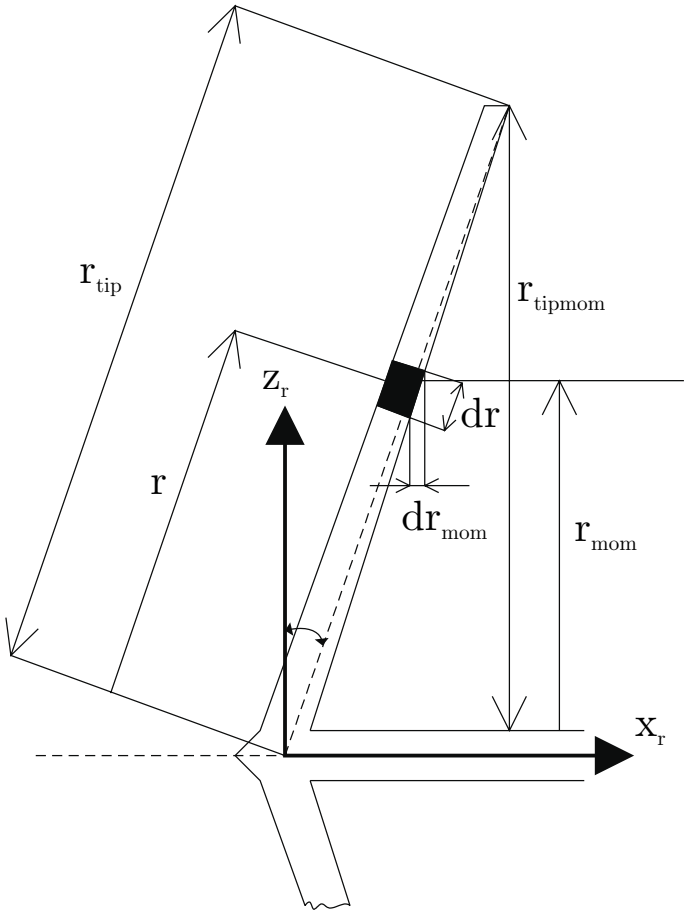

Figure 7.4: Geometric definitions of the rotor.

Other parameters used in order to predict wind loads are, for instance, the wind velocity and the upcoming velocity on each blade element. The wind velocity used in the calculations is described by three components, one in each global direction. The wind data are derived either manually in case of constant wind speed, or, if turbulence is present, by a wind data generator like SOSIS-W, see Section 7.3. The velocity of each blade element is obtained using nodal velocities given by SOLVIA.

The BEM theory requires information about the lift and drag aerofoil coefficients C_L and C_D. If the torsional pitching moment of the blades is taken into account, it

is necessary to specify C_M. The coefficients are specified as functions of the angle of attack and are essential for accurate calculations. Each particular aerofoil has its own data table describing the coefficients. The range of angles of attack in each aerofoil data table must cover the angles of attack that will be encountered during the calculations. If the calculated angle of attack is outside the input range of the table, the program will halt automatically. There are also parameters that need to be set by the user, for example parameters for calculation of time varying inflow. Further information is given in [2].

The outputs from AERFORCE are the normal and tangential forces in the blade element system. If C_M is present in the aerofoil data table, the blade element pitching moments are also given as output.

7.3 SOSIS-W

SOSIS-W is an artificial wind data generator developed by Ingemar Carlén, Teknikgruppen AB [8]. The program is specially developed for providing time domain series of turbulent wind field. SOSIS-W simulates three dimensional wind vectors, corresponding to gridpoints in a plane uniform Cartesian grid, where the grid plane is perpendicular to the mean wind direction.

In SOSIS-W the wind model spectral densities of u-, v-, and w-component are defined either by the International Electrotechnical Commission (IEC) version of the Kaimal spectra, the IEC-version of the von Karman spectra, or the Engineering Science Data Unit (ESDU) version of the von Karman spectra. For additional information about SOSIS-W and its abilities, see [8].

SOSIS-W creates three output files, one for each global direction. The output data are arranged in rows and columns where each row represents a time series and each element in a time series represents the velocity at a specific coordinate.

Each row in the output files forms a grid were the elements are numbered in columns from below to upwards and from left to right. The grid in Figure 7.5 is observed from an upwind position and has its Y-axis pointing to the left and its Z-axis pointing upwards.

6	.	.	.	.	36
.	.	.	.	.	.
.	.	.	.	.	.
.	.	.	.	.	.
2	8	.	.	.	.
1	7	.	.	.	31

Figure 7.5: SOSIS-W output format.

The program is separated from the aeroelastic code and is used as a stand alone

program for providing the files with the pseudo-random wind field condition before the structural simulation. Depending on the data specified in the input file to SOSIS-W, it is possible to model different types of wind models and situations.

The turbulent wind field is described by specifying a large number of parameters. Information needs for instance, to be specified about the mean wind speed at hub height and the corresponding standard deviation. The increase of wind speed with height is known as wind shear and its effect is included in SOSIS-W by the power law, $V(z) = V_r(\frac{z}{z_r})^{\alpha}$, where z is the height above ground level, V_r is the wind speed at the reference height z_r above ground level, $V(z)$ is the wind speed at height z and α is an exponent which depends on the roughness of the terrain. Typical values of α are in the region 0.14–0.20.

The program is further described in [8] and a complete input file is presented in Appendix B.

7.4 Linking SOLVIA and AERFORCE together

As described in Section 7.2, AERFORCE needs a number of input data in order to give the aerodynamic forces. The parameters are derived in the SOLVIA's user-supplied load *USERSL* subroutine and in a subroutine *input&link* that is the link between the two programs.

All Fortran objective and f-files are linked and compiled with the *Compaq Visual Fortran Standard Edition 6.5.0* [9].

The calculation scheme is broadly described below, assuming the steps are performed inside the SOLVIA's user-supplied load *USERSL* subroutine. A block diagram of the wind turbine simulation tool is illustrated in Figure 7.6.

Called by SOLVIA at each iteration and time step:

1. Save x,y,z displacement components for nodes of interest, e.g. blade nodes and rigid-link nodes.

2. Save x,y,z velocity components for each blade node and the rotational speed of the rotor.

3. Derive the transformation matrices, $\mathbf{S}_{\text{gr}}$ (between the global and the rotor system) and $\mathbf{S}_{\text{ge}}$ (between the global and the element system), based on the x,y,z components saved at step 1. Calculate the transformation matrix between the rotor and the global system as $\mathbf{S}_{\text{re}} = \mathbf{S}_{\text{ge}} \cdot \mathbf{S}_{\text{gr}}^T$.

4. Call subroutine *input&link* by *USERSL*.

   (a) read data from input file, e.g. blade information such as chord length, thickness, area, twist, pitch, profile number etc. Step 4(a) is only performed at the first time step since the values are not time dependent.

(b) process the data read in step 4(a) For instance interpolate data between input aerofoil tables and modify $\mathbf{S}_{\text{re}}$ to include the contributions from twist and pitch.

(c) call subroutine *windgen* by *input&link* and calculate the wind speed acting on each blade element.

(d) call subroutine *AERFORCE* by *input&link* and calculate the forces acting on each blade element.

5. Transform blade element forces to the global load vector.

6. Calculate generator moment and write result to the global load vector.

The data is then transferred back to SOLVIA, where the equilibrium iterations of the time step are performed.

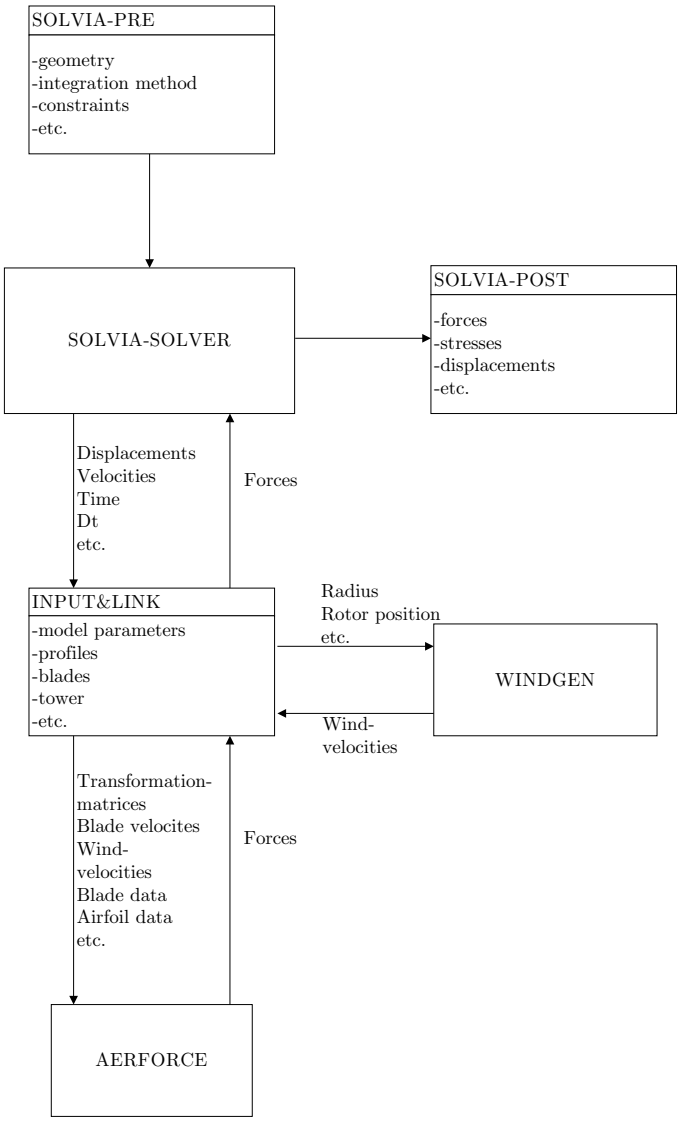

Figure 7.6: Basic block diagram of the wind turbine simulating tool.

When performing the simulation, the pseudo-random wind field is already evaluated.

7.4.1 Derivation of transformation matrices

All transformation matrices are, in the present implementation, derived based on the position of a rigid-link configuration. For instance, to find the transformation matrix between the global system and a system attached to the deformed blade, two help nodes and two rigid links are necessary. The first rigid link is connected between the blade node and a help-node perpendicular to the blade node in the Y,Z-plane. The second rigid link is connected between the blade node and a help-node perpendicular to the blade node in the X-direction, Figure 7.7. The two help nodes are then forced to follow the blade's node motion when elastic deformation and rigid motion is present. With the information available about the coordinates of the two help nodes and the rotor node, two base vectors can be calculated. After normalizing the vectors, the third direction vector is calculated as the vector product between the two base vectors.

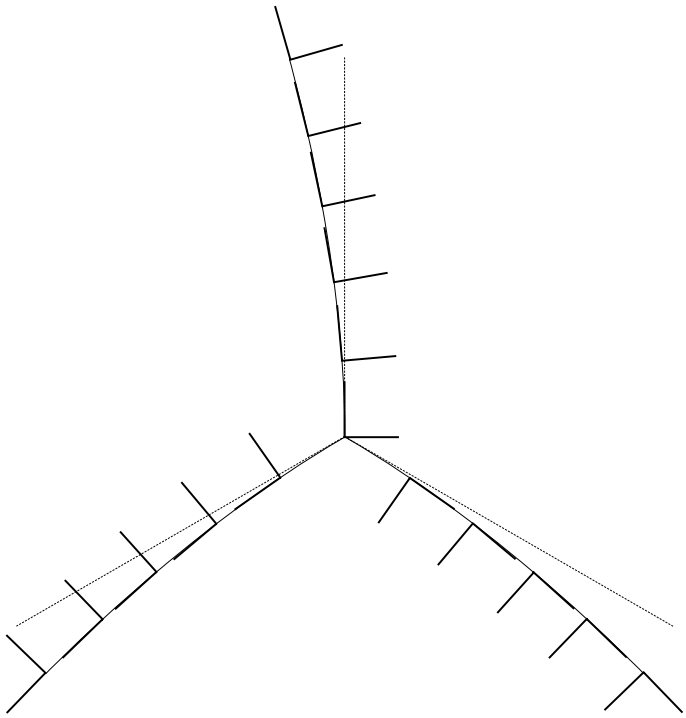

Figure 7.7: Rigid-link configuration on a rotor divided in five elements/blade.

An alternative way to calculate the transformation matrices is to use the nodal rotations. In SOLVIA, the nodal rotations, $\triangle\phi$, $\triangle\theta$ and $\triangle\psi$, are given as incremental rotations at each time step.

7.4.2 Input file

The input file contains the additional information needed by AERFORCE, as geometrical information regarding the blade chord lengths, areas, etc. of the specific structure. Also, it defines the choice of calculation methods and constants. Below follows a short description of the important parts in the input file. A full input file is given in Appendix A.

Identification name:

```
# Turbine name
  Alsvik
```

The coning angle β and the tilt angle τ, Figure 7.1:

```
# Rotor coning angle beta (deg) and tilt angle tau (deg)
                      0.0                          0.0
```

Blade and tower parameters: r_{tip} is the distance from blade root to blade tip and r_{rot} the distance from blade root to the start of the blade section. The other parameters are not used in the present code.

```
# Blade tip radius and rot radius
# hub height and "overhang", xh
#
# th=z for tower top, xh=x for hub position. Positive
# for upwind turbines
# rtip       rrot      th      xh
  11.6       1.0       29.7    1.477
```

Blade element parameters: *Radius* from root to center of each blade element, the same for all blades. Further is the *chord*, *area*, *twist* and *relative thickness* given. To each element is also given a profile number, which corresponds to an aerofoil data table.

```
# ================= BLADE DATA ==========================
# if isetarea=0 the areas from the tabulated values will be used
  0
# Radius  Chord   Area     Twist    rel, thickness profile1 profile2
# m       m       m2       deg      -               -       -
  1.05    0.68    0.340    20.5     30              5       0
    |       |       |      |         |              |       |
  11.3    0.59    0.35     0        15              1       0
# End blade data
```

Parameters for dynamic stall calculations: If *lcncl* = 0 static profile data will be used. All other parameters in the dynamic stall model will then be disregarded. The dynamic stall model is included in AERFORCE and is further described in [3]. The dynamic stall model is not tested in this report. *coeffa1*, *coeffa2*, *coeffb1* and *coeffb2* are coefficients for the inviscid circulatory lift response.

```
# ====Dynamic stall method. common for all aerofoils===========
# If lcncl=0 static profile data will be used. All other parameters in
# the dynamic stall model will then be disregarded
#-------------------------------------------------------------
# lcncl   lpotmeth  lfmeth  lvormeth  lcddyn  ldut
  0       4         4       2         2       0
#-------------------------------------------------------------
# coeffa1     coeffa2      coeffb1     coeffb2
  0.3         0.7          0.13        0.53
# Number of aerofoils (1 row)
  5
```

Aerofoil data: The first input line is a path and the file name of the first aerofoil data file. The other parameters are used if dynamic stall model is used. The number of profiles must be the same as specified above.

```
# ++++++++++++ New profil ++++++++++++++++++++++++++++++++++++++++
# File name with "sep-data" (1 row)
  D:\vindverket\profildata\alvid15v1_360.cla
# aerofoil number
  1
# rel thickness
  15
# tf data (3 rows)
  0.0  0.5  0.1
  5
  0
# ------------------------------------------------------------
# vortex parameters (1 row)
# tv, tvl, tvs, cn1pos, cn1neg
  2   1    1    2       -1
# ======== End of profile data ================================
```

Method data: The first parameter $at1$ is the induction factor. The $con\_vec(1)$ parameter is used to calculate a single time constant if $lval(2) = 2$. *lval* is further described in Section 7.2.

```
# For constants and choice of method. See AERFORCE-manual
#
# default: at1=0.32
```

```
# luitan=1
# time-const int-method luitan
# at1,     con_vec(1),    lval(2), lval(1)
  0.32     .2             1        1
#
```

Air data: Also needed is the information about the air density and the size of the wind grid net given. In this example the area of the grid net is 24×24 m, and each grid is of the size 2×2 m.

```
# ========== Wind, mech, etc. ================================
# Air density (rho)
  1.225
# gridpo: Number of gridpoints along an edge, must be the same number
# as specified in SOSIS. N=gridpo*gridpo e.g. 144=12*12
# grsteps: Grid size in meters
# gridpo grstep
  12      2
```

The data given in the input file is mainly used for the prediction of the aerodynamic loads. Input files are also needed for the generation of the FEM model and for postprocessing the results.

7.4.3 Windgen subroutine

The *windgen* subroutine gives each blade element a unique wind speed vector, containing the global velocity components in X,Y,Z-direction, depending on the blades position and the time passed. The turbulent wind series are created by the program SOSIS-W, [8].

As described in Section 7.3, the SOSIS-W output series are limited to be of length *SLENGTH=TSTEP*8190*. To create a longer time series, it is necessary to interpolate between the fixed time steps to match the time step needed in the time integration of the wind turbine dynamics. However, the limitation in SOSIS-W is not a problem when simulating the turbulent wind, since the resolution of the wind rarely exceeds 10 Hz. It is therefore possible to model time series of a length about 800 s. The interpolation in time is performed by using a Matlab procedure, [43].

The windgen subroutine is called with the parameters:

phi	main shaft position angle.
$first\_call$	flag used to open database in first call.
wind	output from subroutine, wind vector acting in points of blade element origins.
r	radius to blade element origins.
gridpo	number of grid-points along an edge, must be the same number

as specified in SOSIS-W.
grsteps grid size in meters.

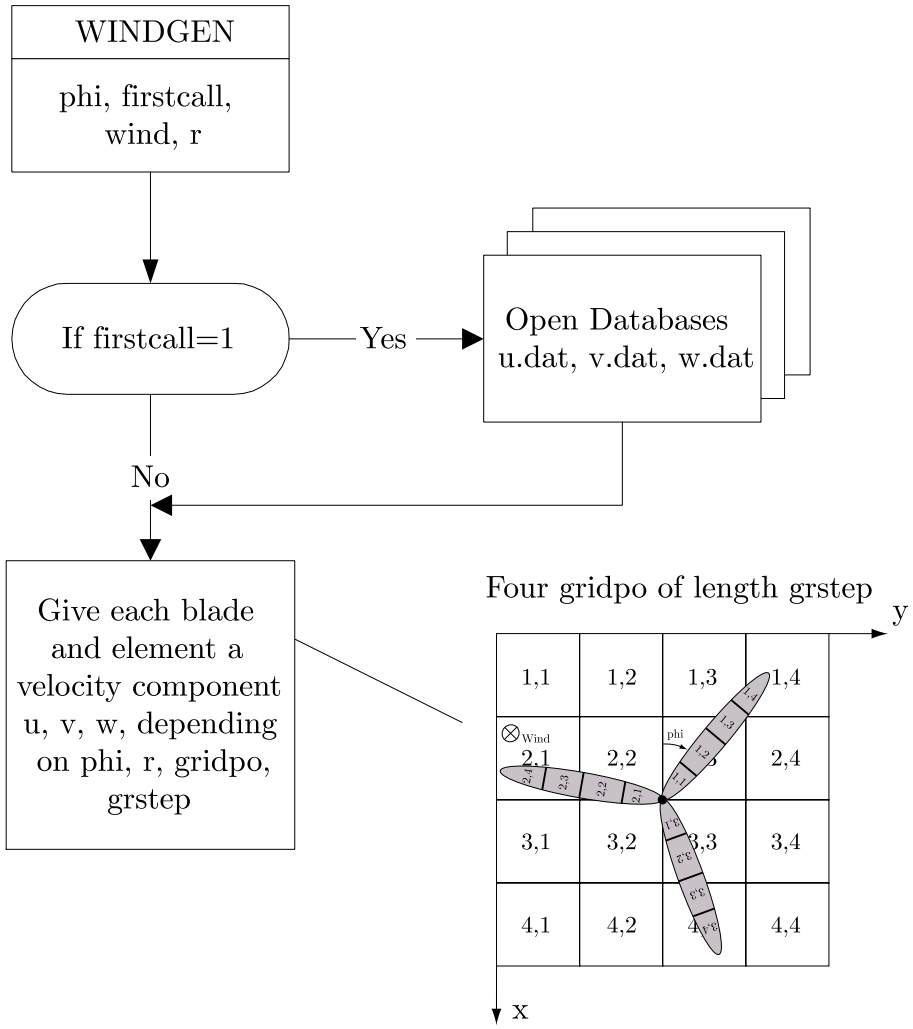

Figure 7.8: Principal function of the windgen subroutine.

For instance, to find the row and column index for a blade depending on the above mentioned variables, the algorithm may look like:

```
xpos=nint((gridpo*grstep/2+r(j)*cos(pi-phi))/grstep)
ypos=nint((gridpo*grstep/2+r(j)*sin(pi-phi))/grstep)
```

where the *nint* function is the command for rounding off a real value to the nearest integer. Possible values for *xpos* and *ypos* will be one to the number of grid-points along a side.

7.4.4 Conclusions

To make a simulation, the program needs input from three different input files. The analysis models are defined by input to the SOLVIA-PRE input file and results in form of plots or listings, etc. can be carried out in SOLVIA-POST via a post input file. The third input file, described in Section 7.4.2 above, is required by the aerodynamic subroutine. Further, is one file needed for each aerofoil table used in the simulation. At this stage of the project, the simulation program needs to be re-compiled if e.g. the generator parameters are changed. However, it is possible, with some modification of the program, to handle most of the possible wind turbine configurations via input files.

Chapter 8

Numerical example

8.1 Alsvik turbine

The wind turbine studied, is one of four turbines located on the west shoreline in Alsvik of the island Gotland in the Baltic sea.

The wind farm is specifically designed for the purpose of experimental measurements and consists of four strategically placed wind turbines, Figure 8.1 and Figure 8.2. Three of the turbines stand on a line that runs along the shoreline in a NNW-SSE direction. The fourth turbine is located to the east of this row, thus deliberately subjected to wind turbine wakes during westerly winds. The land behind them, to the northeast, is low and flat consisting mainly of grazed grasslands and a low growing pine forest. Since the Alsvik wind farm was intended for experimental measurements, it was equipped with two meteorological masts, each being 52 m high. The masts measure the wind speed and the direction on seven elevations above ground.

Figure 8.1: Alsvik wind turbine park. Reproduced from [15].

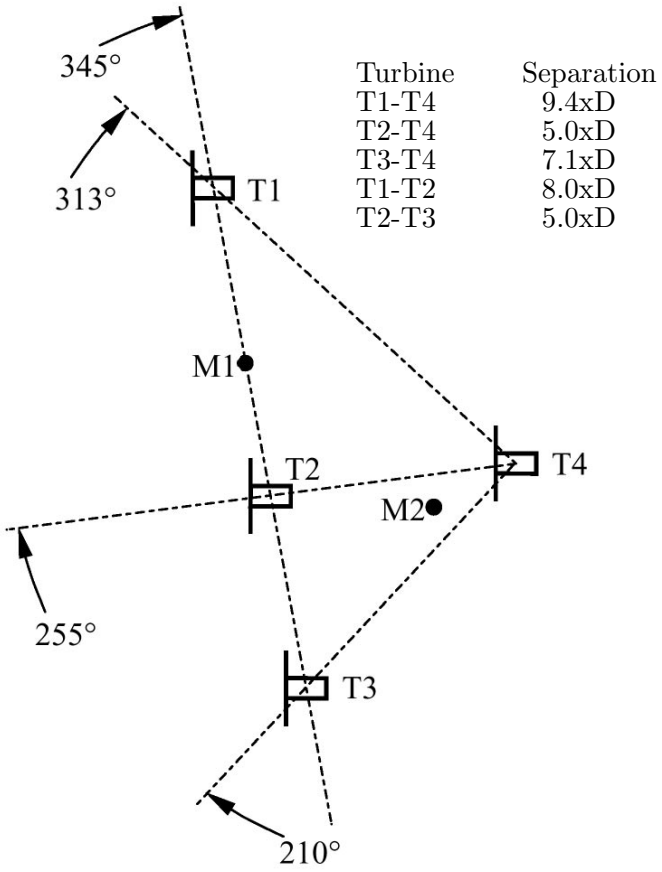

Figure 8.2: Layout of the wind farm at Alsvik, with turbines T1-T4 and masts M1, M2. Reproduced from [15].

The wind turbines are three-bladed and stall regulated with a rated power of 180 kW each. The rotor, which rotates at 42 r.p.m., has a diameter of approximately 23 m and is connected to a 30 m high tower. A more detailed description is given in Appendix A.

8.2 FEM-model of the Alsvik turbine

The FEM-model of the Alsvik turbine is divided into four element groups: The rotor, tower, bedplate and drivetrain. The complete model consists of approximately 280 degrees of freedom.

8.2.1 Rotor

The rotor is modelled with pipe elements. The pipe element is chosen because of a limitation in SOLVIA that prevents the use of beam elements in extremely long time

simulations together with large rotation calculations. A beam formulation should have been preferred since the blades have different properties in different direction.

Each blade is modelled with ten elements and a rigid link configuration attached to each node. The rigid links are used to calculate the transformation matrices needed by AERFORCE to keep track of the position and torsion of the blades.

The mass of the blade is given as concentrated node masses and can be found together with the blade coordinates and the stiffness properties in the Appendix A, Table A.1. Because of the limitation to chose pipe elements, the stiffness properties in edge and flap direction are taken as the mean value for each radial position.

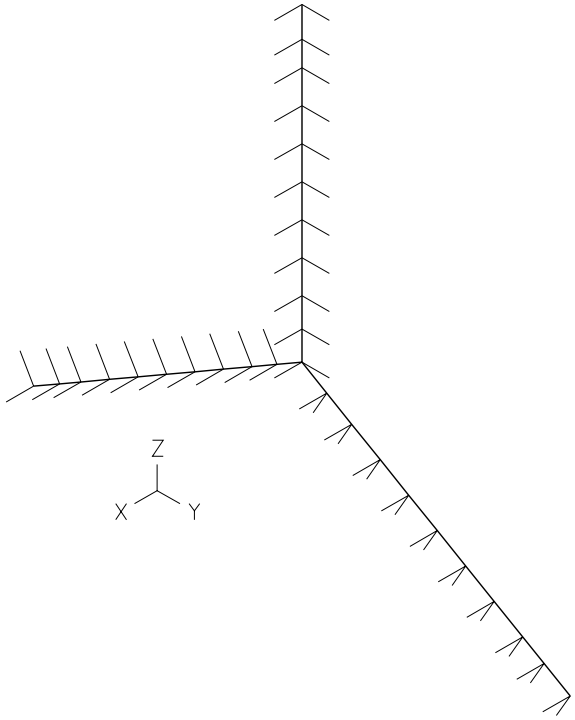

Figure 8.3: FEM-model of the rotor.

8.2.2 Tower

The tower is also modelled with ten pipe elements. The tower data can be found in Appendix A, Table A.2. The mass of the tower is calculated based on the geometrical data and the density of steel, 7850 kg/m^3, specified in the SOLVIA input file. The base of the tower is modelled as rigidly attached to the ground and the top is connected to the bedplate.

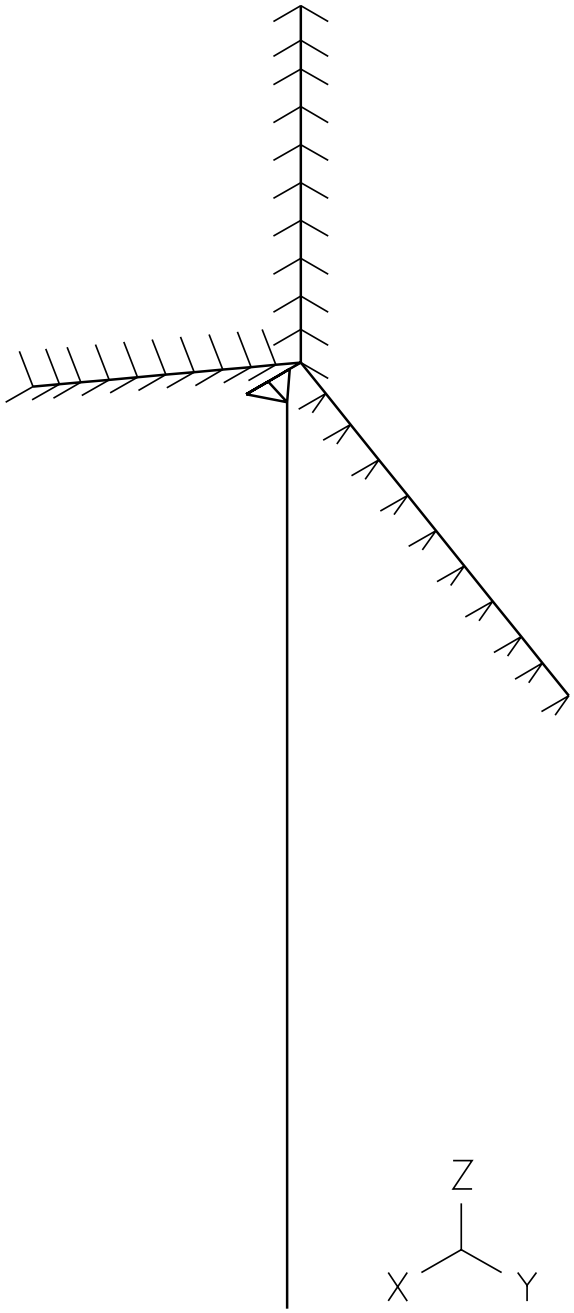

Figure 8.4: FEM-model of the complete wind turbine.

8.2.3 Bedplate

The bedplate is modelled with four beams according to Figure 8.5. The bedplate base between node B and F is divided into four elements. Further, the top of the tower node G is connected to the bedplate base in nodes B,D and F by one element each. The beams are modelled with pipe elements with the outer diameter 0.5 m and the thickness 0.1 m. The mass of the bedplate is given as a concentrated mass, in all three directions, of 6500 kg in the top tower node G.

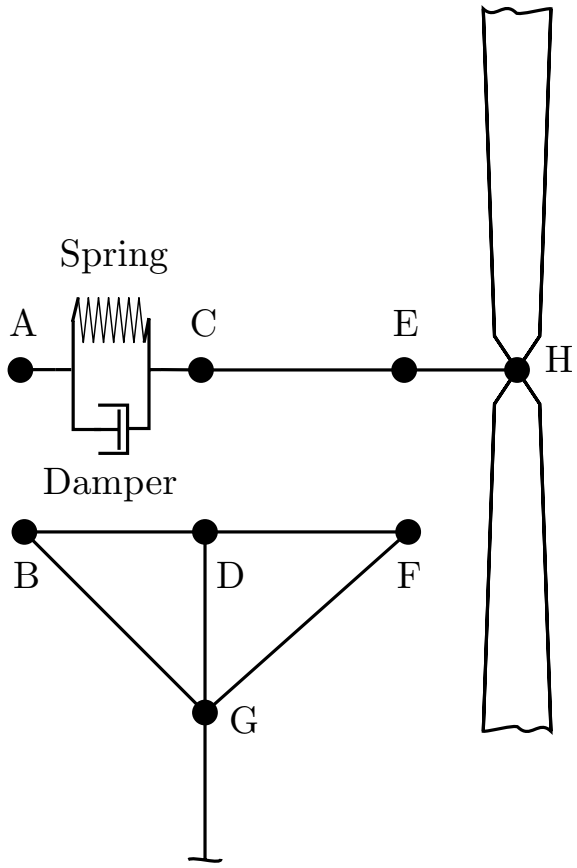

Figure 8.5: Bedplate and drive train.

8.2.4 Drive train

The drive train is made up by the rotor shaft, divided into three pipe elements, between nodes C and H, and the spring-damper configuration between nodes A and C, Figure 8.5. Spring and damping constants are taken as $11.4{\cdot}10^6$ Nm/rad and $10.0{\cdot}10^3$ Nms/rad, based on a similar drive train described in [4], respectively.

Further, node H is given a concentrated mass of 900 kg and a concentrated moment of inertia of 2000 kgm^2, about the rotating shaft, representing the mass properties of the hub. The generator moment of inertia is 2548 kgm^2 and is applied to node A.

The connection between rotor and bedplate is achieved by using constraint equations on nodes A-B, C-D and E-F. The constraint equations are further described in Section 6.3.

8.2.5 Integration method and tolerances

The time integration method used is the Hilber-Hughes method with the parameter $\gamma = -0.3$. The integration parameter is chosen to damp high frequencies in the simulations.

For equilibrium iteration, the full-Newton method is used together with the line search option activated. The tolerance method used is the energy convergence criteria with the parameter $ETOL = 10^{-10}$, which is considered extremely low.

8.3 Results obtained from the numerical simulations

The results presented in this chapter are examples of possible output data, like power, edge and flap moments, etc. Other data may, of course, also be extracted from the FEM simulation, such as stresses, bending and torsion moments, displacements, velocities, accelerations, etc. The method also gives the opportunity to calculate natural frequencies and to perform different kinds of frequency responses.

8.3.1 Power curve

The power curve of a wind turbine is a graph that indicates how large the electrical power output from the turbine will be at different wind speeds.

In Figure 8.6, the measured power curve, [15], is compared to the calculated one. When the wind passes approximately 12 m/s the wind turbine reaches its peak power value 180 kW. Normally the cutout speed is 25 m/s and the power should therefore be constant in the region 12.5–25 m/s, but due to lack of measured data (wind speeds above 13 m/s is not so common) the curve will differ at wind speeds above 13 m/s.

The simulated power curve ends at 16 m/s. The curve follows the measured curve well up to approximately 11 m/s. The differences at higher wind speeds are due to the absence of power regulation in the simulations.

The simulated power curve is calculated with the wind coming directly towards the front of the turbine. For the measured power curve, local turbulence and complex terrain may mean that wind gusts hit the rotor from varying directions. It may therefore be difficult to reproduce the power curve exactly in any given location.

A simple test based on the power given at 6 and 10 m/s gives that the power varies as the exponential 3.15 of the wind speed, which agrees well with the theoretical value 3.

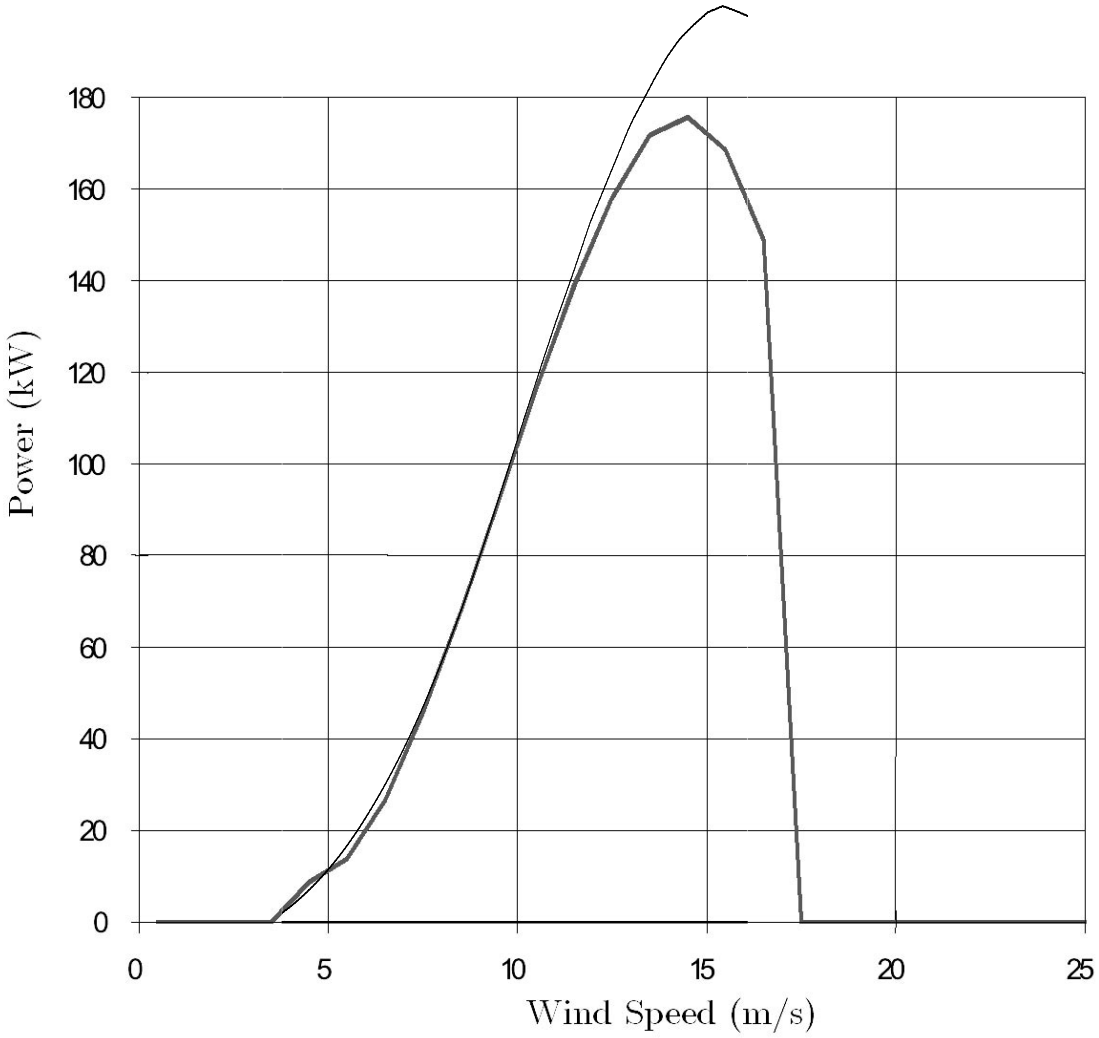

Figure 8.6: Simulated power curve for the Alsvik turbine (light line) compared to measured (heavy line. Redrawn from [15]).

8.3.2 Alsvik turbine running at a constant speed of 12 m/s

It is difficult to check a relatively complex model such as the present wind turbine, where a large number of components interact, for errors. The first basic test was to assure that the model was stable running at a constant wind speed. The Figures 8.7–8.11 show that the rotor speed, power, flap moment, edge moment, flap and edge displacement (at blade tip of blade 1) are approximately constant for, at least, the first 600 s of simulation. The variation of the edge displacement is due to the gravity and the aerodynamically tangential forces acting on the blades. The simulation was made with a wake velocity of 12 m/s acting in X-direction.

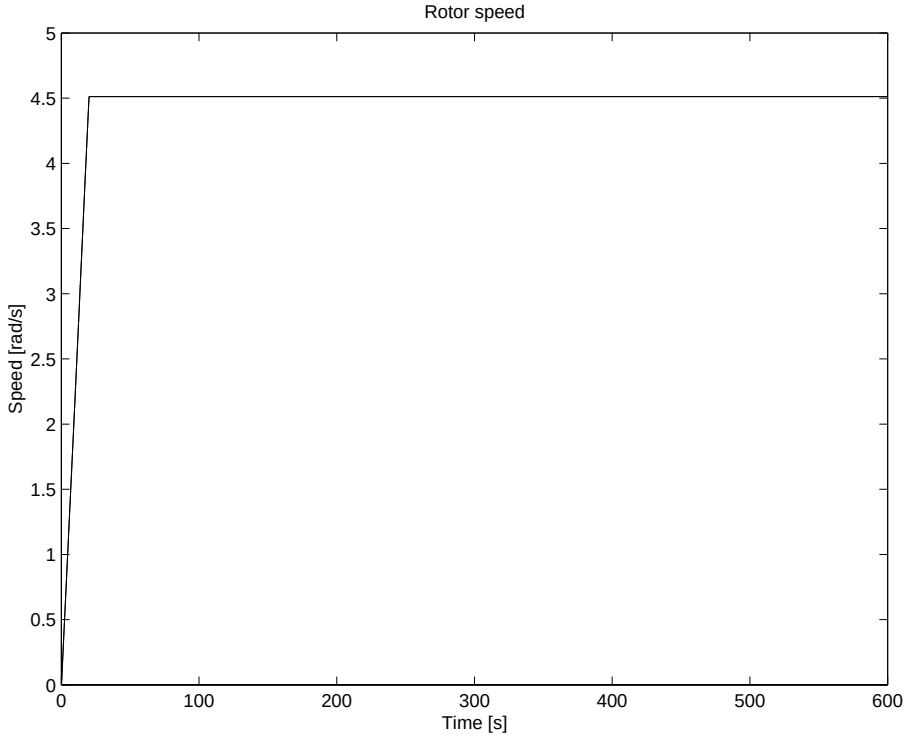

Figure 8.7: Rotor speed for the Alsvik turbine simulated as running at constant speed 12 m/s.

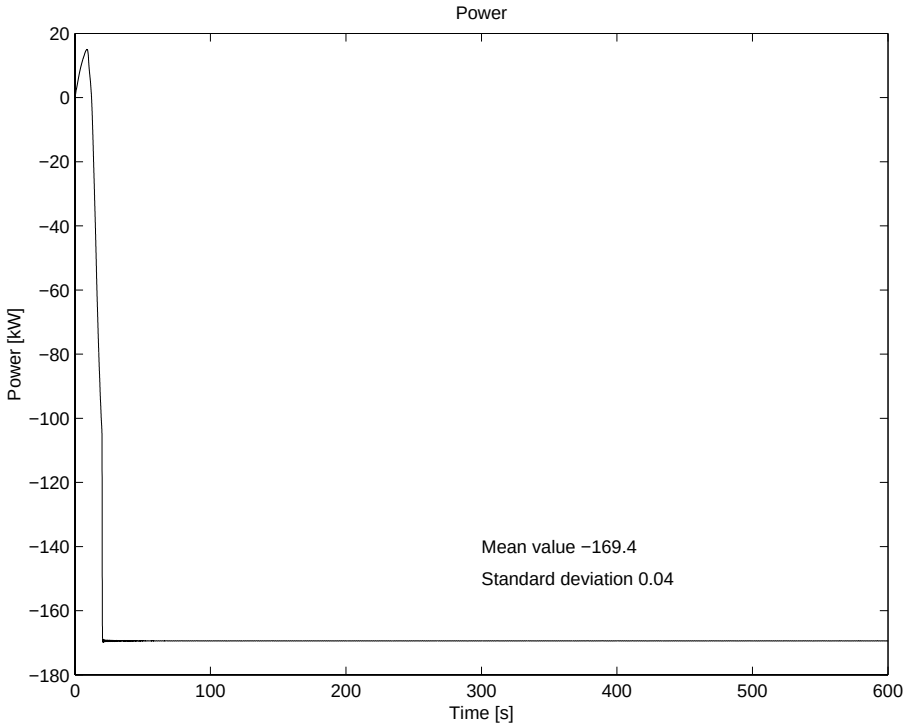

Figure 8.8: Power for the Alsvik turbine simulated as running at constant speed 12 m/s.

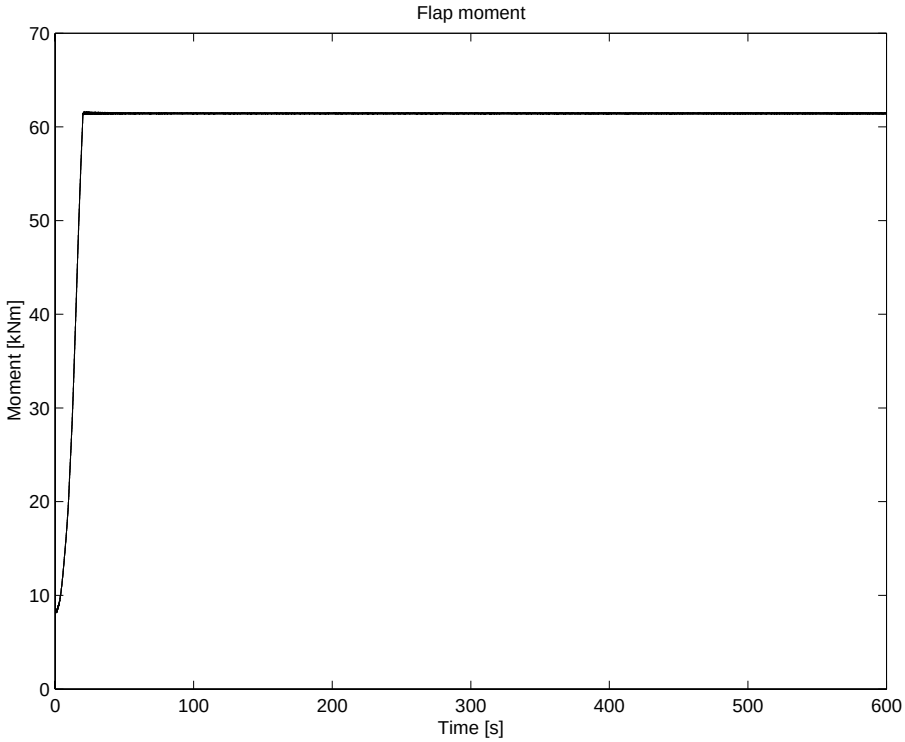

Figure 8.9: Flap moment for the Alsvik turbine simulated as running at constant speed 12 m/s.

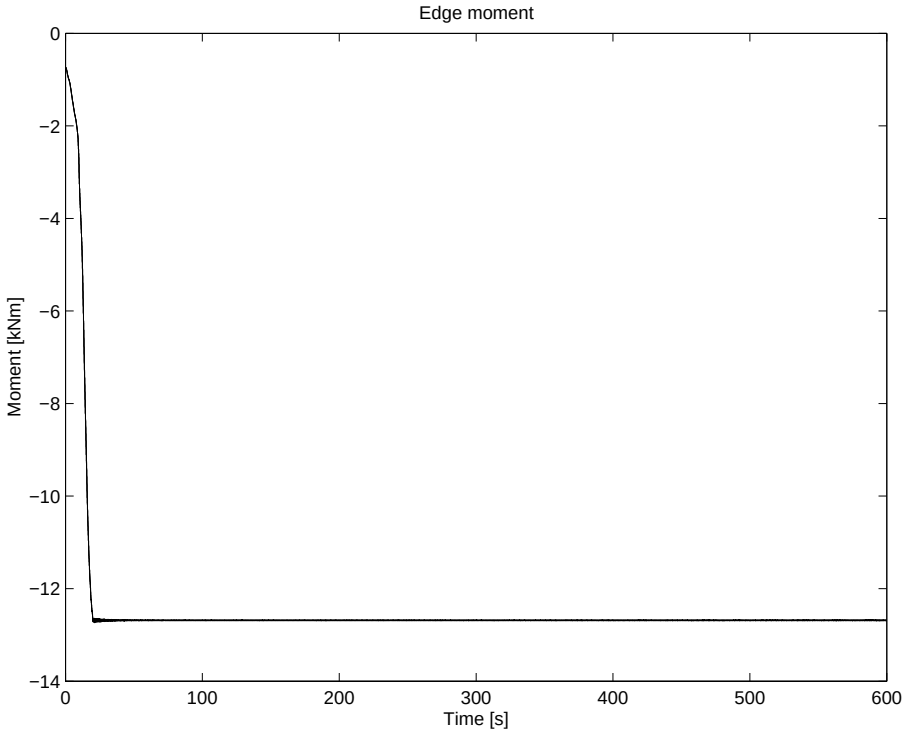

Figure 8.10: Edge moment for the Alsvik turbine simulated as running at constant speed 12 m/s.

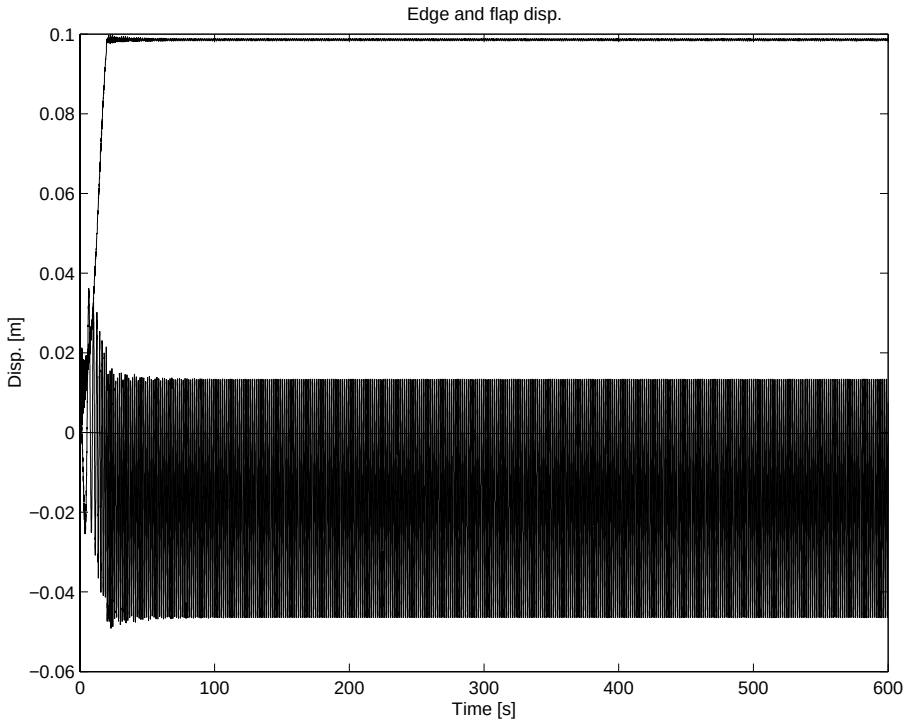

Figure 8.11: Edge (below 0) and flap (above 0) displacements based on the Alsvik turbine simulated as running at constant speed 12 m/s.

The moments plotted in Figure 8.9 and 8.10 are based on the aerodynamic forces only. The constant moments are possible due to the zero tilt angle in the simulation. Contribution from the gravity is not visible in the figures, but is possible to extract from the SOLVIA postprocessor with minor effort. The gravity has of course a great impact on the edge moment, since the rotor is spinning.

8.3.3 Alsvik turbine running at constant speed 12 m/s with yawed flow

Field measurements have shown that it is common for the nacelle to be slightly misaligned with respect to the wind direction [15]. When the turbine is perfectly aligned with the wind, the yaw angle is said to be zero. The yaw angle is defined as the angle between the rotor normal vector and the wind speed vector. In cases were the yaw angle is different from zero, the angle of attack will vary with a frequency corresponding to the frequency of the rotation of the rotor. The crosswind therefore leads to a cyclic increasing and decreasing aerodynamic load distribution over the blades.

In this example, the wind hit the turbine at an angle that varies between $-30°$ and $30°$, Figure 8.12. The following results were obtained from simulations during a period of 600 s. The representative velocity for calculation of the wake skew angle is 10 m/s in X-direction.

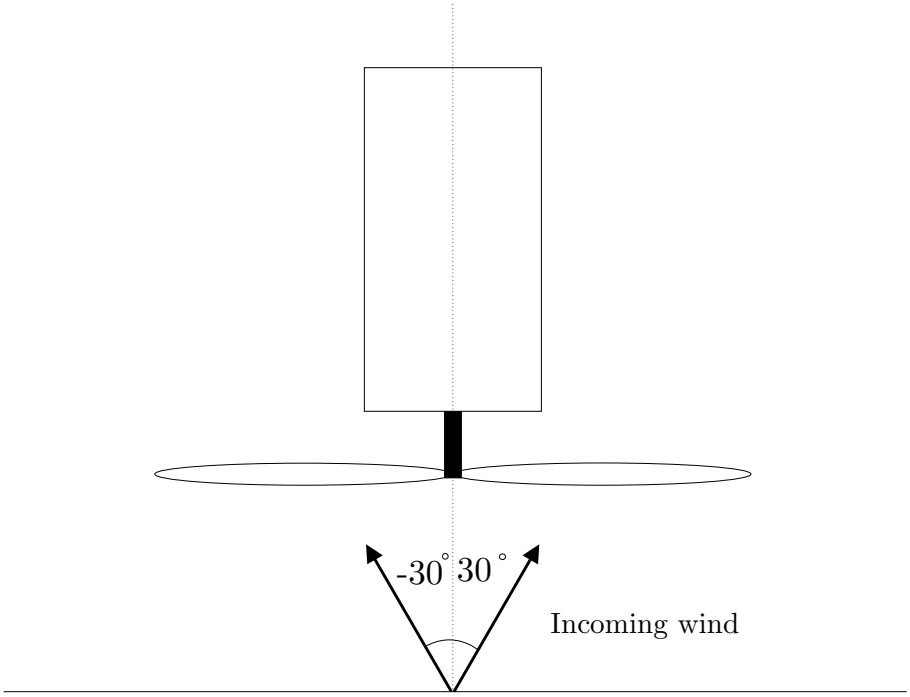

Figure 8.12: Wind angle when the turbine is seen from above.

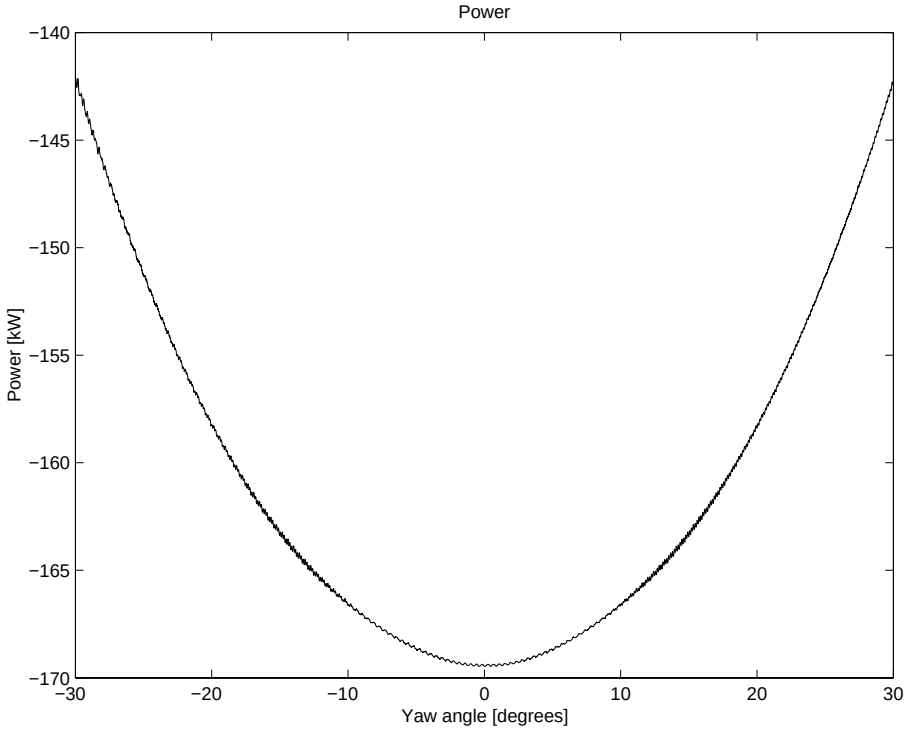

Figure 8.13: Power curve for the Alsvik turbine simulated as running at constant speed 12 m/s with varying yaw angle.

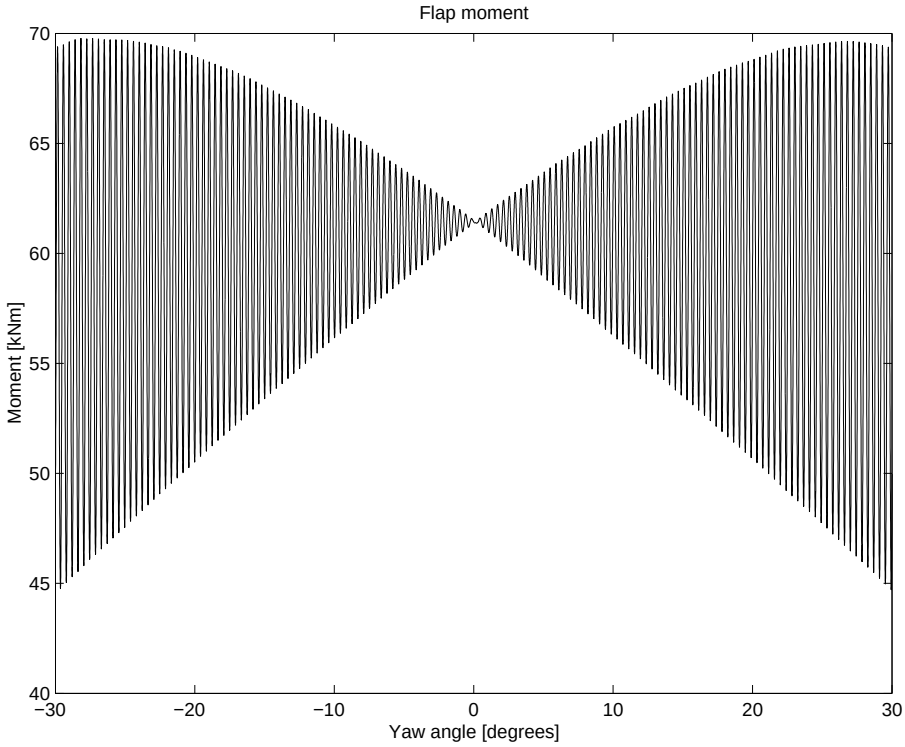

Figure 8.14: Flap moment for the Alsvik turbine simulated as running at constant speed 12 m/s with varying yaw angle.

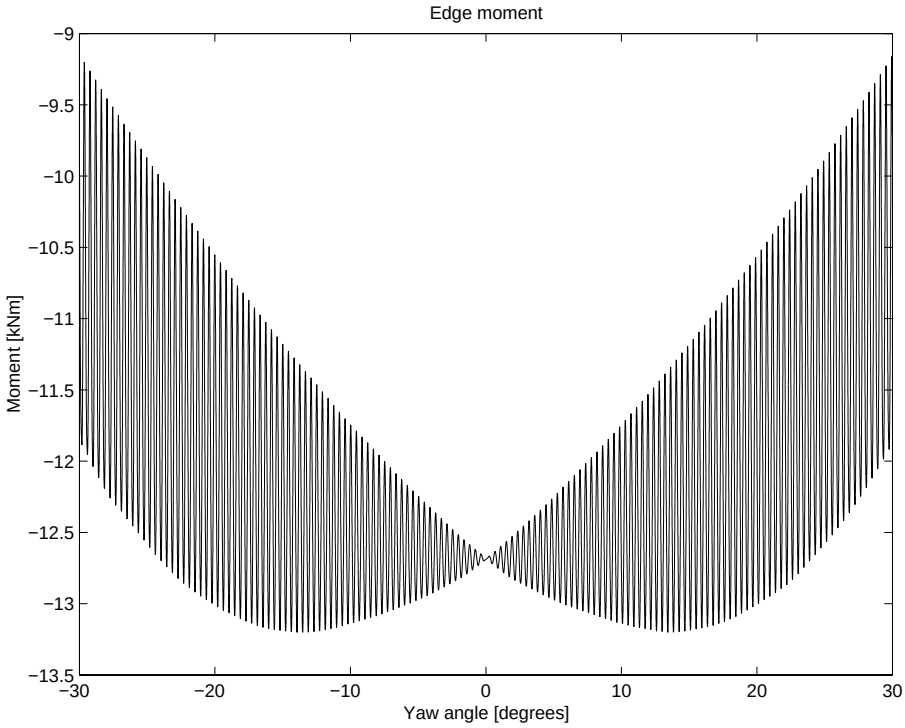

Figure 8.15: Edge moment for the Alsvik turbine simulated as running at constant speed 12 m/s with varying yaw angle.

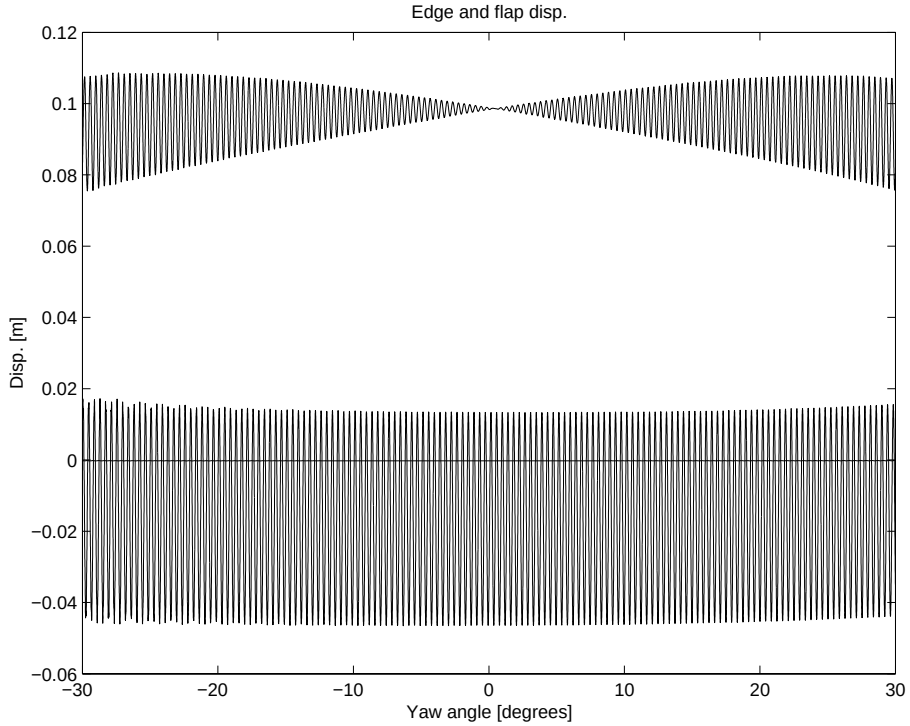

Figure 8.16: Edge (below 0) and flap (above 0) displacements based on the Alsvik turbine simulated as running at constant speed 12 m/s with varying yaw angle. Results given at blade tip.

It is obvious from the results that wind turbines can experience significant time varying aerodynamic loads that potentially causes adverse effects on structures, mechanical components, and power production. For instance, the flap moment is varying ±9 kNm around its mean value 60 kNm at 20-degree yaw angle.

8.3.4 Alsvik turbine running at turbulent wind speed

The SOSIS-W wind data generator was used to create turbulent wind input for the time domain aeroelastic simulations. The results presented in the following section is based on the SOSIS-W input file presented in Appendix B.

Eight different cases were investigated, namely:

1. Mean value 10 m/s, standard deviation $u, v, w = (1.5, 1.2, 0.75)$ and seed A
2. Mean value 10 m/s, standard deviation $u, v, w = (1.5, 1.2, 0.75)$ and seed B
3. Mean value 10 m/s, standard deviation $u, v, w = (0.75, 0.6, 0.375)$ and seed A
4. Mean value 10 m/s, standard deviation $u, v, w = (0.75, 0.6, 0.375)$ and seed B
5. Mean value 5 m/s, standard deviation $u, v, w = (0.75, 0.6, 0.375)$ and seed A

6. Mean value 5 m/s, standard deviation $u, v, w = (0.75, 0.6, 0.375)$ and seed B
7. Mean value 5 m/s, standard deviation $u, v, w = (0.375, 0.3, 0.1875)$ and seed A
8. Mean value 5 m/s, standard deviation $u, v, w = (0.375, 0.3, 0.1875)$ and seed B

where seed A and B, are 890505 and 793505, respectively, in the SOSIS-W input file. The initial seed for random number generator is recommended to be of the order 100000, which guarantees independence of the pseudo-random sequences.

The results presented for each case are the power, as well as the edge and flap moment, as functions of time. The edge and flap displacements (at blade tip of blade 1), in the rotating rotor system are given for case 1, Figure 8.20. The corresponding graphs for the other seven simulations are not shown. Representative velocities for calculation of the wake skew angle given in the global system are for the two standard deviation cases 4 and 9 m/s, respectively.

8.3.4.1 Case 1

Figures 8.17–8.20 show the results obtained for case 1. It is seen that the power graph was varying around its mean value 117.7 kW with a standard deviation of 32.8 kW. The wind loads produced a flap-wise deflection of the blade tip on blade 1, varying around 0.1 m. The edge-wise deflection is in the region -0.05–0.03 and occurred due to the gravity and aerodynamically tangential forces acting on the blade.

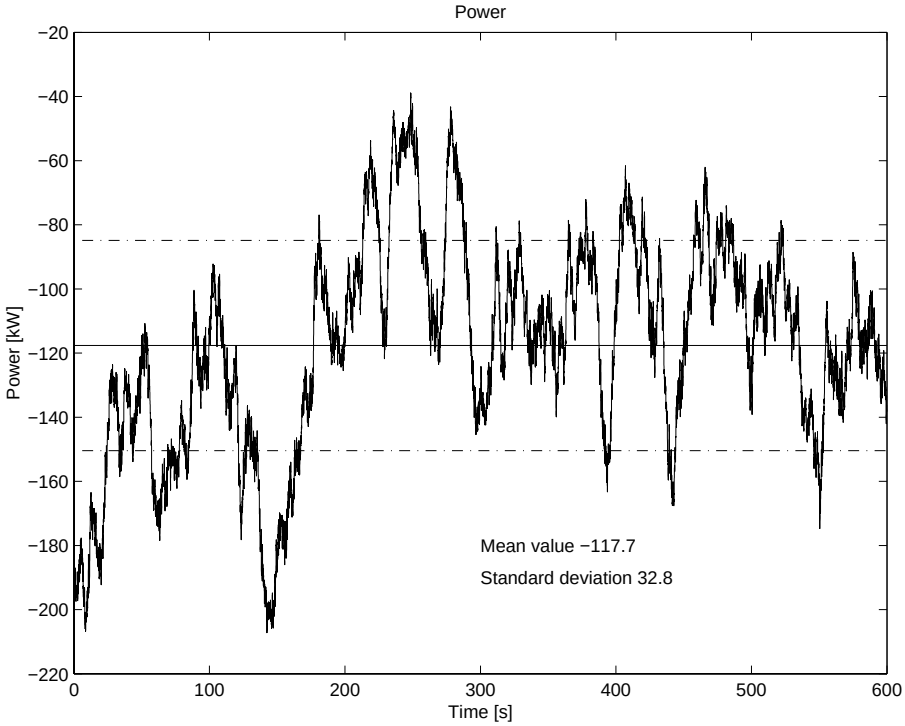

Figure 8.17: Simulated power for case 1.

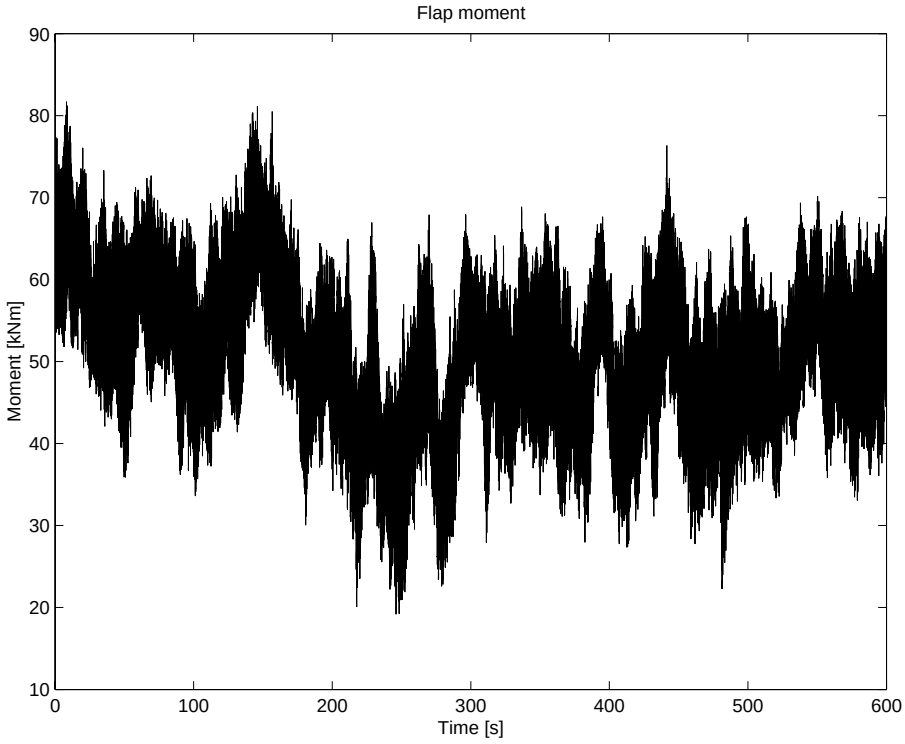

Figure 8.18: Simulated flap moment (blade 1,2 and 3) for case 1.

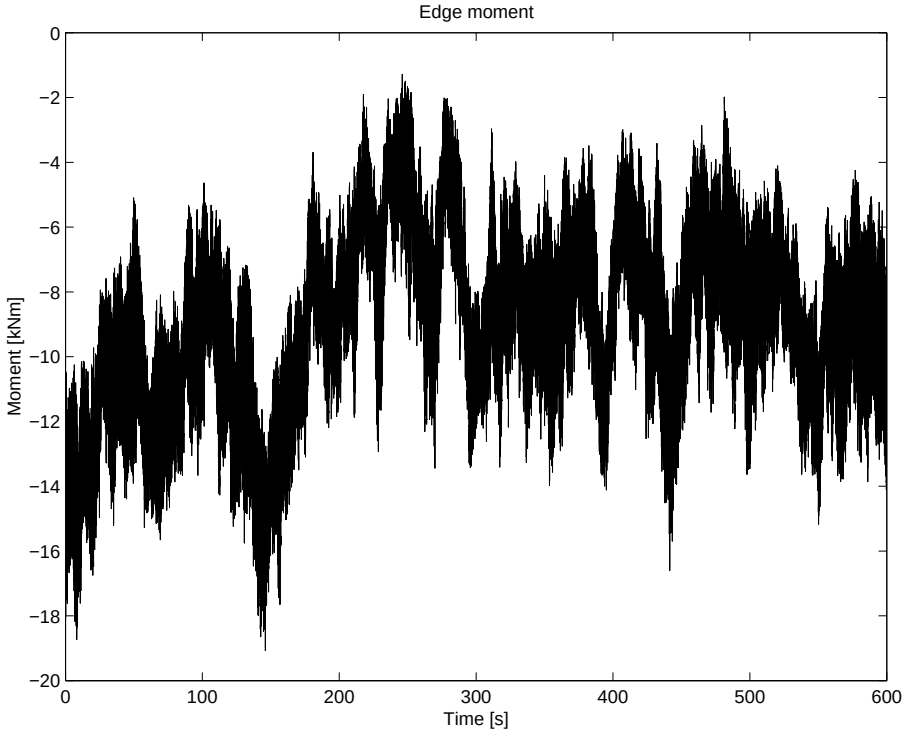

Figure 8.19: Simulated edge moment (blade 1,2 and 3) for case 1.

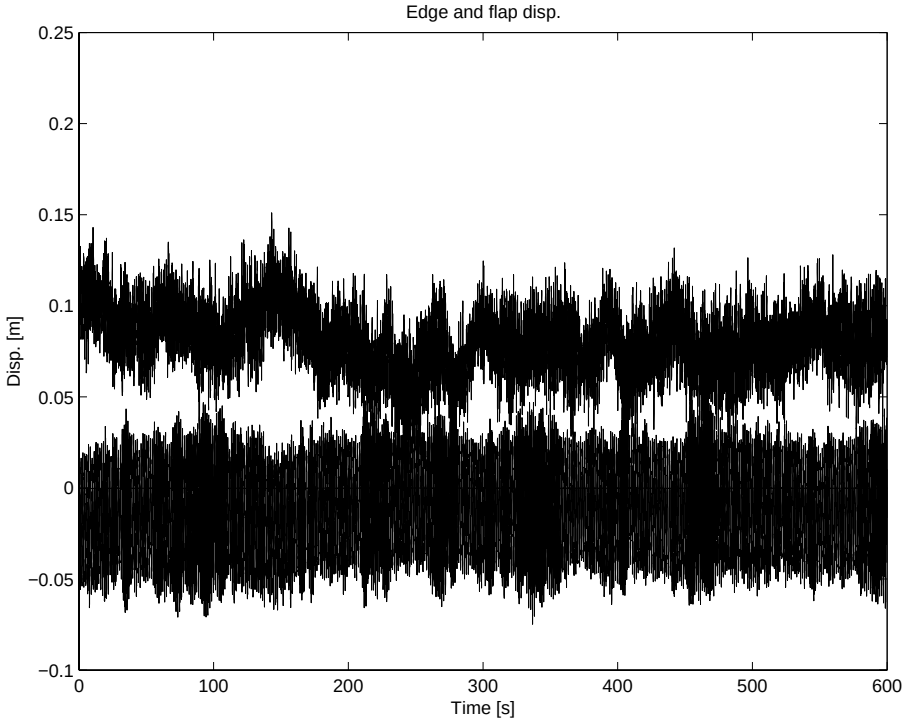

Figure 8.20: Edge (below 0) and flap (above 0) displacements for case 1.

8.3.4.2 Case 2

Figures 8.21–8.23 show the results obtained for case 2. It is seen that the power graph was varying around its mean value 126.9 kW with a standard deviation of 31.0 kW. The mean value and standard deviation were similar to case 1, since the only difference is the value of seed in the input file.

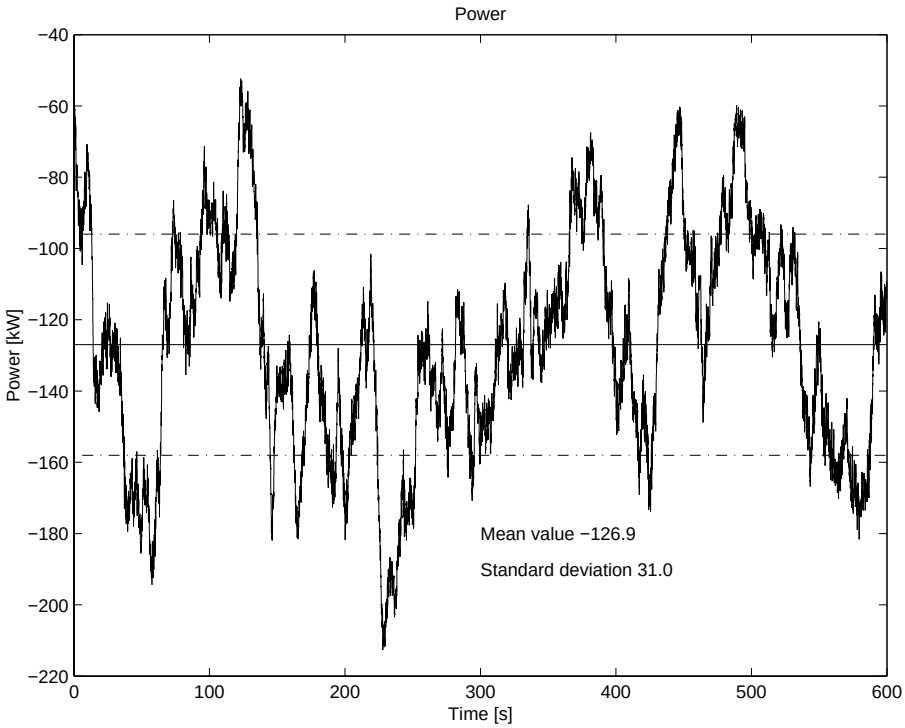

Figure 8.21: Simulated power for case 2.

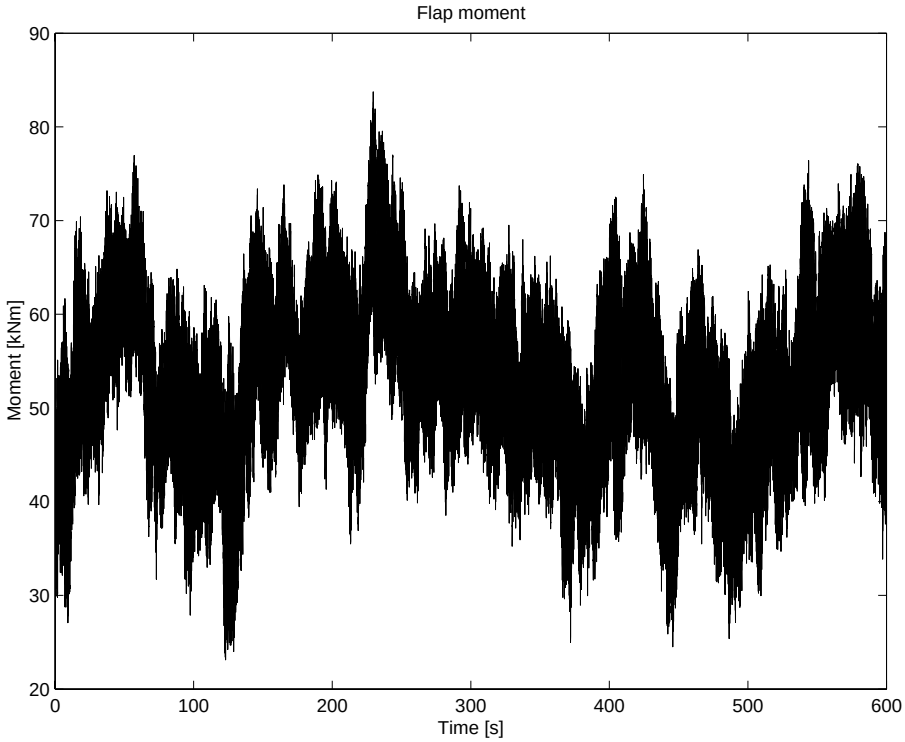

Figure 8.22: Simulated flap moment (blade 1,2 and 3) for case 2.

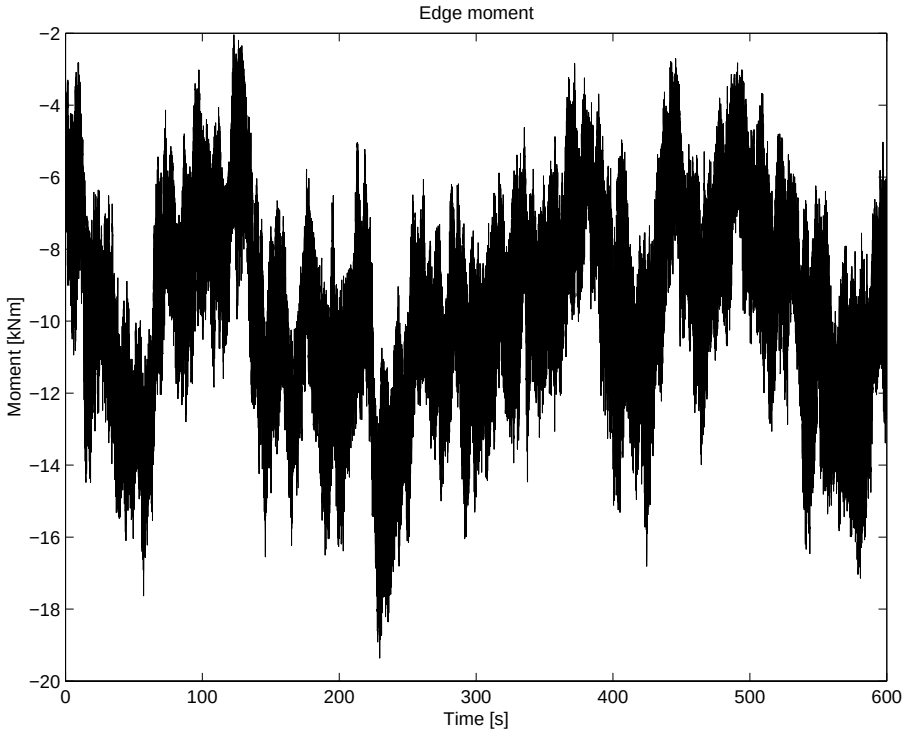

Figure 8.23: Simulated edge moment (blade 1,2 and 3) for case 2.

8.3.4.3 Case 3

Figures 8.24–8.26 show the results obtained for case 3. It is seen that the power graph was varying around its mean value 117.5 kW with a standard deviation of 17.6 kW. When the standard deviation of the wind was halved compared to case 1, the standard deviations of case 1 and 2, yielded 17.6 kW and 32.8 kW, respectively .

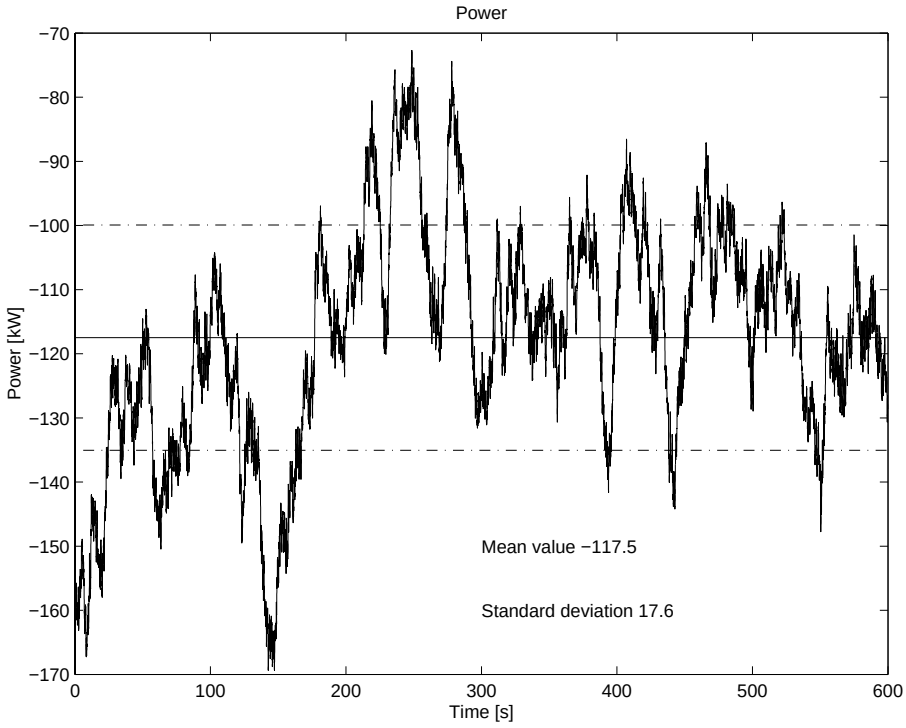

Figure 8.24: Simulated power for case 3.

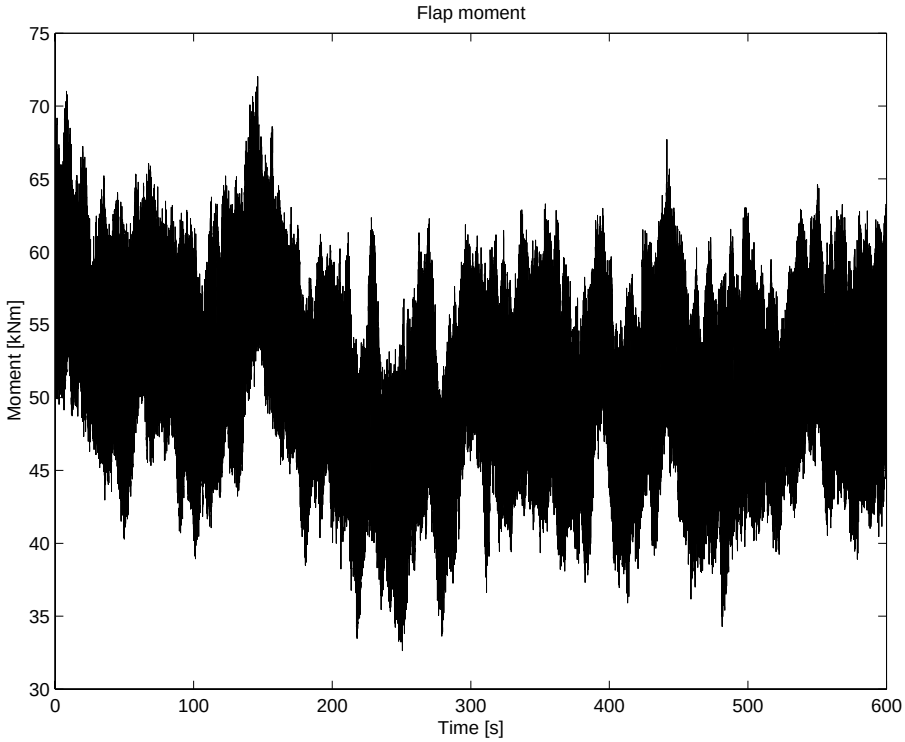

Figure 8.25: Simulated flap moment (blade 1,2 and 3) for case 3.

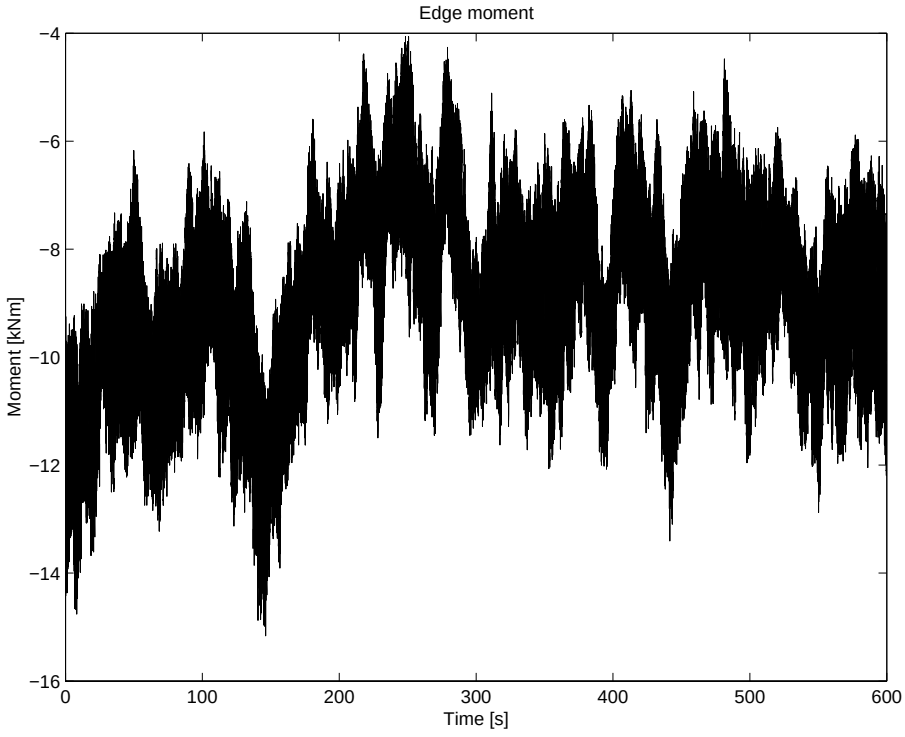

Figure 8.26: Simulated edge moment (blade 1,2 and 3) for case 3.

8.3.4.4 Case 4

Figures 8.27–8.29 show the results obtained for case 4. It is seen that the power graph was varying around its mean value 122.4 kW with a standard deviation of 16.5 kW. The corresponding values of mean value and standard deviation in case 2 were 126.9 kW and 31.0 kW, respectively.

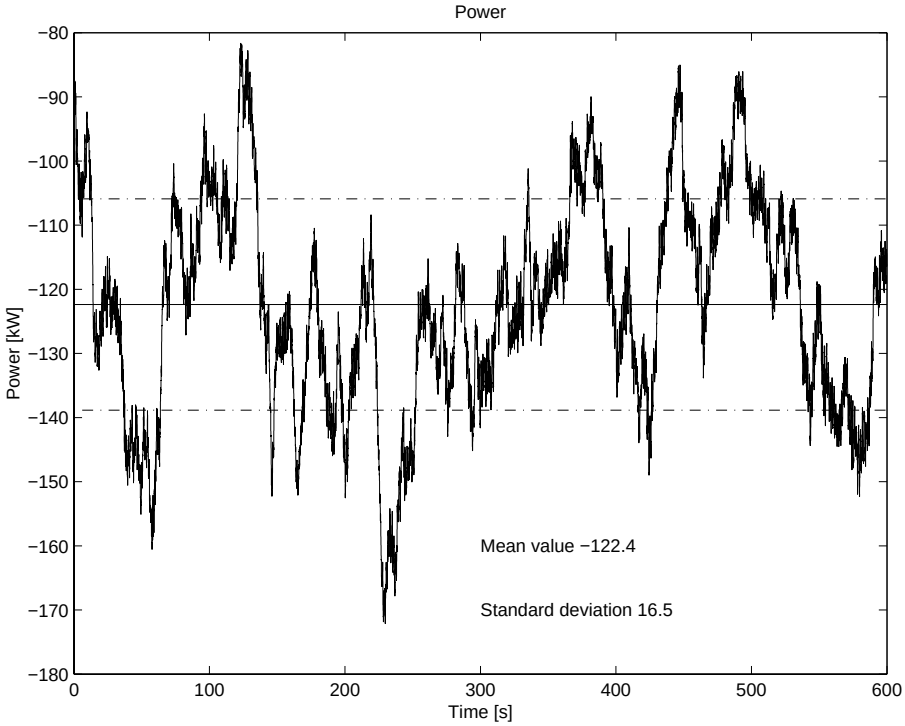

Figure 8.27: Simulated power for case 4.

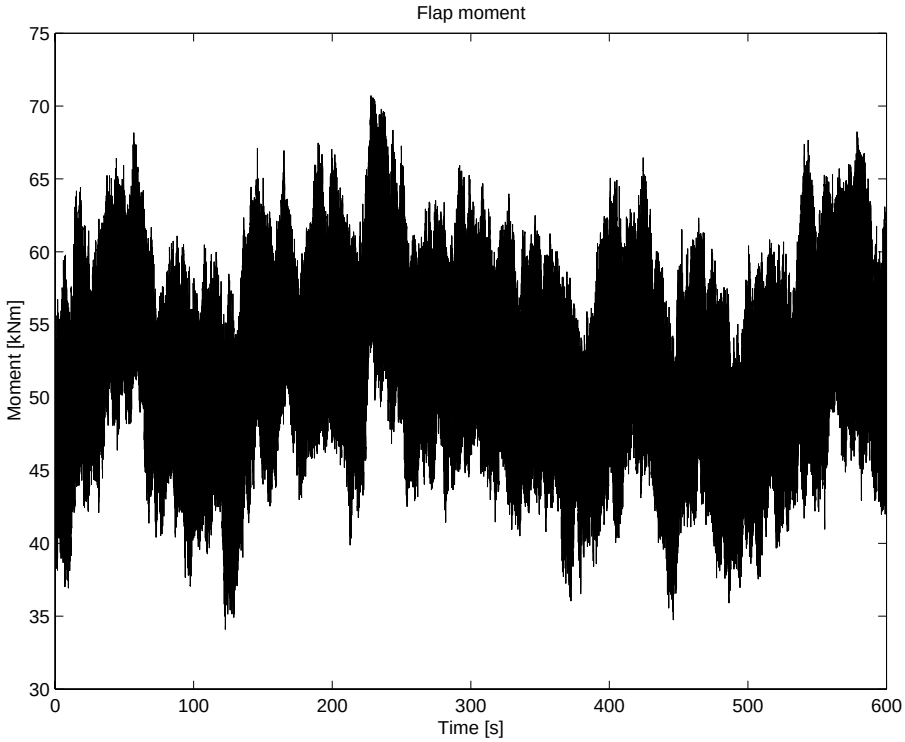

Figure 8.28: Simulated flap moment (blade 1,2 and 3) for case 4.

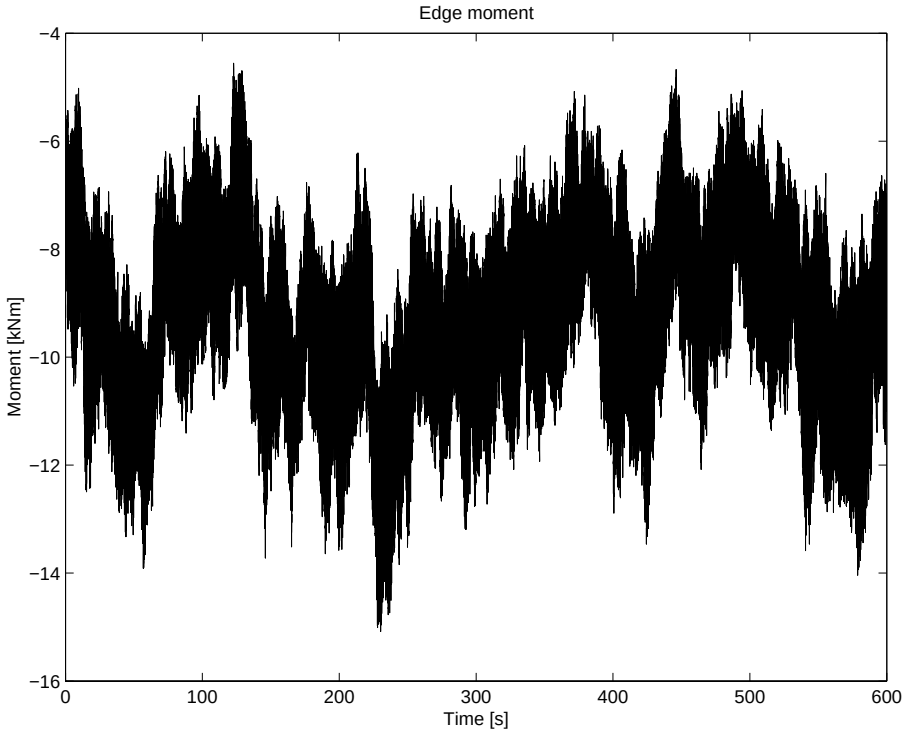

Figure 8.29: Simulated edge moment (blade 1,2 and 3) for case 4.

8.3.4.5 Case 5

Figures 8.30–8.32 show the results obtained for case 5. It is seen that the power graph was varying around its mean value 12.7 kW with a standard deviation of 6.6 kW. It follows that the mean power value varied with the exponent 3.2 when the wind was halved compared to case 3.

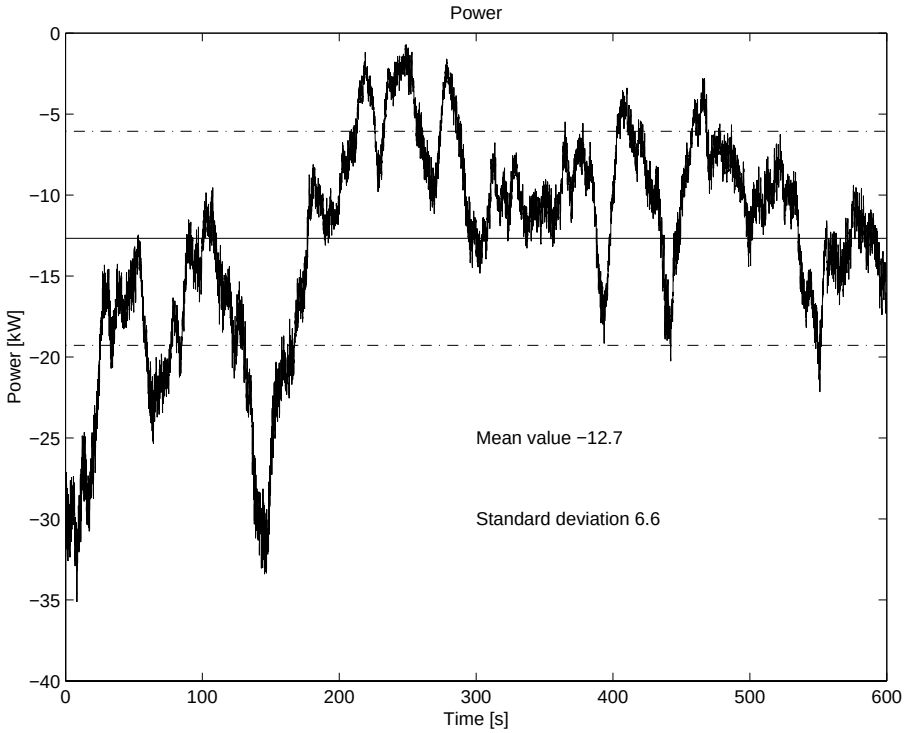

Figure 8.30: Simulated power for case 5.

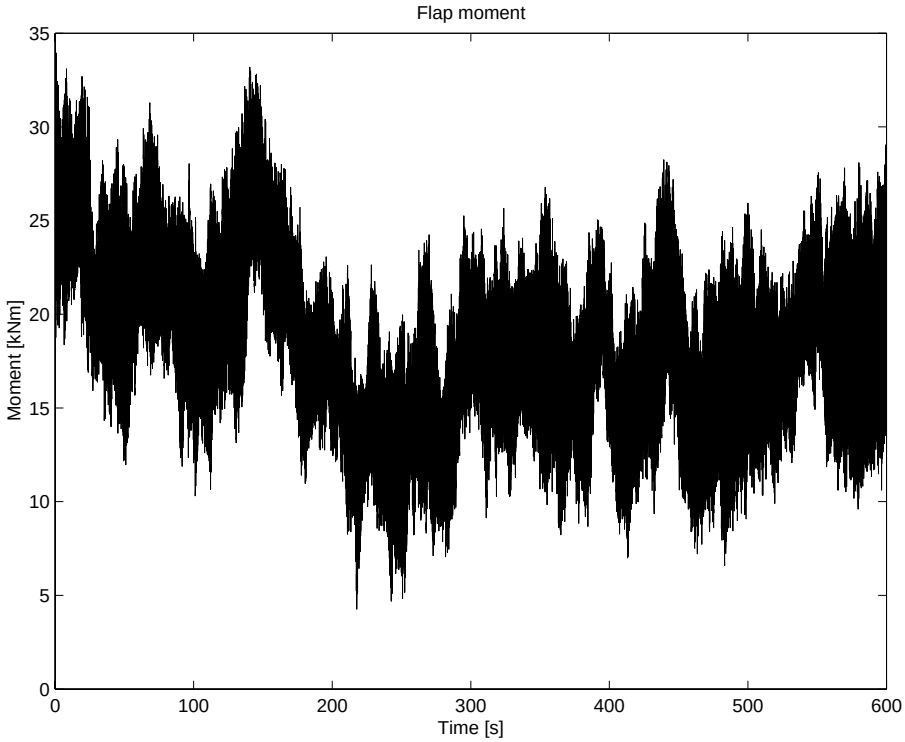

Figure 8.31: Simulated flap moment (blade 1,2 and 3) for case 5.

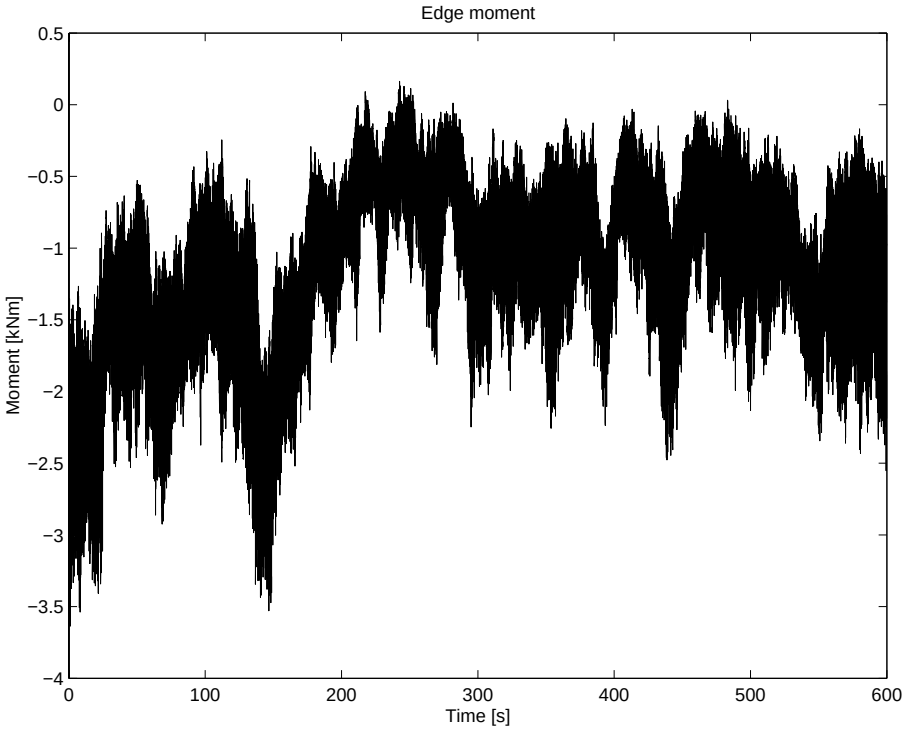

Figure 8.32: Simulated edge moment (blade 1,2 and 3) for case 5.

8.3.4.6 Case 6

Figures 8.33–8.35 show the results obtained for case 6. It is seen that the power graph was varying around its mean value 14.6 kW with a standard deviation of 6.1 kW. The mean value and standard deviation was similar as in case 5, since the only difference was the value of seed in the input file. It follows that the mean power value varied with the exponent 3.1 when the wind was halved compared to case 4.

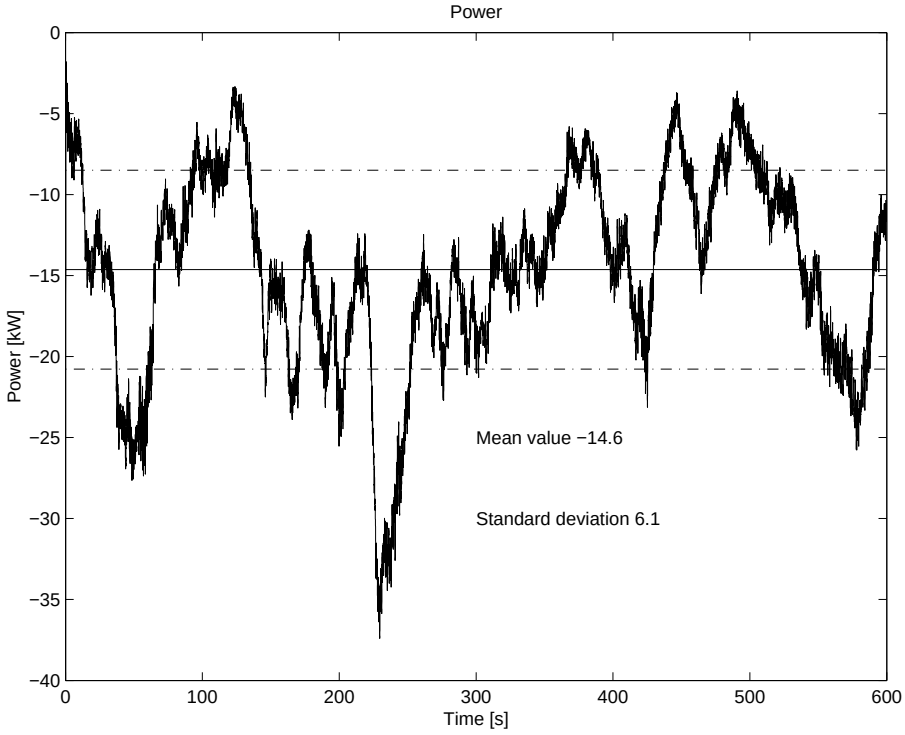

Figure 8.33: Simulated power for case 6.

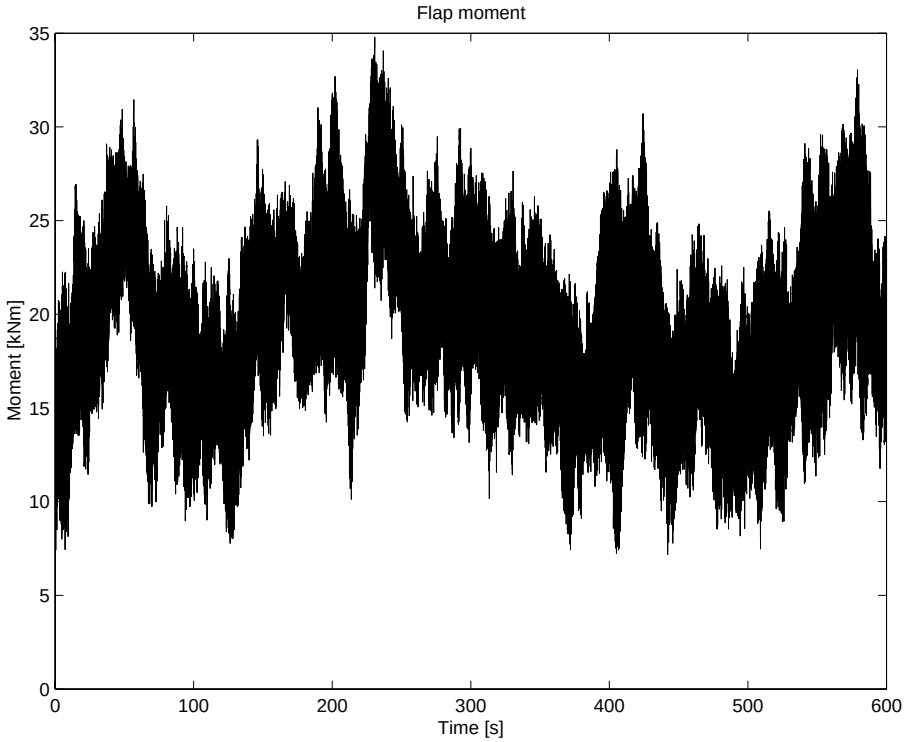

Figure 8.34: Simulated flap moment (blade 1,2 and 3) for case 6.

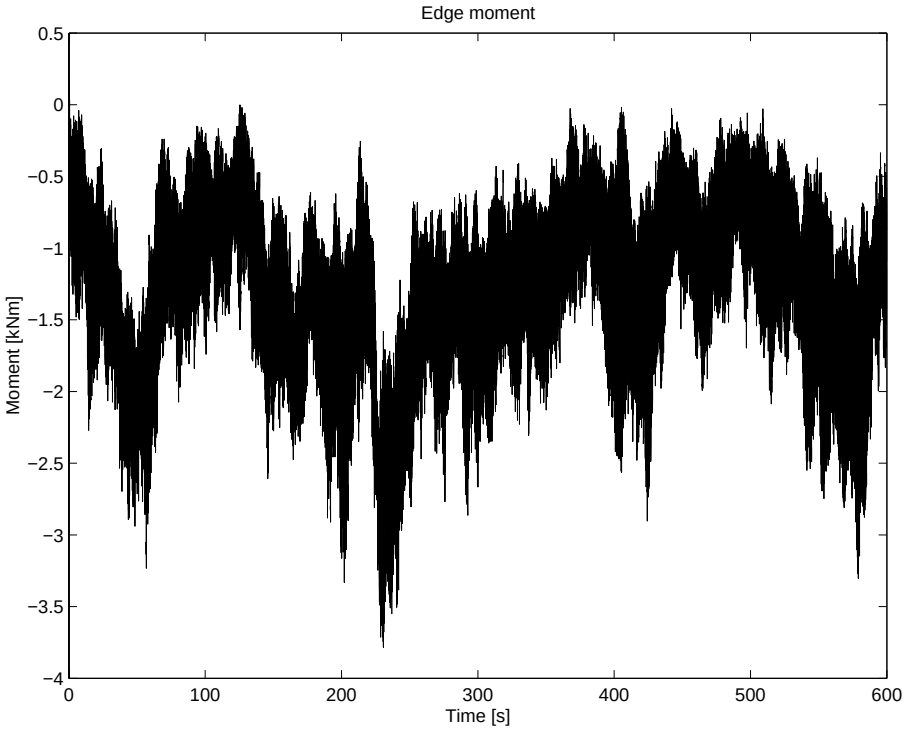

Figure 8.35: Simulated edge moment (blade 1,2 and 3) for case 6.

8.3.4.7 Case 7

Figures 8.36–8.38 show the results obtained for case 7. It is seen that the power graph was varying around its mean value 11.9 kW with a standard deviation of 3.4 kW. When the standard deviation of the wind was halved compared to case 1, the standard deviations of case 7 and 5, yields 3.4 kW and 6.6 kW, respectively.

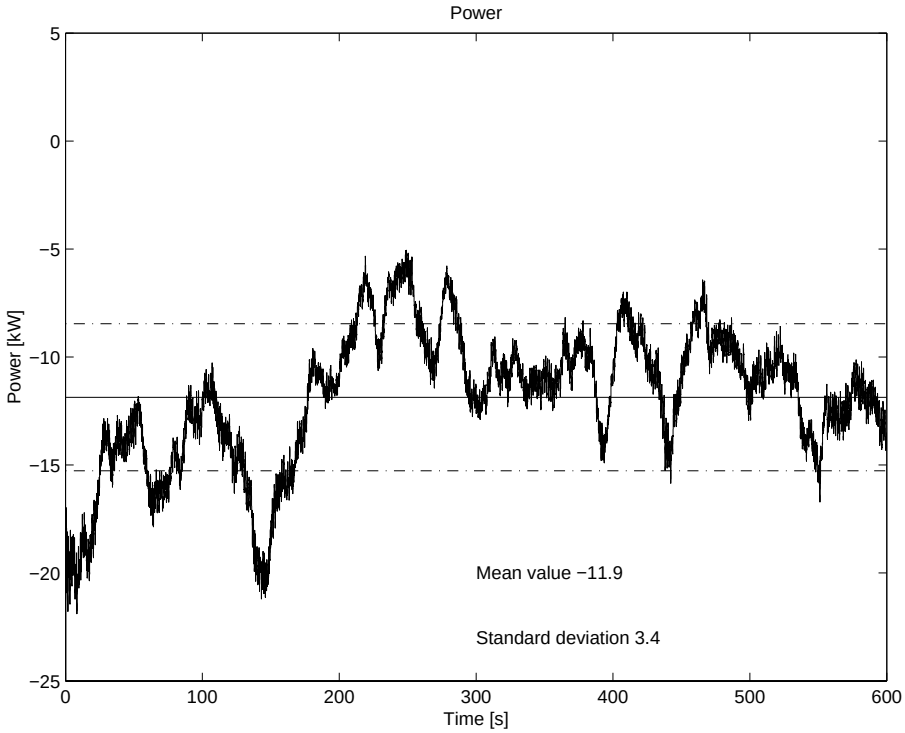

Figure 8.36: Simulated power for case 7.

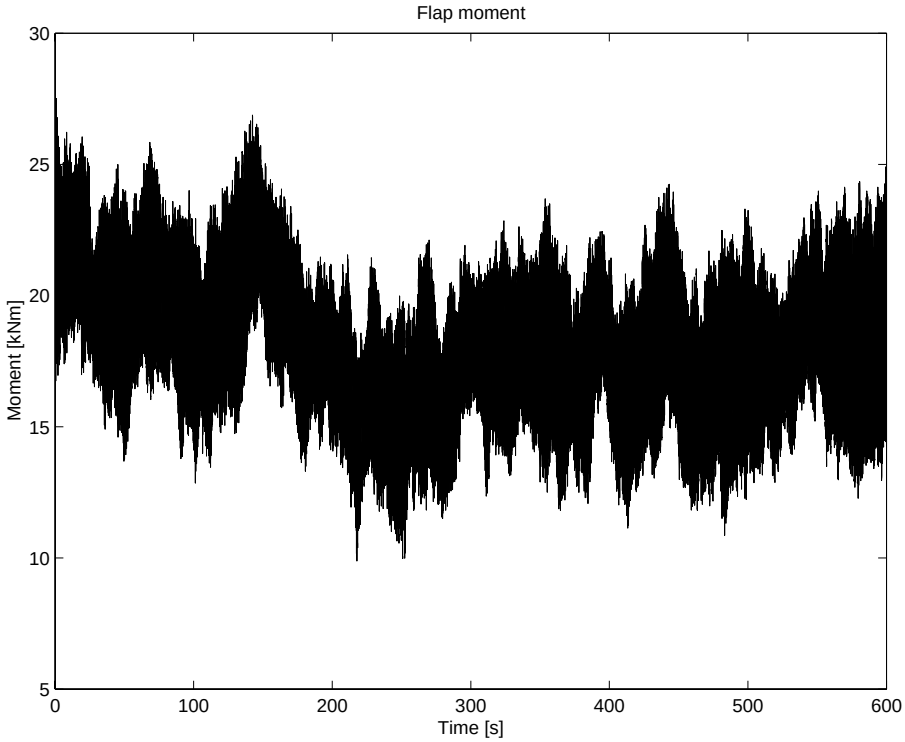

Figure 8.37: Simulated flap moment (blade 1,2 and 3) for case 7.

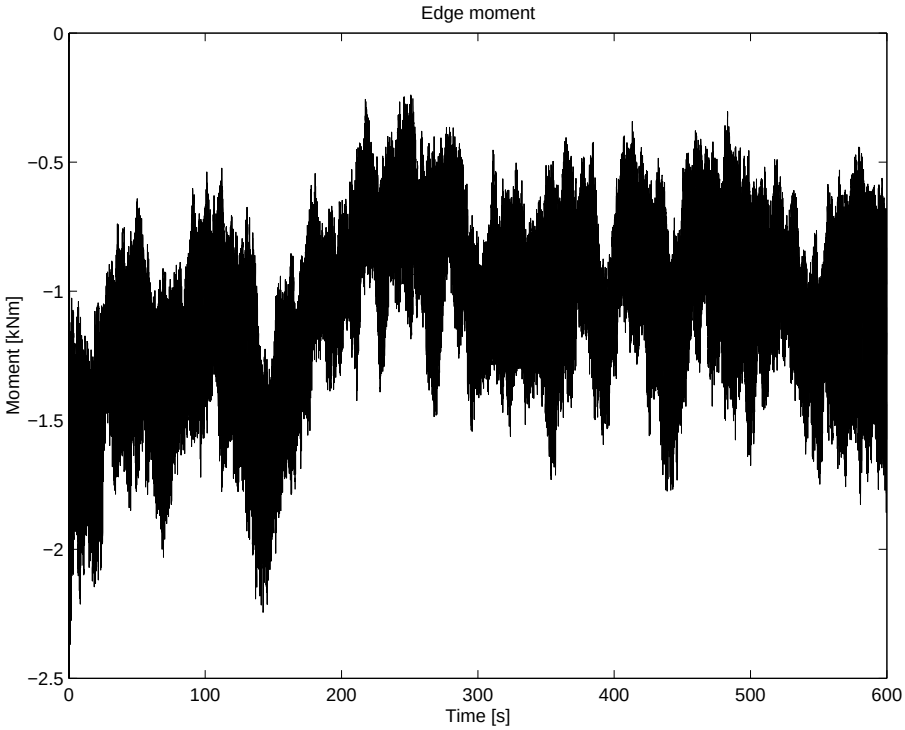

Figure 8.38: Simulated edge moment (blade 1,2 and 3) for case 7.

8.3.4.8 Case 8

Figures 8.39–8.41 show the results obtained for case 8. It is seen that the power graph was varying around its mean value 12.9 kW with a standard deviation of 3.1 kW.

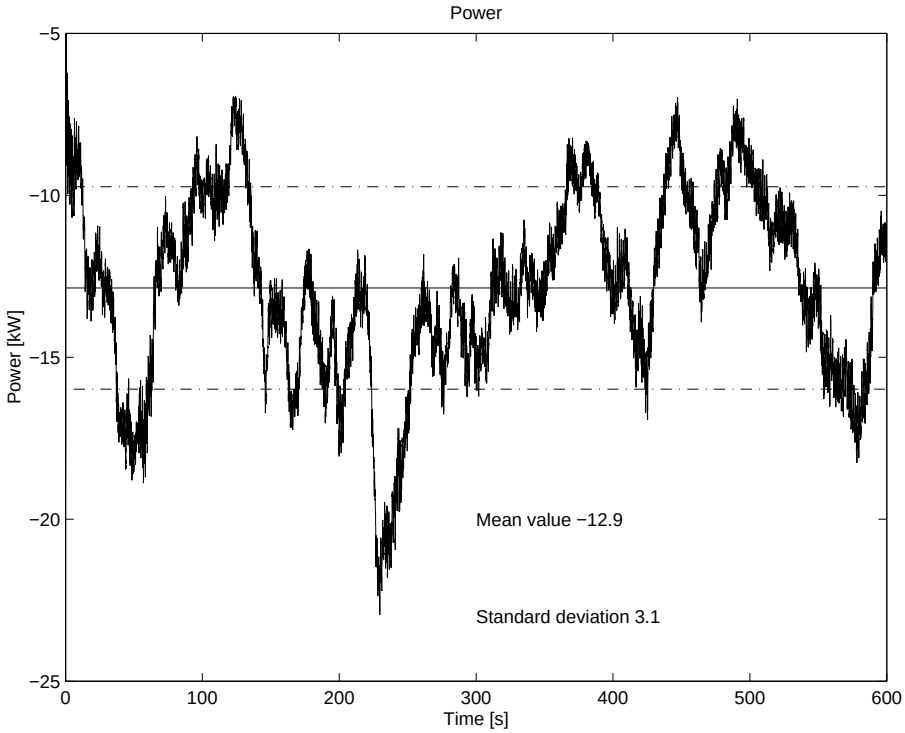

Figure 8.39: Simulated power for case 8.

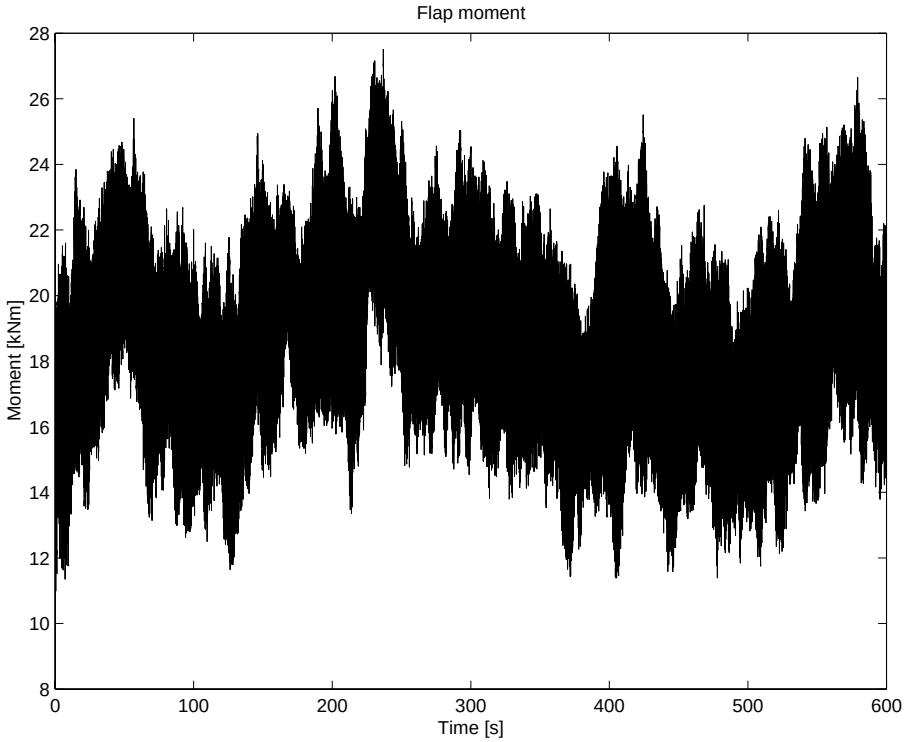

Figure 8.40: Simulated flap moment (blade 1,2 and 3) for case 8.

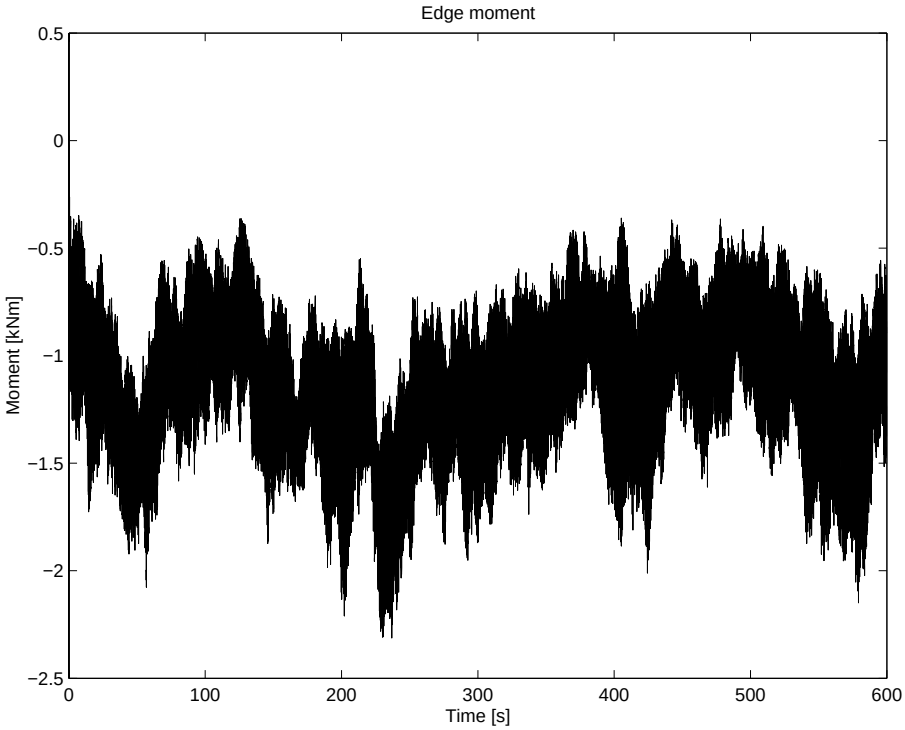

Figure 8.41: Simulated edge moment (blade 1,2 and 3) for case 8.

8.3.4.9 Tabulated results

Table 8.1 shows the results from the simulations in case 1–8.

Table 8.1: Collected results from the simulations in case 1–8.

Case	$\mathbf{P}_{\text{mean}}$ **[kW]**	$\mathbf{P}_{\text{std}}$ **[kW]**	$\mathbf{P}_{\text{min}}$ **[kW]**	$\mathbf{P}_{\text{max}}$ **[kW]**	**mean wind [m/s]**	**wind std [m/s]**	**seed**
1	117.7	32.8	38.9	207.2	10	1.5, 1.2, 0.75	A
2	126.9	31.0	52.4	212.6	10	1.5, 1.2, 0.75	B
3	117.5	17.6	72.7	169.4	10	0.75, 0.6, 0.375	A
4	122.4	16.5	81.6	172.1	10	0.75, 0.6, 0.375	B
5	12.7	6.6	0.7	36.8	5	0.75, 0.6, 0.375	A
6	14.6	6.1	1.8	37.4	5	0.75, 0.6, 0.375	B
7	11.9	3.4	5.1	26.8	5	0.375, 0.3, 0.1875	A
8	12.9	3.1	4.9	22.9	5	0.375, 0.3, 0.1875	B

The results are commented in each of the cases 1–8, see Sections 8.3.4.1–8.3.4.8. Concentrating on the results obtained by using seed A in the calculations, a few observations can be made. The halving of the standard deviation in case 3 compared to case 1 yields almost the same mean power output (117.5 kW compared to 117.7 kW) and a standard deviation that is roughly half of the one in case 1 (17.6 kW compared to 32.8 kW). A halving of the mean wind speed in case 5 compared to case 3 gives that the mean power value and the standard deviation varies as the exponential 3.2 and 1.41, respectively. Again halving the standard deviation, case 7 compared to case 5, gives the same principal trends as the halving in case 3 compared to case 1.

8.4 Comments on simulations

It is, again, worth mentioning that the results presented are examples of possible output data. The results obtained with SOLVIA are saved in a database containing information about all nodal and element displacements and stress results. Postprocessing, such as plots, listings and searching for extreme results can be carried out in SOLVIA-POST.

With the discretisation used in the present work (approximately 300 DOFs) the required computer time was about 60 times the real time on a DELL Dimension Pentium II 450 MHz with 256 Mb ram. The 600 seconds of simulation in the examples would therefor require 10 hours of computer time.

An important part of simulating a wind turbine, in order to predict fatigue loads, power generation etc, is to simulate the wind properly. Is it more accurate to model one sequence of e.g. 6000 s, than ten independent simulations of 600 s? A

deeper understanding of generated wind data and its required time length, may be obtained by studying real sampled wind data fields. But that kind of wind data field investigations, would be out of the scope of this thesis.

Chapter 9

Conclusion and future work

9.1 Conclusions

A tool has been developed for the dynamical simulation of horizontal axis wind turbines.

The project has chosen the finite element method as a means to accurately predict the wind turbine loading and response. The main advantage with the FEM-formulation, and especially using a commercial FEM-package, is the possibility to relatively easily change properties and different configurations of the model. It is also easy to postprocess the results to study e.g. forces, moments, stresses etc. acting on the structure. The user may also easily change the number of DOFs in the model depending on the specific study. The drawbacks are for example the computational costs and difficulties to introduce damping in the model. With the discretisation used in the present work, the required computer time is approximately 60 times the real time, on a Pentium II 400 MHz 256 Mb ram, for a typical simulation. A typical simulation uses a time step of 8 ms and converges within four iteration. Hence simulating a 10 minute period requires 10 hours of computer time.

In the thesis, numerical simulations based on properties of the Danwin 180 kW turbine, were performed. The main goal with the simulations, was to show that the model behaved as expected. Efforts were made to simulate the turbine as closely as possible to the available data. However, it is important to point out that the main effort was made to create a general simulation tool for wind turbine applications and not to model a particular turbine.

The developed tool simulates the operation of wind turbines with 2 or 3 blades at fixed speed. Features like variable speed and pitch controlled power regulations are not included in the present code, but may relatively easily be implemented in later versions.

The subroutine package AERFORCE [2] has been found to work well as a part of the simulation tool. Incorporated features like the dynamic stall model and the model for tower shade effects have, however, not been tested although both models

are included in the simulation code.

All simulations have been done with the SOLVIA FEM program [38]. The program's subroutine based interface has been fairly straight forward to work with and include all possible data needed for wind turbine applications. Unfortunately, the user is limited to work with the pipe-element for large rotation element groups. The limitation is particularly obvious when modelling the blades whose cross sections generally are modelled as orthotropic. However, SOLVIA is aware of the limitation and will work out a solution.

SOSIS-W, [8], is the tool for providing the turbulent wind series. The program is limited to give time series of a length about 800 s with a resolution of 10 Hz. Choosing a lower resolution frequency will lengthen the time series.

9.2 Future research

There are many possible areas to improve or study further.

A natural improvement of today's model must be to include a more extensive control system. A control system that makes it possible to model all kind of generators and power regulation types, as variable or constant speed generators, stall or pith power regulation. For instance, the already built-in stall regulation feasibility needs to be tested. To make the code more convenient to work with, for a wider group of users, a more user-friendly interface may also need to be developed.

The other approach is to use the model as a tool to study specific phenomena. Especially instability problems like blade flutter is an important phenomenon that needs to be investigated further. Another difficult task, connected with e.g. flutter, is the damping properties of the structure and how the damping can be introduced in the model. The damping is today introduced as a numerical damping, to assure numerical stability. The numerical damping is considered to has a relatively slight impact on the structural dynamic behaviour of the wind turbine. The code may also be used for parameter studies, efficiency optimisation, the development of lighter and more optimised turbines, etc. This is very important when maximum values for studied quantities are deduced from random simulations of limited lengths. The possibilities to describe the distribution of high stress levels, based on the simulations, are a very important area of studies. Both the realistic description of variable wind speeds and directions and the statistical interpretation of the obtained results are main topics of future research.

A very important aspect is the interpretation of the results from the pseudo-random time simulations and the use of simulations in order to study e.g. fatigue characteristic. Other questions of similar types are how the simulations should be performed. For instance: are ten independent simulations of 600 s preferred to one 6000 s?

Bibliography

[1] M. E. Bechly. Studies in structural dynamics and manufacture of composite wind turbine blades. Technical report, Mechanical Engineering Department, University of Newcastle, Callaghan, NSW, 2308, 1997.

[2] A. Björk. Aerforce: Subroutine package for unsteady blade-element/momentum calculations. Technical Report TN 2000-07, FFA, Bromma, Sweden, 2000.

[3] A. Björk. Dynstall: Subroutine package with a dynamic stall model. Technical Report FFAP-V-110, FFA, Bromma, Sweden, 2000.

[4] P. Bongers, W. Bierbooms, S. Dijkstra, and T. van Holten. An integrated dynamic model of a flexible wind turbine. Technical Report memt 6, Delft University of Technology, The Netherlands, 1990.

[5] Bonus Energy. General technical description.
Internet online, 06 June 2000.
http://www.bonus.dk/uk/produkter/tekbe_2000_beskrivelse.html.

[6] BTM Consult. The top-10 list of suppliers 1999.
Internet online, 27 Mars 2000.
http://www.btm.dk./overheads/wmu99/sld022.htm.

[7] T. Burton, D. Sharpe, N. Jenkins, and E. Bossanyi. *Wind Energy Handbook*. John Wiley & Sons, Chichester, 2001.

[8] I. Carlen. Sosis-w version 1.3. Technical report, Teknikgruppen AB, Sollentuna, Sweden, 2000.

[9] Compaq Fortran. Language reference manual. Technical Report AA-Q66SD-TK, Compaq Computer Corporation, Houston, Texas, 1999.

[10] R. Cook, D. Malkus, and M. Plesha. *Concepts and application of finite element analysis*. John Wiley & Sons, Chichester, 1989.

[11] A. Crispin, editor. *Wind Directions—How many blades is best?* Arthouros Zervos, Magazine of the European wind energy association, Hockpitt Farm, Nether Stowey, Bridgwater, Somerset, March 2000.

[12] Danish Wind Turbine Manufacturers Association. The wind energy pioneer — Poul la Cour.

Internet online, 23 April 2000.
http://www.windpower.dk/pictures/lacour.htm.

[13] Danish Wind Turbine Manufacturers Association. The wind turbine yaw mechanism.
Internet online, 20 June 2000.
http://www.windpower.dk/tour/wtrb/yaw.htm.

[14] Danish Wind Turbine Manufacturers Association. Wind turbine generators.
Internet online, 29 Maj 2000.
http://www.windpower.dk/tour/wtrb/electric.htm.

[15] E. Djerft and H. Mattson. Evaluation of the software program windfarm and comparisons with measured data from Alsvik. Technical Report TN 2000-30, FFA, Bromma, Sweden, 2000.

[16] R. Edinger and S. Kaul. *Renewable Resources for Electric Power: Prospects and challenges*. Quorum, Westport, 2000.

[17] D. Eggleston and F. Stoddard. *Wind Turbine Engineering Design*. John Wiley & Sons, Chichester, 1987.

[18] T. Ekelund. *Modeling and Linear Quadratic Optimal Control of Wind Turbines*. PhD thesis, School of Electrical and Computer engineering, Chalmers University of Technology, Göteborg, Sweden, 1997.

[19] Enercon. Enercon E-40.
Internet online, 4 June 2000.
http://www.enercon.de/englisch/produkte/e_40_daten.html.

[20] Energy Engineering Board-Commission on Engineering and Technical Systems. Assessment of research needs for wind turbine rotor materials technology. Technical report, National Research Council, Washington, D.C., 1991.

[21] F. Enoksson, J. Olsson, Å. Persson, M. Ringkvist, and C. Wagner. Vindkraft till havs. Technical report, Projektlinjen i matematik, Fysikum Stockholms Universitet, Stockholm, 1999.

[22] European Wind Energy Association. *A plan for action in Europe: Wind Energy—The Facts*. Office for Official Publications of the European Commuunities, Luxembourg, 1999.

[23] Flender Loher. Loher asynchronous generators. Technical Brochure, 2000. LOHER AG Egelstrasse 21, Berlin.

[24] H. Ganander and B. Olsson. Vidyn simuleringsprogram för horisontalaxlade vindkraftverk. Technical Report TG-R-98-14, Teknikgruppen AB, 1998.

[25] Garrad Hassan and Partners. Bladed for windows, a design tool for wind turbine performance and loading.
Internet online, 27 Mars 2001.
http://www.garradhassan.com/bladed/index.htm.

[26] P. Gipe. *Wind energy comes of age*. John Wiley & Sons, New York, 1995.

[27] M. Géradin and D. Rixen. *Mechanical Vibrations*. John Wiley & Sons, Chichester, 1997.

[28] A. Grauers. Design of direct-driven permanent-magnet generators for wind turbines. Technical report, Chalmers, Department of Electric Power Engineering, Techical Report No. 292, Göteborg, Sweden, 1996.

[29] A. C. Hansen and D. J. Laino. USER's GUIDE: YawDyn and AeroDyn for ADAMS. Technical report, Mechanical Engineering Department, University of Utah, Salt Lake City, UT 84112, 1998.

[30] O. L. Hansen. Basic rotor aerodynamics applied to wind turbines. Technical report, Department of Energy Engineering, Fluid Mechanics, Technical University of Denmark, 1998.

[31] R. Harrison, E. Hau, and H. Snel. *Large wind turbines*. John Wiley & Sons, Chichester, 2000.

[32] E. Hau. *Windturbines: fundamentals, technologies, application and economics*. Springer, München, 2000.

[33] R. L. Hills. *Power from wind: a history of windmill technology*. Cambridge University Press, Cambridge, 1994.

[34] J. Holmqvist. Optimization of wind turbine rotors. Technical Report TN 1998-19, FFA, Bromma, Sweden, 1998.

[35] INTEGRATED ENERGIES. Airfoil lift theory revisited.
Internet online, 11 July 2002.
http://home.inreach.com/integener/IE010309AG/.

[36] M. Kuhn and W. Bierbooms. Delft university wind energy converter simulation program.
Internet online, 27 Mars 2001.
http://www.ct.tudelft.nl/windenergy/resduwec.htm.

[37] Å. Larsson. Vindkraft i lokala och regionala nät—elektriska egenskaper och elkvalitet. Technical report, Elforsk Rapport 98:20, Elforsk AB, Stockholm, 1998.

[38] G. Larsson. Solvia, finite element system version 99.0. Technical Report Report SE 99-6, SOLVIA Engineering AB, Västerås, Sweden, 2000.

[39] C. Lindenburg and T. Hegberg. Phatas-IV user's manual. Program for horizontal axis wind turbine analysis and simulation. Version IV. Technical Report ECN-C−99-093, Netherlands Energy Research Foundation ECN, Petten, 2000.

[40] LM Glasfiber A/S. LM lightning protection. Technical Brochure, 2000. Denmark.

[41] LM Glasfiber A/S. Rotor blades development, vortex generators. Technical Brochure, June 2000. Denmark.

[42] J. F. Manwell, J. G. McGowan, and A. L. Rogers. *Wind Energy Explained*. John Wiley & Sons, Chichester, 2002.

[43] Mathworks. Matlab manual.
Internet online, 17 June 2002. http://www.mathworks.com/.

[44] D. Molenaar. State-of-the-art of wind turbine design codes: Main features overview for cost-effective generation. *Wind engineering*, 23:295–311, 1999.

[45] Nordex AG. Products and service.
Internet online, 23 April 2000.
http://www.nordex-online.com/_e/produkte_und_service/index.html.

[46] Ny Teknik. ABB skrotar vindkraftsatsning.
Internet online, 5 July 2002.
http://www.nyteknik.se/pub/ipsart.asp?art_id=19775.

[47] S. Øye. Flex4, simulation of wind turbine dynamics. In B. Maribo Pedersen, editor, *State of the Art of Aerolastic Codes for Wind Turbine Calculations*, pages 71–76, Lyngby, Denmark, 1996.

[48] Professional Services Group. ADAMS/WT 2.0 User's Guide. Technical report, Mechanical Dynamics, 6530 E. Virginia St. Mesa, AZ 85215, 1998.

[49] D. C. Quarton. Wind turbine design calculations the state of the art. In A. Zervos, H. Ehmann, and P. Helm, editors, *European union wind energy conference 1996*, pages 10–15, Göteborg, Sweden, 1996.

[50] M. Rapolder and W. Wunderlich. Adaptive integration algorithms for the dynamic finite element analysis of contact and plasticity. In *European Congress on Computational Methods in Applied Sciences and Engineering ECCOMAS 2000*.

[51] T. Soerensen and M. H. Brask. Lightning protection of wind turbines. Technical report, DEFU, Risoe, Denmark, 1999.

[52] D. A. Spera. *Wind turbine technology: fundamental concepts of wind turbine engineering*. ASME PRESS, New York, 1994.

[53] Statens Kärnkraftinspektion. Kärnkraft.
Internet online, 24 May 2000. http://www.ski.se/karnkraft/index.htm.

[54] Stentec B.V. Wind Energy. Twister.
Internet online, 28 Mars 2001. http://www.stentec.com/windframe.html.

[55] H. Stiesdal. Bonus Energy A/S, The wind turbines components and operation. Technical Brochure, 2000. Fabriksvej 4, Box 170, 7330 Brande, Denmark.

[56] J. Svensson. Grid-connected voltage source converter-control principles and wind energy applications. Technical report, Chalmers, Department of Electric Power Engineering, Techical Report No. 331, Göteborg, Sweden, 1998.

[57] United States Department of Energy Wind Energy Program. History of wind energy use.
Internet online, 19 April 2000. http://www.eren.doe.gov/wind/history.html.

[58] V. A. Vasilis and S. G. Voutsinas. Gast: A general aerodynamic and structural prediction tool for wind turbines. In *European union wind energy conference 1997*, Dublin, Ireland, 1997.

[59] Vattenfall Utveckling AB. Nordic 1000 Utvecklingen av ett vindkraftverk enligt den svenska linjen. Technical report, Vattenfall Utveckling AB, Älvkarleby, 1997.

[60] Vestasvind Svenska AB. Teknisk beskrivning av optislip® i vestas vindkraftverk.
Brochure, 30 Mars 2000. Item Nr 947525.R2.

[61] Vgstol. Vortex generators for single engine Cessnas.
Internet online, 4 June 2002. http://www.vgstol.com/vgstol/.

[62] B. Visser. The aeroelastic code FLEXLAST. In B. Maribo Pedersen, editor, *State of the Art of Aeroelastic Codes for Wind Turbine Calculations*, pages 161–166, Lyngby, Denmark, 1996.

[63] J. Walker and N. Jenkins. *Wind energy technology.* John Wiley & Sons, Chichester, 1997.

[64] B. Wilson. Fast_ad advanced dynamics code. Technical Report OSU/NREL REPORT 99-01, NREL, Oregon State University, Corvallis, Oregon, 2000.

[65] B. Wilson. An aerodynamics and dynamics analysis code for horizontal-axis wind turbines.
Internet online, 27 Mars 2001. http://wind2.nrel.gov/designcodes/fastad/.

[66] Wind Power Monthly. Wind energy facts and figures from windpower monthly.
Internet online, 11 July 2002.
http://windpower-monthly.com/WPM:WINDICATOR:208758#breakdown.

Appendix A

Alsvik data

A.1 Detailed description of the Alsvik 180 kW wind turbine

The wind turbine modelled in the numerical example is a stall regulated DANWIN generator with the following properties:

- Angular velocity 42 r.p.m.
- Cut-in speed 5 m/s
- Cut-out speed 25 m/s
- Hub height 35 m
- Rated power 180 kW
- Rated wind speed 12 m/s
- Rotor diameter 23.2 m

A.1.1 Blade properties

Table A.1: Geometrical and structural data of the Alsvik turbine blades.

Radial pos. (m)	**Chord (m)**	**Area (m)**	**Twist (deg.)**	**Mass (kg)**	**EI flap (Nm^2)**	**EI edge (Nm^2)**
1.05	0.68	0.34	20.5	137	$6.0 \cdot 10^7$	$6.0 \cdot 10^7$
1.55	1.05	0.52	20.6	77.2	$6.0 \cdot 10^7$	$6.0 \cdot 10^7$
2.1	1.35	0.81	20.1	64.6	$5.0 \cdot 10^7$	$6.5 \cdot 10^7$
2.7	1.47	0.88	17.0	50.7	$3.5 \cdot 10^7$	$6.8 \cdot 10^7$
3.3	1.39	0.83	12.1	42.7	$2.5 \cdot 10^7$	$5.0 \cdot 10^7$
3.9	1.33	0.80	8.47	37.2	$1.7 \cdot 10^7$	$3.7 \cdot 10^7$
4.5	1.27	0.76	6.04	34.8	$1.1 \cdot 10^7$	$3.1 \cdot 10^7$
5.1	1.21	0.72	4.37	32.0	$7.0 \cdot 10^6$	$2.5 \cdot 10^7$
5.7	1.15	0.69	3.04	28.8	$4.5 \cdot 10^6$	$2.2 \cdot 10^7$
6.3	1.09	0.65	2.05	26.7	$3.4 \cdot 10^6$	$1.8 \cdot 10^7$
6.9	1.03	0.62	1.33	24.9	$2.4 \cdot 10^6$	$1.6 \cdot 10^7$
7.5	0.97	0.58	0.78	23.7	$1.7 \cdot 10^6$	$1.3 \cdot 10^7$
8.1	0.91	0.54	0.42	22.2	$1.1 \cdot 10^6$	$1.1 \cdot 10^7$
8.7	0.85	0.51	0.22	21.0	$8.0 \cdot 10^5$	$9.1 \cdot 10^6$
9.3	0.79	0.47	0.11	18.2	$6.5 \cdot 10^5$	$6.5 \cdot 10^6$
9.8	0.74	0.29	0	14.0	$6.5 \cdot 10^5$	$5.3 \cdot 10^6$
10.2	0.70	0.28	0	13.5	$6.5 \cdot 10^5$	$4.9 \cdot 10^6$
10.7	0.65	0.39	0	16.0	$6.5 \cdot 10^5$	$4.6 \cdot 10^6$
11.3	0.59	0.35	0	16.2	$6.5 \cdot 10^5$	$4.5 \cdot 10^6$

A.1.2 Tower properties

Table A.2: Geometrical and structural data of the Alsvik tower.

Height (m)	**Outer diameter (m)**	**Thickness (m)**	**Extra Mass (kg)**	**E-mod. (N/m^2)**	**Density (kg/m^3)**
1.0	2.200	0.01	0.0	$213 \cdot 10^9$	7850
2.0	2.168	0.01	0.0	$213 \cdot 10^9$	7850
3.0	2.135	0.01	0.0	$213 \cdot 10^9$	7850
4.0	2.103	0.01	0.0	$213 \cdot 10^9$	7850
5.0	2.070	0.01	0.0	$213 \cdot 10^9$	7850
6.0	2.038	0.01	0.0	$213 \cdot 10^9$	7850
7.0	2.006	0.01	0.0	$213 \cdot 10^9$	7850
8.0	1.974	0.01	0.0	$213 \cdot 10^9$	7850
9.0	1.941	0.01	0.0	$213 \cdot 10^9$	7850
10.0	1.909	0.01	0.0	$213 \cdot 10^9$	7850
11.0	1.877	0.008	0.0	$213 \cdot 10^9$	7850
12.0	1.845	0.008	0.0	$213 \cdot 10^9$	7850
13.0	1.812	0.008	0.0	$213 \cdot 10^9$	7850
14.0	1.780	0.008	0.0	$213 \cdot 10^9$	7850
15.0	1.747	0.008	0.0	$213 \cdot 10^9$	7850
16.0	1.715	0.008	0.0	$213 \cdot 10^9$	7850
17.0	1.683	0.008	0.0	$213 \cdot 10^9$	7850
18.0	1.651	0.008	0.0	$213 \cdot 10^9$	7850
19.0	1.618	0.008	0.0	$213 \cdot 10^9$	7850
20.0	1.586	0.008	0.0	$213 \cdot 10^9$	7850
21.0	1.554	0.006	0.0	$213 \cdot 10^9$	7850
22.0	1.522	0.006	0.0	$213 \cdot 10^9$	7850
23.0	1.489	0.006	0.0	$213 \cdot 10^9$	7850
24.0	1.457	0.006	0.0	$213 \cdot 10^9$	7850
25.0	1.424	0.006	0.0	$213 \cdot 10^9$	7850
26.0	1.392	0.006	0.0	$213 \cdot 10^9$	7850
27.0	1.360	0.006	0.0	$213 \cdot 10^9$	7850
28.0	1.327	0.006	0.0	$213 \cdot 10^9$	7850
29.0	1.295	0.006	950.0	$213 \cdot 10^9$	7850
29.8	1.262	0.006	0.0	$213 \cdot 10^9$	7850

Appendix B

Input files

B.1 Example of SOSIS-W input file

```
# DEMONSTRATION INPUT DATA FILE FOR SOSIS-W VERSION 1.3
#
# RUN PARAMETERS:
# ID OF RUN
#
   demo
#
# GRID PARAMETERS:
# HUB HEIGHT , WIND SPEED AT HUB HEIGHT , INCLINATION , POWER
#
     35.0              10.0                10.0        0.2
#
# NUMBER OF GRID POINTS , GRID SIZE
#
          144                2.0
#
# SIGNAL PARAMETERS:
# TIMESTEP (s) , LENGTH OF SIGNALS (s) , SPECFLAG
#
     0.1                600.0              1
#
# STANDARD DEVIATIONS OF TURBULENCE (AMBIENT AND WAKE):
# STANDARD DEV u   ,  STANDARD DEV v   ,  STANDARD DEV w
#
     1.5  1.5           1.2   1.2          0.75   0.75
#
# LENGTH SCALES OF TURBULENCE (AMBIENT AND WAKE):
#       Lu         ,       Lv           ,     Lw
#
  350.0   350.0       50.0   50.0       12.2  12.2
```

```
#
# COHERENCE DECAY FACTORS AND LENGTH SCALE:
# U-COMPONENT , V-COMPONENT , W-COMPONENT , LENGTH SCALE
#
      8.8           8.8           8.8         10000.0
#
# WAKE PARAMETERS:
#  DIAM    ,   DEFICIT   ,  YOFF  ,  ZOFF  ,  SIGMAY   ,  SIGMAZ
#
   37.0          0.001        0.0     -0.0       0.4        0.37
#
# SEED     CORRECTION1  CORRECTION2   OUTFLAG
#
  890505       0.1          0.5          4
#
```

B.2 The Alsvik input file

```
# Turbine name
  Alsvik
# Rotor coning angle beta (deg) and tilt angle tau (deg)
                     0.0                        0.0
# a check number 888.88 should be on next line
  888.88
# Blade tip radius and rot radius
# hub height and "overhang", xh
#
# th=z for tower top, xh=x for hub position. Positive
# for upwind turbines
# rtip       rrot      th      xh
  11.6       1.0       29.7    1.477
# ================= BLADE DATA ==========================
# if isetarea=0 the areas from the tabulated values will be used
  0
# Radius  Chord     Area     Twist    rel, thickness   profile1 profile2
# m       m         m2       deg      -                -       -
  1.05    0.68      0.44     20.5     30               5       0
  2.1     1.35      1.07     20.1     35               5       0
  3.3     1.39      1.64     12.1     31               5       0
  4.5     1.27      1.60     6.04     27               5       0
  5.7     1.15      1.45     3.04     22.5             4       0
  6.9     1.03      1.31     1.33     19               3       2
  8.1     0.91      1.16     0.42     17               2       1
  9.3     0.79      1.02     0.11     15               1       0
  10.2    0.7       0.67     0        15               1       0
```

```
  11.3    0.59      0.71     0        15               1       0
# End blade data
# ====Dynamic stall method. common for all aerofoils===========
# If lcncl=0 static profile data will be used. All other parameters in the
# dynamic stall model will then be disregarded
#-------------------------------------------------------------
# lcncl   lpotmeth  lfmeth  lvormeth  lcddyn  ldut
  0       4         4       2         2       0
#-------------------------------------------------------------
# coeffa1     coeffa2      coeffb1     coeffb2
  0.3         0.7          0.13        0.53
# Number of aerofoils (1 row)
  5
# ++++++++++++ Ny profil ++++++++++++++++++++++++++++++++++++++++
# File name with "sep-data" (1 row)
  D:\vindverket\profildata\alvid15v1_360.cla
# aerofoil number
  1
# rel thickness
  15
# tf data (3 rows)
  0.0  0.5  0.1
  5
  0
# ------------------------------------------------------------
# vortex parameters (1 row)
# tv, tvl, tvs, cn1pos, cn1neg
  2   1    1    2       -1
# ++++++++++++ New profile ++++++++++++++++++++++++++++++++++++++++
# File name with "sep-data" (1 row)
  D:\vindverket\profildata\alvid18v1_360.cla
# aerofoil number
  2
# rel thickness
  18
# tf data (3 rows)
  0.0  0.5  0.1
  5
  0
# ------------------------------------------------------------
# vortex parameters (1 row)
# tv, tvl, tvs, cn1pos, cn1neg
  2   1    1    2       -1
# ++++++++++++ New profile ++++++++++++++++++++++++++++++++++++++++
# File name with "sep-data" (1 row)
  D:\vindverket\profildata\alvid21v1_360.cla
```

```
# aerofoil number
  3
# rel thickness
  21
# tf data (3 rows)
  0.0  0.5  0.1
  5
  0
# ------------------------------------------------------------
# vortex parameters (1 row)
# tv, tvl, tvs, cn1pos, cn1neg
  2   1    1    2       -1
# ++++++++++++ New profile ++++++++++++++++++++++++++++++++++++++++
# File name with "sep-data" (1 row)
  D:\vindverket\profildata\alvidnr4_360.cla
# aerofoil number
  4
# rel thickness
  24
# tf data (3 rows)
  0.0  0.5  0.1
  5
  0
# ------------------------------------------------------------
# vortex parameters (1 row)
# tv, tvl, tvs, cn1pos, cn1neg
  2   1    1    2       -1
# ++++++++++++ New profile ++++++++++++++++++++++++++++++++++++++++
# File name with "sep-data" (1 row)
  D:\vindverket\profildata\alvidnr5_360.cla
# aerofoil number
  5
# rel thickness
  27
# tf data (3 rows)
  0.0  0.5  0.1
  5
  0
# ------------------------------------------------------------
# vortex parameters (1 row)
# tv, tvl, tvs, cn1pos, cn1neg
  2   1    1    2       -1
# ======== End of profile data ================================
# For constants and choice of method. See AERFORCE-manual
#
# default: at1=0.32
```

```
# luitan=1
# time-const int-method luitan
# at1,     con_vec(1),    lval(2), lval(1)
  0.32     .2             1        1
#
# =========== Wind, mech, etc. ================================
# Air density (rho)
  1.225
# gridpo: Number of gridpoints along an edge, must be the same number as
# specified in SOSIS. N=gridpo*gridpo e.g. 144=12*12
# grsteps: Grid size in meters
# gridpo grstep
  12      2
# a check-number 888.88 should be on next line
  888.88
#-------------------------------------------------------------
```